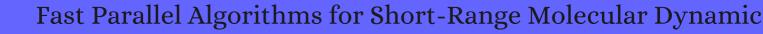
CITATION REPORT List of articles citing



DOI: 10.1006/jcph.1995.1039 Journal of Computational Physics, 1995, 117, 1-19.

Source: https://exaly.com/paper-pdf/25849643/citation-report.pdf

Version: 2024-04-28

This report has been generated based on the citations recorded by exaly.com for the above article. For the latest version of this publication list, visit the link given above.

The third column is the impact factor (IF) of the journal, and the fourth column is the number of citations of the article.

#	Paper	IF	Citations
2201	Gas-Flow-Driven Aligned Growth of Graphene on Liquid Copper.		
2200	•		
2199	Revealing the Intermolecular Interactions of Asphaltene Dimers by Quantum Chemical Calculations.		
2198	Tunable Primary and Secondary Encapsulation of a Charged Nonspherical Nanoparticle: Insights from Brownian Dynamics Simulations.		
2197	Robust Aluminum and Iron Phosphinate MetalOrganic Frameworks for Efficient Removal of Bisphenol A.		
2196	New Patchy Particle Model with Anisotropic Patches for Molecular Dynamics Simulations: Application to a Coarse-Grained Model of Cellulose Nanocrystal.		
2195	Making the Best of a Bad Situation: A Multiscale Approach to Free Energy Calculation.		
2194	•		
2193	StructureProperty Relationships in Amorphous Microporous Polymers.		
2192	Rotational Dynamics in Ionic Liquids from NMR Relaxation Experiments and Simulations: Benzene and 1Ethyl-3-Methylimidazolium.		
2191	Extent of Surface Force Additivity on Chemically Heterogeneous Substrates at Varied Orientations.		
2190	Molecular Modeling of Structure and Dynamics of Nafion Protonation States.		
2189	Molecular Adsorption and Transport at Liposome Surfaces Studied by Molecular Dynamics Simulations and Second Harmonic Generation Spectroscopy.		
2188	Surfing Multiple Conformation-Property Landscapes via Machine Learning: Designing Single-Ion Magnetic Anisotropy.		
2187	Understanding Chemical versus Electrostatic Shifts in Xray Photoelectron Spectra of Organic Self-Assembled Monolayers.		
2186	Accurate Force Field Parameters and pH Resolved Surface Models for Hydroxyapatite to Understand Structure, Mechanics, Hydration and Biological Interfaces.		
2185	Describing the Diverse Geometries of Gold from Nanoclusters to BulkA First-Principles-Based Hybrid Bond-Order Potential.		

2168

2167

ReaxFF Molecular Dynamics Study.

Nonfluorinated Copolymers.

Atomistic and Mesoscopic Simulations of the Structure of CO2 with Fluorinated and

2184 . 2183 Mechanism of Intact Adsorbed Molecules Ejection Using High Intensity Laser Pulses. 2182 Existence of Multiple Phases of Water at Nanotube Interfaces. Proton-Selective Ion Transport in ZSM5 Zeolite Membrane. 2181 2180 Doped Amorphous Ti Oxides To Deoptimize Oxygen Reduction Reaction Catalysis. Correction to Relating Molecular Morphology to Charge Mobility in Semicrystalline Conjugated 2179 Polymers. Effects of Embedded Dipole Layers on Electrostatic Properties of Alkanethiolate Self-Assembled Monolayers. Multiscale Modeling of the HKUST-1/Poly(vinyl alcohol) Interface: From an Atomistic to a Coarse Graining Approach. Insights on the Role of Many-Body Polarization Effects in the Wetting of Graphitic Surfaces by 2176 Water. Enhanced Hydrogen Purification in Nanoporous Phosphorene Membrane with Applied Electric 2175 2174 First-Principles-Derived Force Fields for CH4 Adsorption and Diffusion in Siliceous Zeolites. Adsorption Contraction Mechanics: Understanding Breathing Energetics in Isoreticular 2173 MetalOrganic Frameworks. 2172 Ice Nucleation on a Graphite Surface in the Presence of Nanoparticles. Atomistic Simulations of Al(100) and Al(111) Surface Oxidation: Chemical and Topological Aspects of the Oxide Structure. 2170 Density, Structure and Stability of Citrate3 and H2citrate on Bare and Coated Gold Nanoparticles. 2169 Adsorption of Hexacontane on Hexagonal Boron Nitride. Surface Reactivity and Leaching of a Sodium Silicate Glass under an Aqueous Environment: A

Significant Temperature Dependence of the Isosteric Heats of Adsorption of Gases in Zeolites 2166 Demonstrated by Experiments and Molecular Simulations. Size-Dependent Photocatalytic Activity of Cubic Boron Phosphide Nanocrystals in the Quantum 2165 Confinement Regime. Defects in Self-Assembled Monolayers on Nanoparticles Prompt Phospholipid Extraction and Bilayer-Curvature-Dependent Deformations. 2163 Stress Field Characteristics and Collective Mechanical Properties of Defective Graphene. Classical Magnetic Dipole Moments for the Simulation of Vibrational Circular Dichroism by ab Initio 2162 Molecular Dynamics. Strong Coupling between Nanofluidic Transport and Interfacial Chemistry: How Defect Reactivity Controls LiquidSolid Friction through Hydrogen Bonding. 2160 Atomistic Hydrodynamics and the Dynamical Hydrophobic Effect in Porous Graphene. Universal Repulsive Contribution to the Solvent-Induced Interaction Between Sizable, Curved 2159 Hydrophobes. SolidLiquid Thermal Transport and Its Relationship with Wettability and the Interfacial Liquid 2158 Structure. Free Volume Theory of Hydrocarbon Mixture Transport in Nanoporous Materials. 2156 Liquid-Phase Exfoliation of MoS2 Nanosheets: The Critical Role of Trace Water. Molecular Origin of Electric Double-Layer Capacitance at Multilayer Graphene Edges. 2154 Nanoscale Dynamics versus Surface Interactions: What Dictates Osmotic Transport?. Role of Surface Stress on the Reactivity of Anatase TiO2(001). 2152 Spatially Distributed Rheological Properties in Confined Polymers by Noncontact Shear. Predicted Structures of the Active Sites Responsible for the Improved Reduction of Carbon Dioxide 2151 by Gold Nanoparticles. Kinetic-Dominated Charging Mechanism within Representative Aqueous Electrolyte-based Electric 2150 Double-Layer Capacitors.

2149 Self-Assembly of Mesophases from Nanoparticles.

Ab Initio Molecular Dynamics and Lattice Dynamics-Based Force Field for Modeling Hexagonal 2148 Boron Nitride in Mechanical and Interfacial Applications. Understanding Fast and Robust Thermo-osmotic Flows through Carbon Nanotube Membranes: Thermodynamics Meets Hydrodynamics. 2146 Concerted Metal Cation Desorption and Proton Transfer on Deprotonated Silica Surfaces. 2145 Theory of the Double Layer in Water-in-Salt Electrolytes. 2144 Combining Metadynamics and Integrated Tempering Sampling. Prediction of the Glass Transition Temperatures of Zeolitic Imidazolate Glasses through Topological Constraint Theory. 2142 Many-Body Effects Determine the Local Hydration Structure of Cs+ in Solution. 2141 Exfoliation of Two-Dimensional Materials: The Role of Entropy. 2140 Protein Short-Time Diffusion in a Naturally Crowded Environment. Revealing Transition States during the Hydration of Clay Minerals. Mechanism of Water Content on the Electrochemical Surface Area of the Catalyst Layer in the 2138 Proton Exchange Membrane Fuel Cell. Anisotropic Epitaxial Behavior in the Amorphous Phase-Mediated Hydroxyapatite Crystallization 2137 Process: A New Understanding of Orientation Control. 2136 Controlled Pore Generation in Single-Layer Graphene Oxide for Membrane Desalination. Universality Scaling, and Collapse in Supercritical Fluids. 2134 Sustaining Superheated Liquid within Hydrophilic Surface Texture.

2131 Capillary Stress and Structural Relaxation in Moist Granular Materials.

How Hydrophobic Hydration Destabilizes Surfactant Micelles at Low Temperature: A

2133 Surface Stresses and a Force Balance at a Contact Line.

Coarse-Grained Simulation Study.

2132

2130 Wetting Transition of Ionic Substrate by Modulating Surface Charge Distribution. 2129 Log-Rolling Block Copolymer Cylinders. 2128 Combs and Bottlebrushes in a Melt. Quantitative Comparison of Atomistic Simulations with Experiment for a Cross-Linked Epoxy: A 2127 Specific VolumeCooling Rate Analysis. 2126 Computer Simulations of Continuous 3D Printing. 2125 Energy Renormalization Method for the Coarse-Graining of Polymer Viscoelasticity. Structurally Tailored and Engineered Macromolecular (STEM) Gels as Soft Elastomers and 2124 Hard/Soft Interfaces. Decoding Liquid Crystal Oligomer Phase Transitions: Toward Molecularly Engineered Shape 2123 Changing Materials. Topological Effect on Effective Local Concentration and Dynamics in Linear/Linear, Ring/Ring, and 2122 Linear/Ring Miscible Polymer Blends. Tuning the Mechanical Properties of Metallopolymers via Ligand Interactions: A Combined Experimental and Theoretical Study. 2120 Defect-Free Carbon Nanotube Coils. 2119 High Strain Rate Tensile Testing of Silver Nanowires: Rate-Dependent Brittle-to-Ductile Transition. 2118 Nanodroplet-Mediated Assembly of Platinum Nanoparticle Rings in Solution. Metallic Nanoislands on Graphene as Highly Sensitive Transducers of Mechanical, Biological, and 2117 Optical Signals. 2116 Frictional Properties of Nanojunctions Including Atomically Thin Sheets. Phonons, Localization, and Thermal Conductivity of Diamond Nanothreads and Amorphous 2115 Graphene. Radiation-Induced Helium Nanobubbles Enhance Ductility in Submicron-Sized Single-Crystalline 2114 Copper. 2113 Liquid Sulfur Impregnation of Microporous Carbon Accelerated by Nanoscale Interfacial Effects.

- 2112 Grain-Size-Controlled Mechanical Properties of Polycrystalline Monolayer MoS2. 2111 Strain Modulation of Graphene by Nanoscale Substrate Curvatures: A Molecular View. 2110 Controlling Cargo Trafficking in Multicomponent Membranes. Enhanced Thermoelectric Properties in a New Silicon Crystal Si24 with Intrinsic Nanoscale Porous 2109 Structure. 2108 Multiscale Mechanics of Triply Periodic Minimal Surfaces of Three-Dimensional Graphene Foams. 2107 Self-Assembly of Quantum DotGold Heterodimer Nanocrystals with Orientational Order. 2106 Electrical Double Layer of Supported Atomically Thin Materials. Plasmon-Mediated Synthesis of Periodic Arrays of Gold Nanoplates Using Substrate-Immobilized 2105 Seeds Lined with Planar Defects. 2104 Unexpected Strong Thermally Induced Phonon Energy Shift for Mapping Local Temperature. 2103 Twists and the Electronic Structure of Graphitic Materials. 2102 Stochastic Stress Jumps Due to Soliton Dynamics in Two-Dimensional van der Waals Interfaces. Rational Construction of Porous MetalOrganic Frameworks for Uranium(VI) Extraction: The Strong 2101 Periodic Tendency with a Metal Node. Competing Dissolution Pathways and Ligand Passivation-Enhanced Interfacial Stability of Hybrid 2100 Perovskites with Liquid Water. Emulsion-Based RIR-MAPLE Deposition of Conjugated Polymers: Primary Solvent Effect and Its Implications on Organic Solar Cell Performance. Comparison of Methods for Determining the Mechanical Properties of Semiconducting Polymer Films for Stretchable Electronics.
- 2095 Thermal Transport in Supported Graphene Nanomesh.

Ultrafast Sodiation of Single-Crystalline Sn Anodes.

2096 Asymmetric Junctions Boost in-Plane Thermal Transport in Pillared Graphene.

2094	Enhanced Polymer Crystallinity in Mixed-Matrix Membranes Induced by MetalOrganic Framework Nanosheets for Efficient CO2 Capture.
2093	Atomistic Assessments of Lithium-Ion Conduction Behavior in GlassCeramic Lithium Thiophosphates.
2092	Bio-Inspired NanoVilli Chips for Enhanced Capture of Tumor-Derived Extracellular Vesicles: Toward Non-Invasive Detection of Gene Alterations in Non-Small Cell Lung Cancer.
2091	Integration of Fullerenes as Electron Acceptors in 3D Graphene Networks: Enhanced Charge Transfer and Stability through Molecular Design.
2090	Deformation-Controlled Design of Metallic Nanocomposites.
2089	Hierarchical TiO2:Cu2O Nanostructures for Gas/Vapor Sensing and CO2 Sequestration.
2088	Addition of Short Polymer Chains Mechanically Reinforces Glassy Poly(2-vinylpyridine)Silica Nanoparticle Nanocomposites.
2087	Structures of Partially Fluorinated Bottlebrush Polymers in Thin Films.
2086	Anomalous Vascular Dynamics of Nanoworms within Blood Flow.
2085	Combining Experiment and Theory To Unravel the Mechanism of Two-Electron Oxygen Reduction at a Selective and Active Co-catalyst.
2084	Neural-Network-Biased Genetic Algorithms for Materials Design: Evolutionary Algorithms That Learn.
2083	New Insights into Mossy Li Induced Anode Degradation and Its Formation Mechanism in LiS Batteries.
2082	Strain Effect in Bimetallic Electrocatalysts in the Hydrogen Evolution Reaction.
2081	Quantifying Single-Ion Transport in Percolated Ionic Aggregates of Polymer Melts.
2080	Molecular Simulations of Solute Transport in Polymer Melts.
2079	Influence of Dielectric Constant on Ionic Transport in Polyether-Based Electrolytes.
2078	Measurement of Cohesion and Adhesion of Semiconducting Polymers by Scratch Testing: Effect of Side-Chain Length and Degree of Polymerization.
2077	Diffusion in Lamellae, Cylinders, and Double Gyroid Block Copolymer Nanostructures.

- Effect of Polymer Polarity on Ion Transport: A Competition between Ion Aggregation and Polymer 2076 Segmental Dynamics. 2075 Phagocyte-Inspired Smart Microcapsules. 2074 . Influence of Host Polarity on Correlating Salt Concentration Molecular Weight, and Molar Conductivity in Polymer Electrolytes. 2072 Identifying Nonaffine Softening Modes in Glassy Polymer Networks: A Pathway to Chemical Design. 2071 Brush-Like Polymers and Entanglements: From Linear Chains to Filaments. Enhanced Dynamics of Confined Polymers near the Immiscible PolymerPolymer Interface: Neutron Reflectivity Studies. 2069 Low Energetic Disorder in Small-Molecule Non-Fullerene Electron Acceptors. 2068 Petascale Simulations of the Morphology and the Molecular Interface of Bulk Heterojunctions. Molecular Tuning of the Vibrational Thermal Transport Mechanisms in Fullerene Derivative 2067 Solutions. 2066 Compressible, Dense, Three-Dimensional Holey Graphene Monolithic Architecture. 2065 Bias-Controlled Optical Transitions in GaN/AlN Nanowire Heterostructures. 2064 Griffith Criterion for Nanoscale Stress Singularity in Brittle Silicon.
- Highly Porous Silicon Embedded in a Ceramic Matrix: A Stable High-Capacity Electrode for Li-Ion Batteries.
- Carbon Nanotube Dispersion in Solvents and Polymer Solutions: Mechanisms, Assembly, and Preferences.
- A Programmable DNA Origami Platform for Organizing Intrinsically Disordered Nucleoporins within Nanopore Confinement.
- 2060 Mimicking a Dogs Nose: Scrolling Graphene Nanosheets.
- 2059 Janus Segregation at the Carbon NanotubeCatalyst Interface.

Exclusively Proton Conductive Membranes Based on Reduced Graphene Oxide Polymer Composites. Composites. Composites. Composites. Composites. Composites. Continuous Curvature Change into Controllable and Responsive Onion-like Vesicles by Rigid SphereRod Amphiphiles. Continuous Curvature Change into Controllable and Responsive Onion-like Vesicles by Rigid SphereRod Amphiphiles. Polymides Containing Phosphaphenanthrene Skeleton: Gas-Transport Properties and Molecular Organic Simulations. Covalent and Selective Grafting of Polyethylene Clycol Brushes at the Surface of ZIF8 for the Processing of Membranes for Pervaporation. Covalent and Selective Grafting of Polyethylene Clycol Brushes at the Surface of ZIF8 for the Processing of Membranes for Pervaporation. Covalent and Selective Grafting of Polyethylene Clycol Brushes at the Surface of ZIF8 for the Processing of Membranes for Pervaporation. Low-Noise Nanopore Enables In-Situ and Label-Free Tracking of a Trigger-Induced DNA Molecular Machine at the Single-Molecular Level. Nature of the Active Sites for CO Reduction on Copper Nanoparticles; Suggestions for Optimizing Performance. Nature of the Active Sites for CO Reduction on Copper Nanoparticles; Suggestions for Optimizing Performance. Nature of the Active Sites for CO Reduction by Soluble Molecules. Nature of the Active Sites for Control of the Electrostatic Potential of Quantum Dots through the Formation of Interfacial ion Pairs. Nature of the Active Sites for Control of Structures in Ligand-Exchange Reaction. Nature of the Active Sites for Control of Metallacycle-linked Star Polymers Driven by Simple Phosphine Ulgand-Exchange Reaction. Nature of the Active Sites for Control of Metallacycle-linked Star Polymers Driven by Simple Phosphine Ulgand-Exchange Reaction. Nature of the Active Sites for Control of the Coexistence of Two Types of Local Structures in Liquid Water.	2058	Metal-Level Thermally Conductive yet Soft Graphene Thermal Interface Materials.
Supramolecular Metallocarbohydrates through Hierarchical Self-Assembly: The Balance between Metallacycles and Saccharides. Continuous Curvature Change into Controllable and Responsive Onion-like Vesicles by Rigid SphereRod Amphiphiles. Hierarchically Patterned Elastomeric and Thermoplastic Polymer Films through Nanoimprinting and Ultraviolet Light Exposure. Polymindes Containing Phosphaphenanthrene Skeleton: Gas-Transport Properties and Molecular Dynamics Simulations. Covalent and Selective Grafting of Polyethylene Glycol Brushes at the Surface of ZIF8 for the Processing of Membranes for Pervaporation. Low-Noise Nanopore Enables in-Situ and Label-Free Tracking of a Trigger-Induced DNA Molecular Machine at the Single-Molecular Level. Molecular Mechanism of Facilitated Dissociation of Fis Protein from DNA. Nature of the Active Sites for CO Reduction on Copper Nanoparticles; Suggestions for Optimizing Performance. Noncovalent Control of the Electrostatic Potential of Quantum Dots through the Formation of Interfacial Ion Pairs. Noncovalent Control of the Electrostatic Potential of Quantum Dots through the Formation of Interfacial Ion Pairs. Microscopic Origins of Poor Crystallinity in the Synthesis of Covalent Organic Framework COF5. Microscopic Origins of Poor Crystallinity in the Synthesis of Covalent Organic Framework COF5. Supramolecular Transformation of Metallacycle-linked Star Polymers Driven by Simple Phosphine Ligand-Exchange Reaction. DIPACT Edidence in the Scattering Function for the Coexistence of Two Types of Local Structures in	2057	
Hierarchically Patterned Elastomeric and Thermoplastic Polymer Films through Nanoimprinting and Ultraviolet Light Exposure. Polyminides Containing Phosphaphenanthrene Skeleton: Gas-Transport Properties and Molecular Dynamics Simulations. Covalent and Selective Grafting of Polyethylene Glycol Brushes at the Surface of ZIF8 for the Processing of Membranes for Pervaporation. Low-Noise Nanopore Enables In-Situ and Label-Free Tracking of a Trigger-Induced DNA Molecular Machine at the Single-Molecular Level. Machine at the Single-Molecular Level. Nature of the Active Sites for CO Reduction on Copper Nanoparticles; Suggestions for Optimizing Performance. Noncovalent Control of the Electrostatic Potential of Quantum Dots through the Formation of Interfacial Ion Pairs. Noncovalent Control of Homogeneous Ice Nucleation by Soluble Molecules. Microscopic Origins of Poor Crystallinity in the Synthesis of Covalent Organic Framework COFS. Microscopic Origins of Poor Crystallinity in the Synthesis of Covalent Organic Framework COFS. Supramolecular Transformation of Metallacycle-linked Star Polymers Driven by Simple Phosphine Ligand-Exchange Reaction. DNA Framework-Programmed Cell Capture via Topology-Engineered Receptor Ligand Interactions. DIrect Evidence in the Scattering Function for the Coexistence of Two Types of Local Structures in	2056	Supramolecular Metallocarbohydrates through Hierarchical Self-Assembly: The Balance between
Ultraviolet Light Exposure. 2053 Polyimides Containing Phosphaphenanthrene Skeleton: Gas-Transport Properties and Molecular Dynamics Simulations. 2052 Covalent and Selective Grafting of Polyethylene Glycol Brushes at the Surface of ZIF8 for the Processing of Membranes for Pervaporation. 2051 Low-Noise Nanopore Enables In-Situ and Label-Free Tracking of a Trigger-Induced DNA Molecular Machine at the Single-Molecular Level. 2050 Molecular Mechanism of Facilitated Dissociation of Fis Protein from DNA. 2049 Nature of the Active Sites for CO Reduction on Copper Nanoparticles; Suggestions for Optimizing Performance. 2048 Noncovalent Control of the Electrostatic Potential of Quantum Dots through the Formation of Interfacial Ion Pairs. 2047 Promotion of Homogeneous Ice Nucleation by Soluble Molecules. 2046 Microscopic Origins of Poor Crystallinity in the Synthesis of Covalent Organic Framework COF5. 2047 Supramolecular Transformation of Metallacycle-linked Star Polymers Driven by Simple Phosphine Ligand-Exchange Reaction. 2048 DNA Framework-Programmed Cell Capture via Topology-Engineered ReceptorLigand Interactions. 2049 DNA Framework-Programmed Cell Capture via Topology-Engineered ReceptorLigand Interactions.	2055	
Dynamics Simulations. Covalent and Selective Grafting of Polyethylene Glycol Brushes at the Surface of ZIF8 for the Processing of Membranes for Pervaporation. Low-Noise Nanopore Enables In-Situ and Label-Free Tracking of a Trigger-Induced DNA Molecular Machine at the Single-Molecular Level. Molecular Mechanism of Facilitated Dissociation of Fis Protein from DNA. Nature of the Active Sites for CO Reduction on Copper Nanoparticles; Suggestions for Optimizing Performance. Noncovalent Control of the Electrostatic Potential of Quantum Dots through the Formation of Interfacial Ion Pairs. Microscopic Origins of Poor Crystallinity in the Synthesis of Covalent Organic Framework COF5. Microscopic Origins of Poor Crystallinity in the Synthesis of Polymers Driven by Simple Phosphine Ligand-Exchange Reaction. Direct Evidence in the Scattering Function for the Coexistence of Two Types of Local Structures in	2054	
2052 Processing of Membranes for Pervaporation. 2053 Low-Noise Nanopore Enables In-Situ and Label-Free Tracking of a Trigger-Induced DNA Molecular Machine at the Single-Molecular Level. 2050 Molecular Mechanism of Facilitated Dissociation of Fis Protein from DNA. 2049 Nature of the Active Sites for CO Reduction on Copper Nanoparticles; Suggestions for Optimizing Performance. 2048 Noncovalent Control of the Electrostatic Potential of Quantum Dots through the Formation of Interfacial Ion Pairs. 2047 Promotion of Homogeneous Ice Nucleation by Soluble Molecules. 2048 Microscopic Origins of Poor Crystallinity in the Synthesis of Covalent Organic Framework COF5. 2049 Supramolecular Transformation of Metallacycle-linked Star Polymers Driven by Simple Phosphine Ligand-Exchange Reaction. 2040 DNA Framework-Programmed Cell Capture via Topology-Engineered Receptor Ligand Interactions. 2041 Direct Evidence in the Scattering Function for the Coexistence of Two Types of Local Structures in	2053	
Molecular Mechanism of Facilitated Dissociation of Fis Protein from DNA. Nature of the Active Sites for CO Reduction on Copper Nanoparticles; Suggestions for Optimizing Performance. Noncovalent Control of the Electrostatic Potential of Quantum Dots through the Formation of Interfacial Ion Pairs. Promotion of Homogeneous Ice Nucleation by Soluble Molecules. Microscopic Origins of Poor Crystallinity in the Synthesis of Covalent Organic Framework COF5. Supramolecular Transformation of Metallacycle-linked Star Polymers Driven by Simple Phosphine Ligand-Exchange Reaction. DIrect Evidence in the Scattering Function for the Coexistence of Two Types of Local Structures in	2052	
Nature of the Active Sites for CO Reduction on Copper Nanoparticles; Suggestions for Optimizing Performance. Noncovalent Control of the Electrostatic Potential of Quantum Dots through the Formation of Interfacial Ion Pairs. Promotion of Homogeneous Ice Nucleation by Soluble Molecules. Nicroscopic Origins of Poor Crystallinity in the Synthesis of Covalent Organic Framework COFS. Noncovalent Control of the Electrostatic Potential of Quantum Dots through the Formation of Interfacial Ion Pairs. Noncovalent Control of the Electrostatic Potential of Quantum Dots through the Formation of Interfacial Ion Pairs. Noncovalent Control of the Electrostatic Potential of Quantum Dots through the Formation of Interfacial Ion Pairs. Noncovalent Control of the Electrostatic Potential of Quantum Dots through the Formation of Interfacial Ion Pairs. Noncovalent Control of the Electrostatic Potential of Quantum Dots through the Formation of Interfacial Ion Pairs. Noncovalent Control of the Electrostatic Potential of Quantum Dots through the Formation of Interfacial Ion Pairs. Noncovalent Control of the Electrostatic Potential of Quantum Dots through the Formation of Interfacial Ion Pairs. Noncovalent Control of the Electrostatic Potential of Quantum Dots through the Formation of Ions Interfacial Ion Pairs. Noncovalent Control of the Electrostatic Potential of Quantum Dots through the Formation of Ions Interfacial Ions Ions Ions Ions Ions Ions Ions Ions	2051	
Performance. Noncovalent Control of the Electrostatic Potential of Quantum Dots through the Formation of Interfacial Ion Pairs. Promotion of Homogeneous Ice Nucleation by Soluble Molecules. Nicroscopic Origins of Poor Crystallinity in the Synthesis of Covalent Organic Framework COF5. Supramolecular Transformation of Metallacycle-linked Star Polymers Driven by Simple Phosphine Ligand-Exchange Reaction. NA Framework-Programmed Cell Capture via Topology-Engineered ReceptorLigand Interactions. Direct Evidence in the Scattering Function for the Coexistence of Two Types of Local Structures in	2050	Molecular Mechanism of Facilitated Dissociation of Fis Protein from DNA.
Interfacial Ion Pairs. 2047 Promotion of Homogeneous Ice Nucleation by Soluble Molecules. 2046 Microscopic Origins of Poor Crystallinity in the Synthesis of Covalent Organic Framework COF5. 2045 . 2044 Supramolecular Transformation of Metallacycle-linked Star Polymers Driven by Simple Phosphine Ligand-Exchange Reaction. 2043 . 2042 DNA Framework-Programmed Cell Capture via Topology-Engineered ReceptorLigand Interactions. Direct Evidence in the Scattering Function for the Coexistence of Two Types of Local Structures in	2049	
2046 Microscopic Origins of Poor Crystallinity in the Synthesis of Covalent Organic Framework COF5. 2045 . 2044 Supramolecular Transformation of Metallacycle-linked Star Polymers Driven by Simple Phosphine Ligand-Exchange Reaction. 2043 . 2042 DNA Framework-Programmed Cell Capture via Topology-Engineered ReceptorLigand Interactions. Direct Evidence in the Scattering Function for the Coexistence of Two Types of Local Structures in	2048	
2045 . 2044 Supramolecular Transformation of Metallacycle-linked Star Polymers Driven by Simple Phosphine Ligand-Exchange Reaction. 2043 . 2042 DNA Framework-Programmed Cell Capture via Topology-Engineered ReceptorLigand Interactions. Direct Evidence in the Scattering Function for the Coexistence of Two Types of Local Structures in	2047	Promotion of Homogeneous Ice Nucleation by Soluble Molecules.
Supramolecular Transformation of Metallacycle-linked Star Polymers Driven by Simple Phosphine Ligand-Exchange Reaction. 2043 DNA Framework-Programmed Cell Capture via Topology-Engineered ReceptorLigand Interactions. Direct Evidence in the Scattering Function for the Coexistence of Two Types of Local Structures in	2046	Microscopic Origins of Poor Crystallinity in the Synthesis of Covalent Organic Framework COF5.
Ligand-Exchange Reaction. 2043 . 2042 DNA Framework-Programmed Cell Capture via Topology-Engineered ReceptorLigand Interactions. Direct Evidence in the Scattering Function for the Coexistence of Two Types of Local Structures in	2045	
2042 DNA Framework-Programmed Cell Capture via Topology-Engineered ReceptorLigand Interactions. Direct Evidence in the Scattering Function for the Coexistence of Two Types of Local Structures in	2044	
Direct Evidence in the Scattering Function for the Coexistence of Two Types of Local Structures in	2043	
	2042	DNA Framework-Programmed Cell Capture via Topology-Engineered ReceptorLigand Interactions.
	2041	

2023

Clay.

Nanoarchitecture through Strained Molecules: Cubane-Derived Scaffolds and the Smallest Carbon 2040 Nanothreads. Unveiling the Active Structure of Single Nickel Atom Catalysis: Critical Roles of Charge Capacity and Hydrogen Bonding. Toward Atomistic Resolution Structure of Phosphatidylcholine Headgroup and Glycerol Backbone at Different Ambient Conditions. Parametrization of Chain Molecules in Dissipative Particle Dynamics. Three-Dimensional Non-Close-Packed Structures of Oppositely Charged Colloids Driven by pH 2036 Oscillation. 2035 Interplay of Nanoparticle Rigidity and Its Translocation Ability through Cell Membrane. 2034 Relating Molecular Morphology to Charge Mobility in Semicrystalline Conjugated Polymers. First-Principles Predictions of StructureFunction Relationships of Graphene-Supported Platinum 2033 Nanoclusters. Understanding Aqueous Dispersibility of Boron Nitride Nanosheets from 1H Solid State NMR and 2032 Reactive Molecular Dynamics. Helium and Argon Interactions with Gold Surfaces: Ab Initio-Assisted Determination of the HeAu 2031 Pairwise Potential and Its Application to Accommodation Coefficient Determination. Toward Reliable and Transferable Machine Learning Potentials: Uniform Training by Overcoming 2030 Sampling Bias. Effect of Core Morphology on the Structural Asymmetry of Alkanethiol Monolayer-Protected Gold 2029 Nanoparticles. Tunable Energy Barrier for Intercalation of a Carbon Nanotube into Graphene Nanosheets: A 2028 Molecular Dynamics Study of a Hybrid Self-Assembly. 2027 Connecting Theory with Experiment to Understand the Sintering Processes of Ag Nanoparticles. 2026 Iterative-Learning Strategy for the Development of Application-Specific Atomistic Force Fields. Comparison of Thermomechanical Properties for Weaved Polyethylene and Its Nanocomposite 2025 Based on the CNT Junction by Molecular Dynamics Simulation. 2024 Mechanical Properties and Failure Envelope of Kerogen Matrix by Molecular Dynamics Simulations.

Structural Implications of Interfacial Hydrogen Bonding in Hydrated Wyoming-Montmorillonite

2022 In Situ 3D Imag	ging of Catalysis Induced Strain in Gold Nanoparticles.	
2021 Virtual Screenii	ng for High Carrier Mobility in Organic Semiconductors.	
	of Structure and Dynamics in the Raman Spectrum of Liquid Water over the Full Temperature Range.	
2019 What Controls	the Limit of Supercooling and Superheating of Pinned Ice Surfaces?.	
2018 Widom Delta o	of Supercritical GasLiquid Coexistence.	О
2017 Collective Varia	ables from Local Fluctuations.	
2016 Realistic Atomi Dynamics.	istic Structure of Amorphous Silicon from Machine-Learning-Driven Molecular	
2015 The ClathrateW	Vater Interface Is Oleophilic.	
2014 Experimentally	y Validated Structures of Supported Metal Nanoclusters on MoS2.	
Charge Environ 2013 Computational	nment and Hydrogen Bond Dynamics in Binary Ionic Liquid Mixtures: A l Study.	
2012 Tunable Polaro	on Distortions Control the Extent of Halide Demixing in Lead Halide Perovskites.	
2011 Multi-ion Cond	luction in Li3OCl Glass Electrolytes.	
2010 Understanding and Transferab	Missing Entropy in Coarse-Grained Systems: Addressing Issues of Representability bility.	
	e yet Chemically Separate Reduction and Oxidation Sites in Double-Walled Photocatalytic Hydrogen Generation.	
Anomalies in Su Transformation	upercooled Water at 230 K Arise from a 1D Polymer to 2D Network Topological n.	
2007 Effect of Atom	ic Corrugation on Adhesion and Friction: A Model Study with Graphene Step Edges.	
2006 Amine Dynamic	cs in Diamine-Appended Mg2(dobpdc) MetalOrganic Frameworks.	
2005 Ensemble-Base	ed Molecular Simulation of Chemical Reactions under Vibrational Nonequilibrium.	

- Formation of Hollow Gold Nanocrystals by Nanosecond Laser Irradiation.

 Evidence of Facilitated Transport in Crowded Nanopores.

 Unraveling the Dynamics of Aminopolymer/Silica Composites.

 In-Depth Insights into the Key Steps of Delamination of Charged 2D Nanomaterials.

 Thermally Induced Structural Evolution of Silicon- and Oxygen-Containing Hydrogenated Amorphous Carbon: A Combined Spectroscopic and Molecular Dynamics Simulation Investigation.

 Distribution of Chains in Polymer Brushes Produced by a Grafting From Mechanism.

 Page Dynamics of Bottlebrush Networks.

1994 Supersoft and Hyperelastic Polymer Networks with Brushlike Strands.

Molecular Dynamics Simulation and PRISM Theory Study of Assembly in Solutions of Amphiphilic Bottlebrush Block Copolymers.

Electric-Field-Driven Trapping of Polyelectrolytes in Needle-like Backfolded States.

- 1991 Interphase Structures and Dynamics near Nanofiller Surfaces in Polymer Solutions.
- Modeling Polymer Glass Transition Properties from Empirical Monomer Data with the SAFT Mie Force Field.
- Modeling the Influence of Emergent and Self-Limiting Phase Separations among Nascent Oligomers on Polymer Sequences Formed during Irreversible Step-Growth Copolymerizations.
- 1988 Modeling Supramolecular Polymerization: The Role of Steric Effects and Hydrophobic Interactions.
- 1987 Optimization of the Thermoelectric Figure of Merit in Crystalline C60 with Intercalation Chemistry.

Bottom-up Design of Three-Dimensional Carbon-Honeycomb with Superb Specific Strength and 1986 High Thermal Conductivity. Cooperative Molecular Behavior Enhances the Thermal Conductance of Binary Self-Assembled Monolayer Junctions. 1984 Origin of Reversible Photoinduced Phase Separation in Hybrid Perovskites. Design of Heterogeneous Chalcogenide Nanostructures with Pressure-Tunable Gaps and without 1983 Electronic Trap States. 1982 Impact of Nanoporosity on Hydrocarbon Transport in Shales Organic Matter. Roll-to-Roll Nanoforming of Metals Using Laser-Induced Superplasticity. 1980 Nanoparticle Ligand Exchange and Its Effects at the NanoparticleCell Membrane Interface. 1979 . 1978 Strengthening Mechanism of a Single Precipitate in a Metallic Nanocube. How the Complementarity at Vicinal Steps Enables Growth of 2D Monocrystals. 1977 Quantum-Dot-Like States in Molybdenum Disulfide Nanostructures Due to the Interplay of Local Surface Wrinkling, Strain, and Dielectric Confinement. Fundamental Limits to the Electrochemical Impedance Stability of Dielectric Elastomers in Bioelectronics. 1974 Few-Wall Carbon Nanotube Coils. Enhanced Transport of Shape and Rigidity-Tuned Lactalbumin Nanotubes across Intestinal Mucus and Cellular Barriers. 1972 Tuning MetalOrganic Framework Nanocrystal Shape through Facet-Dependent Coordination. Fluorinated Copolymer Functionalized with Ethylene Oxide as Novel Water-Borne Binder for a 1971 High-Power Lithium Ion Battery: Synthesis, Mechanism, and Application. 1970 Mechanical Response of Nanocrystalline Ice-Contained Methane Hydrates: Key Role of Water Ice. Nitrogen-Doped Unusually Superwetting, Thermally Insulating and Elastic Graphene Aerogel for 1969 Efficient Solar Steam Generation.

1953

Giant Surface Conductivity Enhancement in a Carbon Nanotube Composite by Ultraviolet Light 1968 Exposure. pH-Switchable Stratification of Colloidal Coatings: Surfaces On Demand. Nanoscale StructureProperty Relationships of Polyacrylonitrile/CNT Composites as a Function of 1966 Polymer Crystallinity and CNT Diameter. Atomistic Insight into Ion Transport and Conductivity in Ga/Al-Substituted Li7La3Zr2O12 Solid 1965 Electrolytes. PhononGrain-Boundary-Interaction-Mediated Thermal Transport in Two-Dimensional 1964 Polycrystalline MoS2. Thermal Engineering of MetalOrganic Frameworks for Adsorption Applications: A Molecular Simulation Perspective. 1962 Nanoengineering Microstructure of Hybrid CSH/Silicene Gel. Ethene Dimerization on Zeolite-Hosted Ni Ions: Reversible Mobilization of the Active Site. What Can Infrared Spectra Tell Us about the Crystallinity of Nanosized Interstellar Silicate Dust 1960 Grains?. Uniaxial Extension of Surfactant Micelles: Counterion Mediated Chain Stiffening and a Mechanism 1959 of Rupture by Flow-Induced Energy Redistribution. Glass-Transition and Side-Chain Dynamics in Thin Films: Explaining Dissimilar Free Surface Effects 1958 for Polystyrene vs Poly(methyl methacrylate). 1957 Surface Stress and Surface Tension in Polymeric Networks. Glyco-Platelets with Controlled Morphologies via Crystallization-Driven Self-Assembly and Their Shape-Dependent Interplay with Macrophages. Self-Assembled Saccharide-Functionalized Amphiphilic Metallacycles as Biofilms Inhibitor via Sweet 1955 Talking. 1954 Metal Organic Frameworks for Xenon Storage Applications.

Patchy and Janus Nanoparticles by Self-Organization of Mixtures of Fluorinated and Hydrogenated

1951 Interlocking Friction Governs the Mechanical Fracture of Bilayer MoS2.

1952 Apparent Softening of Wet Graphene Membranes on a Microfluidic Platform.

Alkanethiolates on the Surface of a Gold Core.

1950	Atomic-Scale in Situ Observations of Crystallization and Restructuring Processes in Two-Dimensional MoS2 Films.	
1949	A Paper-Like Inorganic Thermal Interface Material Composed of Hierarchically Structured Graphene/Silicon Carbide Nanorods.	
1948	MetalOrganic Frameworks Invert Molecular Reactivity: Lewis Acidic Phosphonium Zwitterions Catalyze the Aldol-Tishchenko Reaction.	
1947	Explanation of Dramatic pH-Dependence of Hydrogen Binding on Noble Metal Electrode: Greatly Weakened Water Adsorption at High pH.	
1946	Could Mesophases Play a Role in the Nucleation and Polymorph Selection of Zeolites?.	
1945	Polymer Infiltration into MetalOrganic Frameworks in Mixed-Matrix Membranes Detected in Situ by NMR.	
1944	Photovoltaic Blend Microstructure for High Efficiency Post-Fullerene Solar Cells. To Tilt or Not To Tilt?.	
1943	Fluidic Multivalent Membrane Nanointerface Enables Synergetic Enrichment of Circulating Tumor Cells with High Efficiency and Viability.	
1942	Cytoprotective Self-assembled RGD Peptide Nanofilms for Surface Modification of Viable Mesenchymal Stem Cells.	
1941	Thermal Transport in Interpenetrated MetalOrganic Frameworks.	
1940		
1020		
1939	Characterizing Hydration Properties Based on the Orientational Structure of Interfacial Water Molecules.	
	Molecules.	
1938	Molecules. Ab Initio Derived Force Fields for Zeolitic Imidazolate Frameworks: MOF-FF for ZIFs. Enhanced Sampling of Transition States.	2
1938	Molecules. Ab Initio Derived Force Fields for Zeolitic Imidazolate Frameworks: MOF-FF for ZIFs. Enhanced Sampling of Transition States. Massively Parallel Molecular Dynamics Simulations for Many-Body Potentials. 1995, 408, 125	2
1938 1937 1936	Molecules. Ab Initio Derived Force Fields for Zeolitic Imidazolate Frameworks: MOF-FF for ZIFs. Enhanced Sampling of Transition States. Massively Parallel Molecular Dynamics Simulations for Many-Body Potentials. 1995, 408, 125 Structural and Mechanical Properties of a Simulated Nickel Nanophase. 1995, 400, 293	

1932 Parallel Simulations of Rapid Fracture. **1995**, 409, 311

1931 Crack Growth and Propagation in Metallic Alloys. 1995 , 409, 81	
1930 I/O limitations in parallel molecular dynamics. 1995 ,	
1929 Computational limits of classical molecular dynamics simulations. 1995 , 4, 361-364	73
1928 Porting of an empirical tight-binding Molecular Dynamics code on MIMD platforms. 1996 , 197-204	
1927 Domain decomposition for particle methods on the sphere. 1996 , 119-130	1
1926 Cracking a Tough NUT with a Big Computer. 1996 , 463, 187	
1925 Modelling of phenomena within catalyst particles. 1996 , 51, 1543-1567	36
1924 A new parallel method for molecular dynamics simulation of macromolecular systems. 1996 , 17, 326-337	94
O(N) tight-binding molecular dynamics on massively parallel computers: an orbital decomposition approach. 1996 , 94, 89-102	19
1922 Large-scale molecular dynamics simulations of fracture growth in alloys. 1996 , 37, 181-184	1
1921 Lightweight computational steering of very large scale molecular dynamics simulations. 1996 ,	21
1920 Design of a large scale discrete element soil model for high performance computing systems. 1996 ,	7
1919 Portrait of a crack: rapid fracture mechanics using parallel molecular dynamics. 1997 , 4, 66-77	16
The effect of attractions on the structure and thermodynamics of model polymer blends. 1997 , 107, 4024-4032	7
1917 Effect of inhomogeneities on dynamic crack growth in an elastic solid. 1997 , 5, 489-516	24
1916 IMD: A Software Package for Molecular Dynamics Studies on Parallel Computers. 1997 , 08, 1131-1140	237
1915 Comparing high-level and low-level implementations of a molecular dynamics algorithm.	1

1914 Molecular dynamic modeling of supercritical LOX evaporation. 1997,

1913	Massively parallel molecular dynamics simulations with EAM potentials. 1997 , 142, 9-21	38
1912	A domain decomposition parallel processing algorithm for molecular dynamics simulations of systems of arbitrary connectivity. 1997 , 103, 170-186	39
1911	Molecular modelling of polymers 17. Simulation and QSPR analyses of transport behavior in amorphous polymeric materials. 1997 , 7, 199-214	22
1910	A molecular dynamics investigation of rapid fracture mechanics. 1997 , 45, 1595-1619	98
1909	Instability dynamics in three-dimensional fracture: An atomistic simulation. 1997 , 45, 1461-1471	58
1908	Parallel short-range molecular dynamics using the ahta runtime system. 1997 , 102, 28-43	16
1907	Dynamic-domain-decomposition parallel molecular dynamics. 1997 , 102, 44-58	13
1906	Optimization techniques for parallel molecular dynamics using domain decomposition. 1998 , 113, 145-167	35
1905	Massively parallel dual control volume grand canonical molecular dynamics with LADERA II. Gradient driven diffusion through polymers. 1998 , 94, 673-683	43
1904	Development of a parallel molecular dynamics code on SIMD computers: Algorithm for use of pair list criterion. 1998 , 19, 685-694	4
1903	Molecular simulation of complex systems using massively parallel supercomputers. 1998 , 144, 331-342	1
1902	Classical molecular simulations of complex, industrially-important systems on the intel paragon. 1998 , 35, 73-84	3
1901	Ab initiodynamics of rapid fracture. 1998 , 6, 639-670	28
1900	The structure and thermodynamics of energetically and structurally asymmetric polymer blends. 1998 , 109, 806-814	8
1899	Performance analysis and optimization of a parallel carbon molecular dynamic code on a Cray T3E.	
1898	Massively parallel dual control volume grand canonical molecular dynamics with LADERA I. Gradient driven diffusion in Lennard-Jones fluids. 1998 , 94, 659-671	39
1897	Direct molecular simulation of gradient-driven diffusion. 1998 , 109, 6406-6414	68

1896 Chromosome structure predicted by a polymer model. 1998 , 57, 5888-5896	93
1895 Direct simulation of hydrodynamic relaxation in microchannels. 1998 , 109, 196-207	5
1894 Report on a Parallel Molecular Dynamics Implementation. 1998 , 12, 217-220	1
1893 Molecular dynamics using P-threads. 1998 , 878-880	
1892 Parallel Particle Simulations of Thin-Film Deposition. 1999 , 13, 16-32	6
1891 Molecular-dynamics study of ductile and brittle fracture in model noncrystalline solids. 1999 , 60, 7062-7070	156
1890 Large scale simulation of parallel molecular dynamics.	5
1889 Molecular dynamics algorithms for path integrals at constant pressure. 1999 , 110, 3275-3290	165
1888 Spatial correlations of mobility and immobility in a glass-forming Lennard-Jones liquid. 1999 , 60, 3107-19	425
1887 Molecular Dynamics Studies of Thermophysical Properties of Supercritical Ethylene. 1999 , 13, 351-354	8
Interactive Large-Scale Soil Modeling Using Distributed High Performance Computing Environments. 1999 , 13, 33-48	13
1885 Statistical models of brittle deformation Part I: introduction. 1999 , 15, 401-426	10
1884 Efficient parallel algorithms for molecular dynamics simulations. 1999 , 25, 217-230	30
$_{f 1883}$ Data-parallel support for numerical irregular problems. 1999 , 25, 1971-1994	5
NAMD2: Greater Scalability for Parallel Molecular Dynamics. <i>Journal of Computational Physics</i> , 1999 , 4.1	1965
Scalable molecular-dynamics, visualization, and data management algorithms for materials simulations. 1999 , 1, 39-47	21
Simulations of the Effect of Diblock Surfactant Spacer Molecules on Micelle Structure and Function. 1999 , 15, 7426-7431	9
Molecular Dynamics Simulation of Penetrant Diffusion in Amorphous Polypropylene: Diffusion Mechanisms and Simulation Size Effects. 1999 , 32, 5017-5028	78

1878	Large Slip Effect at a Nonwetting Fluid-Solid Interface. 1999 , 82, 4671-4674		628
1877	Large Scale Parallel Molecular Dynamics Simulations. 1999 , 231-280		
1876	A simple dynamic load-balancing scheme for parallel molecular dynamics simulation on distributed memory machines. 1999 , 260-269		1
1875	An XML-based component model for wrapping legacy codes as Java/CORBA components. 2000,		
1874	An Adaptive Load Balancing Method for Parallel Molecular Dynamics Simulations. <i>Journal of Computational Physics</i> , 2000 , 161, 250-263	4.1	27
1873	Parallel molecular dynamics using OpenMP on a shared memory machine. 2000 , 124, 49-59		15
1872	Computational chemistry on Fujitsu vectorparallel processors: Development and performance of applications software. 2000 , 26, 887-911		7
1871	Parallel constrained molecular dynamics. 2000 , 24, 393-405		
1870	Scalable Molecular Dynamics for Large Biomolecular Systems. 2000 , 8, 195-207		1
1869	Scalable Molecular Dynamics for Large Biomolecular Systems. 2000 ,		9
1868	A Wrapper Generator for Wrapping High Performance Legacy Codes as Java/CORBA Components. 2000 ,		7
1867	Constant pressure path integral molecular dynamics studies of quantum effects in the liquid state properties of n-alkanes. 2000 , 112, 870-880		19
1866	Structure of Supercritical Fluid Krypton at Small Scattering Angle Using Parallel Molecular Dynamics Simulation. 2000 , 23, 293-306		10
1865	Effects of dispersion forces on the structure and thermodynamics of fluid krypton. 2000 , 62, 3671-8		14
1864	Generative and Component-Based Software Engineering. 2000,		4
1863	Implementing and evaluating an efficient dynamic load-balancer for distributed molecular dynamics simulation.		5
1862	Molecular Dynamics Simulation of Reverse Micelles in Supercritical Carbon Dioxide. 2000 , 39, 4543-4554		37
1861	Characterizing the function of unstructured proteins: Simulations of charged polymers under confinement. 2001 , 115, 4909-4918		16

(2001-2001)

Effect of pressure, membrane thickness, and placement of control volumes on through thin silicalite membranes: A dual control volume grand canonical mole study. 2001 , 114, 7174-7181	
1859 Atomic and electronic structure of high-energy grain boundaries in silicon and	carbon. 2001 , 20, 351-362 18
Dynamics of Exchange at Gas-Zeolite Interfaces I: Pure Component n-Butane a 105, 5700-5712	nd Isobutane. 2001 ,
DESIGN OF A PARALLEL INTERCONNECT BASED ON COMMUNICATION PATTE CONSIDERATIONS. 2001 , 16, 243-271	RN
1856 6. Computational Approaches to Nanomineralogy. 2001 , 191-216	1
Application of Pfortran and Co-Array Fortran in the Parallelization of the GRON Dynamics Module. 2001 , 9, 61-68	AOS96 Molecular 4
1854 Discrete Element Modelling on a Cluster of Workstations. 2001 , 17, 1-15	10
An approach to simulate the motion of spherical and non-spherical fuel particle chambers. 2001 , 3, 231-266	es in combustion 208
1852 Wrapping MPI-based legacy codes as Java/CORBA components. 2001 , 18, 213-	223 11
$_{f 1}851$ Computational nanoscale plasticity simulations using embedded atom potential	als. 2001 , 37, 49-98 81
1850 Scalability and Performance of Two Large Linux Clusters. 2001 , 61, 1546-1569	6
1849 Granular flow down an inclined plane: Bagnold scaling and rheology. 2001 , 64,	051302 656
1848 MPiSIM: Massively parallel simulation tool for metallic system. 2001 , 8, 185-192	2 2
$_{ m 1847}$ Length scale and time scale effects on the plastic flow of fcc metals. 2001 , 49, $_{ m 1847}$	4363-4374 247
Vectorization of the generalized Born model for molecular dynamics on shared computers. 2001 , 549, 193-201	J-memory 6
1845 Computational Approaches to Nanomineralogy. 2001 , 44, 191-216	4
1844 Molecular Dynamics Simulation of Nanodroplet Evaporation. 2001 , 123, 741-74	18 45
$_{ m 1843}$ Demonstrating the scalability of a molecular dynamics application on a Petaflo	p computer. 2001 , 16

1842	Using AMDAHLE Law as a Metric to Drive Code Parallelization: Two Case Studies. 2001, 15, 75-80	2
1841	Self-consistent integral equation theory for polyolefins: Comparison to molecular dynamics simulations and x-ray scattering. 2001 , 114, 2847-2860	60
1840	Surface-tethered chains entangled in a polymer melt: effects on adhesion dynamics. 2001, 64, 050802	31
1839	Exploiting flexibly assignable work to improve load balance. 2002,	
1838	Distributed load balancing for molecular dynamics simulations.	2
1837	Friction between Alkylsilane Monolayers: Molecular Simulation of Ordered Monolayers. 2002 , 18, 8392-8399	100
1836	Large-Scale Simulation of Adhesion Dynamics for End-Grafted Polymers. 2002 , 35, 566-573	49
1835	Dynamic Load Balancing for Short-range Parallel Molecular Dynamics Simulations. 2002 , 79, 165-177	5
1834	Experiments with parallelizing a tribology application.	
1833	Damascene process simulation using molecular dynamics. 2002 , 92, 7062-7069	2
1833 1832	Damascene process simulation using molecular dynamics. 2002, 92, 7062-7069 A large scale molecular dynamics simulation code using the fast multipole algorithm (FMD): performance and application. 2002, 21, 89-99	10
	A large scale molecular dynamics simulation code using the fast multipole algorithm (FMD): performance and application. 2002 , 21, 89-99	
1832	A large scale molecular dynamics simulation code using the fast multipole algorithm (FMD): performance and application. 2002 , 21, 89-99	10
1832	A large scale molecular dynamics simulation code using the fast multipole algorithm (FMD): performance and application. 2002 , 21, 89-99 Location of phase equilibria by temperature-quench molecular dynamics simulations. 2002 , 203, 1-14	10
1832 1831 1830	A large scale molecular dynamics simulation code using the fast multipole algorithm (FMD): performance and application. 2002, 21, 89-99 Location of phase equilibria by temperature-quench molecular dynamics simulations. 2002, 203, 1-14 The new biology and computational statistical physics. 2002, 146, 77-83 A cell multipole based domain decomposition algorithm for molecular dynamics simulation of	10
1832 1831 1830	A large scale molecular dynamics simulation code using the fast multipole algorithm (FMD): performance and application. 2002, 21, 89-99 Location of phase equilibria by temperature-quench molecular dynamics simulations. 2002, 203, 1-14 The new biology and computational statistical physics. 2002, 146, 77-83 A cell multipole based domain decomposition algorithm for molecular dynamics simulation of systems of arbitrary shape. 2002, 144, 141-153 On the parallelization of molecular dynamics codes. 2002, 147, 711-715	10 37
1832 1831 1830 1829	A large scale molecular dynamics simulation code using the fast multipole algorithm (FMD): performance and application. 2002, 21, 89-99 Location of phase equilibria by temperature-quench molecular dynamics simulations. 2002, 203, 1-14 The new biology and computational statistical physics. 2002, 146, 77-83 A cell multipole based domain decomposition algorithm for molecular dynamics simulation of systems of arbitrary shape. 2002, 144, 141-153 On the parallelization of molecular dynamics codes. 2002, 147, 711-715	10 37 1 2

(2003-2003)

1824	flows. Journal of Computational Physics, 2003 , 191, 1-17 4.1	19
1823	Blue Matter, an application framework for molecular simulation on Blue Gene. 2003 , 63, 759-773	56
1822	Optimization techniques for parallel force-decomposition algorithm in molecular dynamic simulations. 2003 , 154, 121-130	10
1821	Molecular dynamics simulation on burst and arrest of stacking faults in nanocrystalline Cu under nanoindentation. 2003 , 14, 1208-1215	94
1820	Nonequilibrium molecular dynamics simulation of electro-osmotic flow in a charged nanopore. 2003 , 119, 7503-7511	55
1819	Improved United Atom Force Field for Poly(dimethylsiloxane). 2003 , 36, 2122-2129	51
1818	Molecular Modeling of Fluid-Phase Equilibria Using an Isotropic Multipolar Potential. 2003, 42, 4123-4131	28
1817	On the Calculation of Supercritical FluidBolid Equilibria by Molecular Simulation. 2003, 107, 1672-1678	22
1816	Molecular dynamics simulation of dark-adapted rhodopsin in an explicit membrane bilayer: coupling between local retinal and larger scale conformational change. 2003 , 333, 493-514	88
1815	Role of intramolecular energy on polyolefin miscibility: Isotactic polypropylene/polyethylene blends. 2003 , 118, 914-924	52
1814	Validity of effective medium theory for aluminium under tension. 2003 , 11, 127-136	15
1813	Confined granular packings: structure, stress, and forces. 2003 , 67, 041303	123
1812	Solute mobility and packing fraction: A new look at the Doolittle equation for the polymer glass transition. 2003 , 119, 9269-9273	15
1811	Scalability of a low-cost multi-Teraflop Linux cluster for high-end classical atomistic and quantum mechanical simulations.	1
1810	Spreading dynamics of polymer nanodroplets. 2003 , 68, 061603	91
1809	Interactions and structure of poly(dimethylsiloxane) at silicon dioxide surfaces: Electronic structure and molecular dynamics studies. 2003 , 118, 5132-5142	56
1808	Fracture behavior of Lennard-Jones glasses. 2003 , 68, 021802	12
1807	Simulation by Molecular Dynamics. 2003,	

Some observations on the mechanical properties of particulate-reinforced 6061 aluminium metal matrix composites. 2003 , 19, 218	2
Cluster-Based Parallel Simulation for Large Scale Molecular Dynamics in Microscale Thermophysics. 2004 , 200-211	1
Molecular dynamics simulations of palladium cluster growth on flat and rough graphite surfaces. 2004 , 28, 43-50	6
Comparison of random-walk density functional theory to simulation for bead-spring homopolymer melts. 2004 , 121, 2788-97	12
Anomalous mixing behavior of polyisobutylene/polypropylene blends: molecular dynamics simulation study. 2004 , 120, 8883-6	34
1801 A Parallel Engine for Graphical Interactive Molecular Dynamics Simulations.	1
1800 Spreading dynamics of polymer nanodroplets in cylindrical geometries. 2004 , 70, 011606	48
1799 Surface tension of quantum fluids from molecular simulations. 2004 , 120, 8707-15	9
1798 Time and length scales in supercooled liquids. 2004 , 69, 020201	187
1797 Oscillatory behavior of nanodroplets. 2004 , 70, 011505	12
Finite Size Effects in Determination of Thermal Conductivities: Comparing Molecular Dynamics Results With Simple Models. 2004 , 126, 577	81
1795 Parallel implementation of the treecode Ewald method.	
1794 High Performance Scientific and Engineering Computing. 2004 ,	
1793 Characterizing a new class of threads in scientific applications for high end supercomputers. 2004 ,	7
Discrete element simulations of stress distributions in silos: crossover from two to three dimensions. 2004 , 139, 233-239	49
1791 Atomistic simulations of biologically realistic transmembrane potential gradients. 2004 , 121, 10847-	51 133
1790 Experiments with Parallelizing Tribology Simulations. 2004 , 28, 323-343	2
1789 Parallelizing of macro-scale pseudo-particle modeling for particle-fluid systems. 2004 , 47, 434-442	12

(2004-2004)

1788	Multi-scale modeling of polyimides. 2004 , 45, 7001-7010	26
1787	A Note on N-Body Computations with Cutoffs. 2004 , 37, 295	36
1786	Conformational sampling and dynamics of membrane proteins from 10-nanosecond computer simulations. 2004 , 57, 783-91	86
1785	Effect of end-tethered polymers on surface adhesion of glassy polymers. 2004 , 42, 199-208	69
1784	Fracture behavior of triglyceride-based adhesives. 2004 , 42, 3333-3343	22
1783	Parallel programming library for molecular dynamics simulations. 2004 , 96, 530-536	6
1782	Partial rigid-body dynamics in NPT, NPAT and NPgammaT ensembles for proteins and membranes. 2004 , 25, 529-41	125
1781	Hildebrand and Hansen solubility parameters from molecular dynamics with applications to electronic nose polymer sensors. 2004 , 25, 1814-26	261
1780	Industrial property prediction using Towhee and LAMMPS. 2004 , 217, 105-110	50
1779	Effects of chain stiffness and penetrant size on penetrant diffusion in simple polymers: deduced relations from simulation and PRISM theory. 2004 , 45, 3923-3932	17
1778	Simulation of hydrated Li+-, Na+- and K+-montmorillonite/polymer nanocomposites using large-scale molecular dynamics. 2004 , 389, 261-267	42
1777	An adaptive algorithm selection framework.	3
1776	General relationships between the mobility of a chain fluid and various computed scalar metrics. 2004 , 121, 10291-8	28
1775	A comparison of 4X InfiniBand and Quadrics Elan-4 technologies.	12
1774	Interdiffusion of solvent into glassy polymer films: a molecular dynamics study. 2004, 121, 7513-9	21
1773	Mapping molecular models to continuum theories for partially miscible fluids. 2004 , 69, 021505	19
1772	Nanophase-Segregation and Transport in Nafion 117 from Molecular Dynamics Simulations: Effect of Monomeric Sequence. 2004 , 108, 3149-3157	375
1771	Effect of Strain History on Stress and Permanent Set in Cross-Linking Networks: A Molecular Dynamics Study. 2004 , 37, 5468-5473	54

1770	Mechanically Controlled, Seeded Formation of a Nanoscale Metastable Phase in Ionic Compounds. 2004 , 4, 1769-1773		1
1769	Morphology of Evaporated Multiblock Copolymer Membranes Studied by Molecular Dynamics Simulations. 2004 , 37, 9132-9138		20
1768	Frictional dynamics of fluorine-terminated alkanethiol self-assembled monolayers. 2004 , 20, 10007-14		28
1767	Molecular dynamics simulation of solvent-polymer interdiffusion: Fickian diffusion. 2004 , 120, 2989-95		56
1766	Multiscale modelling of nanostructures. 2004 , 16, R1537-R1576		79
1765	Molecular Dynamics Study of the Evaporation Process in Polymer Films. 2004 , 37, 4333-4335		44
1764	Atomistic Simulations of End-Linked Poly(dimethylsiloxane) Networks: Structure and Relaxation. 2004 , 37, 3857-3864		108
1763	Molecular Dynamics Study of a Surfactant-Mediated DecanelWater Interface: Effect of Molecular Architecture of Alkyl Benzene Sulfonate. 2004 , 108, 12130-12140		187
1762	Molecular dynamics simulations of electrostatic layer-by-layer self-assembly. 2004 , 93, 037801		45
1761	Chapter 17 The Challenges in Developing Molecular Simulations of Fluid Properties for Industrial Applications. 2005 , 239-244		
1760	Parallel short range molecular dynamics simulations on computer clusters: Performance evaluation and modeling. 2005 , 42, 783-798		1
1759	Massively parallel implementation of a fast multipole method for distributed memory machines. 2005 , 65, 870-881		31
1758	Performance optimization of irregular codes based on the combination of reordering and blocking techniques. 2005 , 31, 858-876		14
1757	Revisiting and parallelizing SHAKE. <i>Journal of Computational Physics</i> , 2005 , 209, 193-206 4	1	55
1756	Disorder effects on the strain response of model polymer networks. 2005 , 46, 4283-4295		40
1755	The structure of poly(ethylene oxide) liquids: comparison of integral equation theory with molecular dynamics simulations and neutron scattering. 2005 , 46, 6500-6506		14
1754	Molecular dynamics simulations of nanoindentation of 虧iC with diamond indenter. 2005 , 117, 235-240		42
1753	Parallel implementation of macro-scale pseudo-particle simulation for particle \mathbf{f} uid systems. 2005 , 29, 1543-1553		11

Parallel implementation of molecular dynamics simulation for short-ranged interaction. 2005 , 170, 175-18	35 2
1751 Faster neighbour list generation using a novel lattice vector representation. 2005 , 170, 31-41	13
1750 Surface wetting of liquid nanodroplets: droplet-size effects. 2005 , 95, 107801	46
Molecular dynamics simulation of thermal and mechanical properties of polyimidellarbon-nanotube composites. 2005 , 13, 493-507	58
1748 Shape memory and pseudoelasticity in metal nanowires. 2005 , 95, 255504	257
1747 OOPSE: an object-oriented parallel simulation engine for molecular dynamics. 2005 , 26, 252-71	35
A fast, scalable method for the parallel evaluation of distance-limited pairwise particle interactions. 2005 , 26, 1318-28	150
1745 An atomistic investigation of elastic and plastic properties of Au nanowires. 2005 , 57, 62-66	59
1744 Frictional dynamics of perfluorinated self-assembled monolayers on amorphous SiO2. 2005 , 19, 93-98	64
Feature Activated Molecular Dynamics: Parallelization and Application to Systems with Globally Varying Mechanical Fields. 2005 , 12, 17-34	1
Control of silicate nanocomposite morphology in binary fluids: Coarse-grained molecular dynamics simulations. 2005 , 43, 1014-1024	14
1741 Multi-scale Rule-of-Mixtures Model of Carbon Nanotube/Carbon Fiber/Epoxy Lamina. 2005 , 887, 1	2
1740 Recent Advances in Parallel Virtual Machine and Message Passing Interface. 2005 ,	O
Improvement of the Koradi parallel algorithm for molecular dynamics and application to the economic organization and optimization of recycling costs of waste electrical and electronic equipment. 2005 , 71, 845-851	4
1738 The implications of working set analysis on supercomputing memory hierarchy design. 2005 ,	13
1737 Influence of thermodynamic state on nanojet break-up. 2005 , 16, 2838-2845	14
1736 A genetic algorithm for energy minimization in bio-molecular systems.	2
1735 A new dynamical domain decomposition method for parallel molecular dynamics simulation. 2005 ,	13

1734	Phase change of a confined subcooled simple liquid in a nanoscale cavity. 2005 , 71, 041602	11
1733	New theoretical insight into the interactions and properties of formic acid: development of a quantum-based pair potential for formic acid. 2005 , 123, 144702	29
1732	Comparison of density functional theory and simulation of fluid bilayers. 2005 , 72, 041924	16
1731	Temperature-quench Molecular Dynamics Simulations for Fluid Phase Equilibria. 2005 , 31, 33-43	25
1730	Phase Transition of Argon in a Nanocavity. 2005 , 25	
1729	Molecular dynamics simulations of layer-by-layer assembly of polyelectrolytes at charged surfaces: effects of chain degree of polymerization and fraction of charged monomers. 2005 , 21, 6113-22	49
1728	Molecular dynamics simulations of polyelectrolyte multilayering on a charged particle. 2005 , 21, 1118-25	27
1727	Polymer Melt near a Solid Surface: A Molecular Dynamics Study of Chain Conformations and Desorption Dynamics. 2005 , 38, 571-580	53
1726	A preliminary analysis of the MPI queue characterisitics of several applications.	15
1725	Improving load balance with flexibly assignable tasks. 2005 , 16, 956-965	6
1724	Parallel molecular dynamics simulation in NPT ensemble and its application to general anesthesia. 2005 ,	
1724 1723	· · · · · · · · · · · · · · · · · · ·	36
	Healing Surface Defects with Nanoparticle-Filled Polymer Coatings: Effect of Particle Geometry. 2005, 38, 10138-10147	36
1723	2005, Healing Surface Defects with Nanoparticle-Filled Polymer Coatings: Effect of Particle Geometry. 2005, 38, 10138-10147	
1723 1722	Healing Surface Defects with Nanoparticle-Filled Polymer Coatings: Effect of Particle Geometry. 2005, 38, 10138-10147 A new technique to reduce false sharing in parallel irregular codes based on distance functions. Diverse spreading behavior of binary polymer nanodroplets. 2005, 21, 7959-63	2
1723 1722 1721	Healing Surface Defects with Nanoparticle-Filled Polymer Coatings: Effect of Particle Geometry. 2005, 38, 10138-10147 A new technique to reduce false sharing in parallel irregular codes based on distance functions. Diverse spreading behavior of binary polymer nanodroplets. 2005, 21, 7959-63	2
1723 1722 1721 1720	Healing Surface Defects with Nanoparticle-Filled Polymer Coatings: Effect of Particle Geometry. 2005, 38, 10138-10147 A new technique to reduce false sharing in parallel irregular codes based on distance functions. Diverse spreading behavior of binary polymer nanodroplets. 2005, 21, 7959-63 Modeling inelasticity and failure in gold nanowires. 2005, 72, A new parallel environment for interactive simulations implementing safe multithreading with MPI.	2 8 202

(2006-2005)

1716	Interlayer Structure and Bonding in Nonswelling Primary Amine Intercalated Clays. 2005 , 38, 6189-6200	66
1715	Nanophase segregation and water dynamics in the dendrion diblock copolymer formed from the FrEhet polyaryl ethereal dendrimer and linear PTFE. 2005 , 109, 10154-67	55
1714	Hierarchical Modeling of the Dynamics of Polymers with a Nonlinear Molecular Architecture: Calculation of Branch Point Friction and Chain Reptation Time of H-Shaped Polyethylene Melts from Long Molecular Dynamics Simulations. 2005 , 38, 8583-8596	52
1713	Extrapolation of Rheological Properties for Lubricant Components with StokesEinstein Relationships. 2005 , 44, 5828-5835	10
1712	Molecular Dynamics Simulations of Polyampholyte P olyelectrolyte Complexes in Solutions. 2005 , 38, 5300-5312	37
1711	Density Functional Theory and Molecular Dynamics Simulation of Poly(dimethylsiloxane) Melts near Silica Surfaces. 2005 , 38, 8562-8573	7
1710	Detailed Atomistic Molecular Dynamics Simulation of cis-1,4-Poly(butadiene). 2005, 38, 1478-1492	104
1709	Orientational dynamics and dye-DNA interactions in a dye-labeled DNA aptamer. 2005 , 88, 3455-65	87
1708	Solvent evaporation and interdiffusion in polymer films. 2005 , 17, S4119-S4132	36
1707	PROPERTIES OF TRIGLYCERIDE-BASED THERMOSETS. 2005 , 202-255	8
1706	Structures and properties of self-assembled monolayers of bistable [2]rotaxanes on Au (111) surfaces from molecular dynamics simulations validated with experiment. 2005 , 127, 1563-75	185
1705	Mechanical Properties of Nanostructured Materials Determined Through Molecular Modeling Techniques. 2005 ,	2
1704		28
1703	Molecular dynamics simulation of uranyl(VI) adsorption equilibria onto an external montmorillonite surface. 2005 , 7, 3580-6	118
1702	Tribological properties of alkylsilane self-assembled monolayers. 2005 , 21, 11744-8	33
1701	Molecular dynamics simulation of amphiphilic bistable [2]rotaxane langmuir monolayers at the air/water interface. 2005 , 127, 14804-16	90
1700	Slip behavior in liquid films on surfaces of patterned wettability: comparison between continuum and molecular dynamics simulations. 2005 , 71, 041608	204
1699	Permanent Set of Cross-Linking Networks: 'Comparison of Theory with Molecular Dynamics Simulations. 2006 , 39, 5521-5530	43

1698 Langevin Dynamics Study of Polymer Translocation through a Nanopore. 2007 , 159-164	2
1697 Scalable Algorithms for Molecular Dynamics Simulations on Commodity Clusters. 2006 ,	469
General continuum boundary conditions for miscible binary fluids from molecular dynamics simulations. 2006 , 125, 214102	18
1695 Characterization of Scientific Workloads on Systems with Multi-Core Processors. 2006 ,	59
On the application of computer simulation techniques to anionic and cationic clays: A materials chemistry perspective. 2006 , 16, 708-723	119
1693 Atomistic simulations of langmuir monolayer collapse. 2006 , 22, 10016-24	32
Molecular dynamicsScalable algorithms for molecular dynamics simulations on commodity clusters. 2006 ,	578
Investigation of Aromatic/Aliphatic Polyimides as Dispersants for Single Wall Carbon Nanotubes. 2006 , 39, 1731-1739	89
1690 Novel Shape Memory of Metal Nanowires Through Reversible Lattice Reorientations. 2006 ,	
1689 Molecular studies of the structural properties of hydrogen gas in bulk water. 2006 , 32, 269-278	19
1688 . 2006 , 8, 16-25	
$_{ m 1687}$ High performance multiscale simulation or crack propagation.	5
1686 Nature designs tough collagen: explaining the nanostructure of collagen fibrils. 2006 , 103, 12285-90	538
1685 Early evaluation of the Cray XT3. 2006 ,	17
1684 . 2006 ,	2
$_{f 1683}$ Lessons learned building a general purpose cluster for space mission applications.	1
Architectures and APIs: Assessing Requirements for Delivering FPGA Performance to Applications. 2006 ,	8
Moving dislocations in disordered alloys: Connecting continuum and discrete models with atomistic simulations. 2006 , 74,	69

(2006-2006)

1680	2006 , 125, 014504	39
1679	Salt permeation and exclusion in hydroxylated and functionalized silica pores. 2006 , 96, 095504	65
1678	The midpoint method for parallelization of particle simulations. 2006 , 124, 184109	92
1677	Density functional theory and DFT+U study of transition metal porphines adsorbed on Au(111) surfaces and effects of applied electric fields. 2006 , 128, 3659-68	90
1676	Geometric effects on the inelastic deformation of metal nanowires. 2006 , 89, 181916	44
1675	Water structure and aqueous uranyl(VI) adsorption equilibria onto external surfaces of beidellite, montmorillonite, and pyrophyllite: results from molecular simulations. 2006 , 40, 3865-71	118
1674	Modeling of Interface Behavior in Carbon Nanotube Composites. 2006,	1
1673	Parallelization Algorithms for Three-Body Interactions in Molecular Dynamics Simulation. 2006 , 374-382	1
1672	Atomistic and continuum modeling of mechanical properties of collagen: Elasticity, fracture, and self-assembly. 2006 , 21, 1947-1961	217
1671	Structures and properties of Newton black films characterized using molecular dynamics simulations. 2006 , 110, 7992-8001	91
1670	Structure of Strongly Charged Polyelectrolyte Solutions. 2006 , 39, 8467-8472	3
1669	Fast multipole methods for particle dynamics. 2006 , 32, 775-790	21
1668	Liquid nanodroplets spreading on chemically patterned surfaces. 2006 , 22, 4745-9	25
1667	Loop-Level Profiling and Analysis of DoD Applications Using TAU. 2006,	O
1666	Molecular dynamics simulations of ordering of poly(dimethylsiloxane) under uniaxial stress. 2006 , 110, 3588-94	16
1665	Effect of Terminal Group Modification on the Solution Properties of Dendrimers: A Molecular Dynamics Simulation Study. 2006 , 39, 4247-4255	32
1664	Intercalation and in situ polymerization of poly(alkylene oxide) derivatives within M+-montmorillonite (M = Li, Na, K). 2006 , 16, 1082	42
1663	A thermodynamic understanding of clay-swelling inhibition of interlayer potassium ion. 2006 , 70, A365	3

1662	Vibrational spectra of methane clathrate hydrates from molecular dynamics simulation. 2006 , 110, 6428-31	45
1661	Momentum Transfer Between Polydisperse Particles in Dense Granular Flow. 2006 , 128, 62-68	7
1660	Atomistic Molecular Dynamics simulation of short@hain branched polyethylene melts. 2006, 22, 333-357	
1659	Detailed Atomistic Simulation of the Barrier Properties of Linear and Short©hain Branched Polyethylene Melts Through a Hierarchical Modeling Approach. 2006 , 201-239	
1658	Advanced Monte Carlo Methods for the atomistic simulation of polymers with a linear or a non-linear molecular architecture. 2006 , 31-67	2
1657	Computational challenges for modeling and simulating biomacromolecular assemblies. 2006 , 46, 311-315	
1656	Large-scale simulations of the ribosome: a new landmark in computational biology. 2006 , 46, 334-342	11
1655	Characterizing High-Energy-Density Propellants for Space Propulsion Applications. 2006,	3
1654	How a small change in retinal leads to G-protein activation: initial events suggested by molecular dynamics calculations. 2007 , 66, 559-74	20
1653	Computing the mobility of grain boundaries. 2006 , 5, 124-7	197
1653 1652		197 79
1652		
1652	On the thermomechanical deformation of silver shape memory nanowires. 2006 , 54, 2645-2654	79
1652 1651	On the thermomechanical deformation of silver shape memory nanowires. 2006 , 54, 2645-2654 ESPResSolin extensible simulation package for research on soft matter systems. 2006 , 174, 704-727 A parallel molecular dynamics simulation scheme for a molecular system with bond constraints in	79 544
1652 1651 1650 1649	On the thermomechanical deformation of silver shape memory nanowires. 2006, 54, 2645-2654 ESPResSoln extensible simulation package for research on soft matter systems. 2006, 174, 704-727 A parallel molecular dynamics simulation scheme for a molecular system with bond constraints in NPT ensemble. 2006, 174, 263-269 Evaluation of momentum conservation influence in non-equilibrium molecular dynamics methods	79 544 8
1652 1651 1650 1649	On the thermomechanical deformation of silver shape memory nanowires. 2006, 54, 2645-2654 ESPResSoln extensible simulation package for research on soft matter systems. 2006, 174, 704-727 A parallel molecular dynamics simulation scheme for a molecular system with bond constraints in NPT ensemble. 2006, 174, 263-269 Evaluation of momentum conservation influence in non-equilibrium molecular dynamics methods to compute thermal conductivity. 2006, 373, 291-296	79 544 8 42
1652 1651 1650 1649 1648	On the thermomechanical deformation of silver shape memory nanowires. 2006, 54, 2645-2654 ESPResSoBn extensible simulation package for research on soft matter systems. 2006, 174, 704-727 A parallel molecular dynamics simulation scheme for a molecular system with bond constraints in NPT ensemble. 2006, 174, 263-269 Evaluation of momentum conservation influence in non-equilibrium molecular dynamics methods to compute thermal conductivity. 2006, 373, 291-296 Deformation of FCC nanowires by twinning and slip. 2006, 54, 1862-1881 Multiscale diffusion Monte Carlo simulation of epitaxial growth. <i>Journal of Computational Physics</i> ,	79 544 8 42 259

(2006-2006)

1644	Stress-Induced Martensitic Phase Transformation in Intermetallic Nickel Aluminum Nanowires. 2006 , 6, 958-962	92
1643	Atomistic simulations reveal shape memory of fcc metal nanowires. 2006 , 73,	136
1642	An efficient parallelization scheme for molecular dynamics simulations with many-body, flexible, polarizable empirical potentials: application to water. 2006 , 117, 73-84	7
1641	Modeling of interfacial modification effects on thermal conductivity of carbon nanotube composites. 2006 , 47, 5990-5996	185
1640	A general purpose parallel molecular dynamics simulation program. 2006 , 174, 560-568	15
1639	Modified force decomposition algorithms for calculating three-body interactions via molecular dynamics. 2006 , 175, 683-691	6
1638	Parallelization and performance tuning of molecular dynamics code with OpenMP. 2006 , 13, 260-264	3
1637	Stable nanobridge formation in <110> gold nanowires under tensile deformation. 2006 , 54, 1127-1132	38
1636	A thermodynamic understanding of clay-swelling inhibition by potassium ions. 2006 , 45, 6300-3	104
1635	Linear and Nonlinear Viscoelasticity of a Model Unentangled Polymer Melt: Molecular Dynamics and Rouse Modes Analysis. 2006 , 15, 252-262	52
1634	Temperature and Pressure Effects on Local Structure and Chain Packing in cis-1,4-Polybutadiene from Detailed Molecular Dynamics Simulations. 2006 , 15, 381-393	20
1633	A Thermodynamic Understanding of Clay-Swelling Inhibition by Potassium Ions. 2006 , 118, 6448-6451	5
1632	A Cyclic Force Decomposition Algorithm for Parallelising Three-Body Interactions in Molecular Dynamics Simulations. 2006 ,	1
1631	Mesoscale modeling of mechanics of carbon nanotubes: Self-assembly, self-folding, and fracture. 2006 , 21, 2855-2869	142
1630	Atomic Investigation of Al/Ni(001) by Molecular Dynamics Simulation. 2006 , 45, 99-101	7
1629	Performance characterization of molecular dynamics techniques for biomolecular simulations. 2006 ,	8
1628	Big fast crowds on PS3. 2006 ,	60
1627	Capillary waves at the liquid-vapor interface and the surface tension of water. 2006 , 125, 014702	142

1626	Biomolecular simulations on petascale: promises and challenges. 2006 , 46, 327-333	7
1625	Parallel Computation of Large-Scale Molecular Dynamics Simulations. 2006 , 326-328, 341-344	1
1624	Surface identification, meshing and analysis during large molecular dynamics simulations. 2006 , 14, 229-251	7
1623	Entropic Elasticity Controls Nanomechanics of Single Tropocollagen Molecules. 2006 , 975, 1	
1622	Simulating nanoscale dielectric response. 2006 , 96, 230603	35
1621	Boundary slip and wetting properties of interfaces: correlation of the contact angle with the slip length. 2006 , 124, 204701	111
1620	Atomistic simulations of the mechanical behavior of fivefold twinned nanowires. 2006 , 74,	85
1619	Salt-induced collapse and reexpansion of highly charged flexible polyelectrolytes. 2006 , 97, 148301	154
1618	Contact of single asperities with varying adhesion: comparing continuum mechanics to atomistic simulations. 2006 , 74, 026111	118
1617	Atomistic molecular dynamics simulation of the temperature and pressure dependences of local and terminal relaxations in cis-1,4-polybutadiene. 2006 , 124, 084906	33
1616	Liquid friction on charged surfaces: from hydrodynamic slippage to electrokinetics. 2006 , 125, 204716	144
1615	Designing synthetic vesicles that engulf nanoscopic particles. 2007 , 127, 084703	125
1614	Adaptive Load-Balancing for Force-Decomposition Based 3-Body Molecular Dynamics Simulations in A Heterogeneous Distributed Environment with Variable Number of Processors. 2007 ,	O
1613	Zero-copy protocol for MPI using infiniband unreliable datagram. 2007,	8
1612	. 2007,	4
1611	Structures and energies of B asymmetric tilt grain boundaries in copper and aluminium. 2007 , 87, 3147-3173	185
1610	Approximate solutions for the generalized KdV B urgers' equation by He's variational iteration method. 2007 , 76, 161-164	23
1609	SIZE-DEPENDENT ELASTIC PROPERTIES OF NI NANOFILMS BY MOLECULAR DYNAMICS SIMULATION. 2007 , 14, 661-665	17

1608 Molecular flexibility effects upon liquid dynamics. 2007 , 126, 184904	10
1607 Rotational relaxation in simple chain models. 2007 , 127, 214902	10
1606 Decoupling of exchange and persistence times in atomistic models of glass formers. 2007 , 127, 211	101 72
Using the GA and TAO toolkits for solving large-scale optimization problems on parallel computers. 2007 , 33, 11	. 2
Performance Analysis and Evaluation of Mellanox ConnectX InfiniBand Architecture with Multi-Core Platforms. 2007 ,	16
Activation volume and incipient plastic deformation of uniaxially-loaded gold nanowires at very high strain rates. 2007 , 18, 455702	7
MD Simulation of Effect of Crystal Orientation and Cutting Direction on Nanometric Cutting Using AFM Pin Tool. 2007 , 20, 619-624	4
Molecular dynamics study of equilibrium concentration profiles and the gradient energy coefficient in Cu-Pb nanodroplets. 2007 , 76,	t 15
1600 Surface tension of normal and branched alkanes. 2007 , 105, 3155-3163	39
1599 Spontaneous reorientation of bimetal multilayer nanowires. 2007 , 91, 253114	14
Spontaneous reorientation of bimetal multilayer nanowires. 2007 , 91, 253114 Tension-compression asymmetry in homogeneous dislocation nucleation in single crystal copper. 2007 , 90, 121916	14 56
Tension-compression asymmetry in homogeneous dislocation nucleation in single crystal copper.	
Tension-compression asymmetry in homogeneous dislocation nucleation in single crystal copper. 2007 , 90, 121916	56 3
Tension-compression asymmetry in homogeneous dislocation nucleation in single crystal copper. 2007, 90, 121916 Molecular simulations of DNA transport in solution. 2007, 33, 399-403	56 3
Tension-compression asymmetry in homogeneous dislocation nucleation in single crystal copper. 2007, 90, 121916 Molecular simulations of DNA transport in solution. 2007, 33, 399-403 TensionDompression asymmetry and size effects in nanocrystalline Ni nanowires. 2007, 87, 2233-22 Molecular dynamics simulations of coherent optical photon emission from shock waves in crystals.	56 3 44 22
Tension-compression asymmetry in homogeneous dislocation nucleation in single crystal copper. 2007, 90, 121916 Molecular simulations of DNA transport in solution. 2007, 33, 399-403 TensionBompression asymmetry and size effects in nanocrystalline Ni nanowires. 2007, 87, 2233-22 Molecular dynamics simulations of coherent optical photon emission from shock waves in crystals. 2007, 75,	56 3 244 22
Tension-compression asymmetry in homogeneous dislocation nucleation in single crystal copper. 2007, 90, 121916 Molecular simulations of DNA transport in solution. 2007, 33, 399-403 TensionBompression asymmetry and size effects in nanocrystalline Ni nanowires. 2007, 87, 2233-22 Molecular dynamics simulations of coherent optical photon emission from shock waves in crystals. 2007, 75, Molecular dynamics simulation of plastic deformation of nanotwinned copper. 2007, 102, 083511 Molecular dynamics simulation of Ga penetration along B symmetric tilt grain boundaries in an Al	56 3 244 22 6 64

1590 Li	near grain growth kinetics and rotation in nanocrystalline Ni. 2007 , 98, 165502	56
1589 A l	tomistic underpinnings for orientation selection in alloy dendritic growth. 2007 , 98, 125701	70
	tomistic simulations of crack nucleation and intergranular fracture in bulk nanocrystalline nickel. 007 , 76,	60
15 ⁸⁷ 76	hase-change phenomena during electron-beam heating: Molecular dynamics simulations. 2007 , 6,	9
	iscovery, characterization and modelling of novel shape memory behaviour of fcc metal anowires. 2007 , 87, 2191-2220	23
	erformance of a Parallel Molecular Dynamics Program for Computation of Thermal Properties. 007 , 51, 315-331	3
1584 D	escription of dynamics of stock prices by a Langevin approach. 2007 , 16, 975-983	1
1583 Pl	lanar Defects on (112) in BCC Crystals. 2007 , 567-568, 69-72	6
	niaxial Compression Behavior of Bulk Nano-twinned Gold from Molecular Dynamics Simulation. 007 , 1049, 1	1
1581 A I	nton, a special-purpose machine for molecular dynamics simulation. 2007,	69
1580 A l	n Analysis of 10-Gigabit Ethernet Protocol Stacks in Multicore Environments. 2007 ,	14
1 [70	olecular Dynamics Simulations of Polymer Networks Undergoing Sequential Cross-Linking and cission Reactions. 2007 , 40, 131-139	64
	molecular dynamics simulation study of inclusion size effect on polymeric nanocomposites. 2007 , 1, 54-62	58
1577 M	cructures and Transport Properties of Hydrated Water-Soluble Dendrimer-Grafted Polymer dembranes for Application to Polymer Electrolyte Membrane Fuel Cells: Classical Molecular ynamics Approach. 2007 , 111, 2759-2769	47
1576 AI	tomistic simulations of homogeneous dislocation nucleation in single crystal copper. 2007 , 15, 693-709	104
1575 A I	nnealing twins in nanocrystalline fcc metals: A molecular dynamics simulation. 2007, 75,	31
1574 . 2	2007 , 56, 937-945	36
1573 M	olecular Dynamics Study of Melting of Nano Aluminum Particles. 2007 ,	1

(2007-2007)

Molecular Dynamics Simulations of Effects of Pressure and Void Size on Melting of Aluminum. 2007	1
$_{1571}$ Molecular Dynamics Modeling of Ion Adsorption to the Basal Surfaces of Kaolinite. 2007 , 111, 6753-6762	119
1570 Charge inversion of divalent ionic solutions in silica channels. 2007 , 75, 061202	50
Mechanical and transport properties of the poly(ethylene oxide)-poly(acrylic acid) double network hydrogel from molecular dynamic simulations. 2007 , 111, 1729-37	121
1568 Molecular Dynamics Simulations on Commodity GPUs with CUDA. 2007 , 185-196	20
1567 Numerical Simulation in Molecular Dynamics. 2007 ,	2
1566 Anton, a special-purpose machine for molecular dynamics simulation. 2007 , 35, 1-12	74
1565 Strain-induced grain growth and rotation in nickel nanowires. 2007 , 75,	49
1564 Conformation and dynamics of arylthiol self-assembled monolayers on Au(111). 2007 , 23, 12208-16	15
A symmetric transformation for 3-body potential molecular dynamics using force-decomposition in a heterogeneous distributed environment. 2007 ,	1
1562 Effect of Particle Size on Melting of Aluminum at Nano Scales. 2007 , 111, 11776-11783	139
1561 Mechanical response of freestanding Au nanopillars under compression. 2007 , 91, 101907	38
1560 An Application Specific Memory Characterization Technique for Co-processor Accelerators. 2007 ,	0
1559 Atomistic simulations of the interaction between lipid bilayers and substrates. 2007 , 33, 391-397	34
Molecular Dynamics Study of Alkanethiolate Self-Assembled Monolayer coated Gold Nanoparticle. 2007 ,	2
An Inspector/Executor Based Strategy to Efficiently Parallelize N-Body Simulation Programs on Shared Memory Systems. 2007 ,	1
1556 Segue between favorable and unfavorable solvation. 2007 , 111, 9025-30	21
1555 Atomic-level view of inelastic deformation in a shock loaded molecular crystal. 2007 , 76,	72

1554	Structure of Poly(dialkylsiloxane) Melts: Comparisons of Wide-Angle X-ray Scattering, Molecular Dynamics Simulations, and Integral Equation Theory. 2007 , 40, 7036-7043	19
1553	The Use of Processor Groups in Molecular Dynamics Simulations to Sample Free-Energy States. 2007 , 3, 583-92	2
1552	Structure and dynamics of water near the interface with oligo(ethylene oxide) self-assembled monolayers. 2007 , 23, 8508-14	32
1551	Local Dynamics and Primitive Path Analysis for a Model Polymer Melt near a Surface. 2007 , 40, 3797-3804	45
1550	Morphology and Diffusion Mechanism of Platinum Nanoparticles on Carbon Nanotube Bundles 2007, 111, 17905-17913	40
1549	Segmental and Chain Dynamics of Isotactic Polypropylene Melts. 2007 , 40, 2235-2245	37
1548	Surface composition effects on martensitic phase transformations in nickel aluminium nanowires. 2007 , 87, 2159-2168	5
1547	The nanoindentation responses of nickel surfaces with different crystal orientations. 2007 , 33, 905-917	44
1546	Molecular Orientation in Model Asphalts Using Molecular Simulation. 2007, 21, 1102-1111	99
1545	"Effective" negative surface tension: a property of coated nanoaerosols relevant to the atmosphere. 2007 , 111, 5459-64	24
1544	Electrowetting at the Nanoscale. 2007, 111, 505-509	116
1543	Static and Dynamic Properties of Polymer Brushes at Moderate and High Grafting Densities: ´A Molecular Dynamics Study. 2007 , 40, 6721-6730	51
1542	Interlayer structure and dynamics of alkylammonium-intercalated smectites with and without water: A molecular dynamics study. 2007 , 55, 554-564	58
1541	Entropic elasticity controls nanomechanics of single tropocollagen molecules. 2007 , 93, 37-43	156
1540	Segregation of Particulate Material Using the Discrete Element Method. 2007, 341-355	
1539	Molecular nanomechanics of nascent bone: fibrillar toughening by mineralization. 2007 , 18, 295102	216
1538	Relaxation time, diffusion, and viscosity analysis of model asphalt systems using molecular simulation. 2007 , 127, 194502	122
1537	The coupled effects of geometry and surface orientation on the mechanical properties of metal nanowires. 2007 , 18, 305704	44

	Many-body potential for point defect clusters in Fe-C alloys. 2007 , 98, 215501	68
1535	Analyzing Properties of Model Asphalts Using Molecular Simulation. 2007 , 21, 1712-1716	153
1534	Molecular Dynamics Simulation of Size-Dependent Structural and Thermal Properties of Polymer Nanofibers. 2007 , 40, 8483-8489	55
1533	Accurate computation of shear viscosity from equilibrium molecular dynamics simulations. 2007 , 33, 1261-1266	58
1532	Nanoscale organization in room temperature ionic liquids: a coarse grained molecular dynamics simulation study. 2007 , 3, 1395-1400	184
1531	Kinetic coefficient of steps at the Si(111) crystal-melt interface from molecular dynamics simulations. 2007 , 127, 074703	52
1530	Long-range interactions and parallel scalability in molecular simulations. 2007, 176, 14-22	34
1529	The application hosting environment: Lightweight middleware for grid-based computational science. 2007 , 176, 406-418	44
1528	A fine grained parallel smooth particle mesh Ewald algorithm for biophysical simulation studies: Application to the 6-D torus QCDOC supercomputer. 2007 , 177, 362-377	7
1527	Slip length and contact angle over hydrophobic surfaces. 2007 , 441, 273-276	54
1526	Twin nucleation mechanisms at a crack tip in an hcp material: Molecular simulation. 2007 , 55, 2065-2074	
	Twin indeceded in incertainship de d crack up in an incp indecriat. Motecatal simulation. 2001, 55, 2005 2014	41
	Stabilizing nanocrystalline materials with dopants. 2007 , 55, 2329-2336	187
		ŕ
1525	Stabilizing nanocrystalline materials with dopants. 2007 , 55, 2329-2336 Structure and free volume of <1 1 0> symmetric tilt grain boundaries with the E structural unit.	187
1525 1524	Stabilizing nanocrystalline materials with dopants. 2007, 55, 2329-2336 Structure and free volume of <1 1 0> symmetric tilt grain boundaries with the E structural unit. 2007, 55, 3959-3969 A micromechanical continuum model for the tensile behavior of shape memory metal nanowires.	187 91
1525 1524 1523	Stabilizing nanocrystalline materials with dopants. 2007, 55, 2329-2336 Structure and free volume of <1 1 0> symmetric tilt grain boundaries with the E structural unit. 2007, 55, 3959-3969 A micromechanical continuum model for the tensile behavior of shape memory metal nanowires. 2007, 55, 1729-1761	187 91 24
1525 1524 1523 1522	Structure and free volume of <1 1 0> symmetric tilt grain boundaries with the E structural unit. 2007, 55, 3959-3969 A micromechanical continuum model for the tensile behavior of shape memory metal nanowires. 2007, 55, 1729-1761 Vitrification of a monatomic metallic liquid. 2007, 448, 787-90 Structural transformations in single-crystal iron during shock-wave compression and tension:	187 91 24 178

1518	Strengthening in Gold Nanopillars with Nanoscale Twins. 2007, 7, 2056-2062	159
1517	Large-Scale Molecular Dynamics Study of Montmorillonite Clay: Emergence of Undulatory Fluctuations and Determination of Material Properties. 2007 , 111, 8248-8259	122
1516	Polymer brushes near the crystallization density. 2007 , 24, 325-30	21
1515	Emergence of Undulations and Determination of Materials Properties in Large-Scale Molecular Dynamics Simulation of Layered Double Hydroxides. 2007 , 19, 5510-5523	52
1514	Fracture Resistance of Nanocrystalline Ni. 2007 , 38, 2168-2173	23
1513	Shock Compression of Monocrystalline Copper: Atomistic Simulations. 2007 , 38, 2681-2688	45
1512	Atomistic Simulations of the Plasticity Behavior of Shock-Induced Polycrystalline Nickel. 2007, 38, 2716-2720	8
1511	Surface melting of superheated crystals. Atomistic simulation study. 2007 , 177, 34-37	19
1510	An efficient parallel implementation of the smooth particle mesh Ewald method for molecular dynamics simulations. 2007 , 177, 426-431	11
1509	Multiscale simulation of nanoindentation on Ni (100) thin film. 2008, 255, 3240-3250	42
1508	Understanding behavior of machining interface and dielectric molecular medium in nanoscale electro-machining. 2008 , 57, 199-202	13
1507	Implementing peridynamics within a molecular dynamics code. 2008 , 179, 777-783	193
1506	Size effects in indentation response of thin films at the nanoscale: A molecular dynamics study. 2008 , 24, 2016-2031	73
1505	General purpose molecular dynamics simulations fully implemented on graphics processing units. Journal of Computational Physics, 2008 , 227, 5342-5359 4.1	1145
1504	Coarse-grained molecular dynamics simulations of ionic polymer networks. 2008 , 12, 205-220	7
1503	Chain Expulsion out of Dense Polymer Brushes. 2008 , 17, 171-179	6
1502	Theoretical and computational hierarchical nanomechanics of protein materials: Deformation and fracture. 2008 , 53, 1101-1241	144
1501	Large-scale numerical investigation of solids mixing in a V-blender using the discrete element method. 2008 , 181, 205-216	97

(2008-2008)

1500	processors. 2008 , 34, 640-651	5
1499	Thermodynamic and mechanical properties of epoxy resin DGEBF crosslinked with DETDA by molecular dynamics. 2008 , 26, 1269-75	65
1498	Influence of single crystal orientation on homogeneous dislocation nucleation under uniaxial loading. 2008 , 56, 1806-1830	142
1497	Discrete element simulation of liquid-particle flows. 2008 , 32, 841-856	44
1496	A biophysical perspective on the cellulosome: new opportunities for biomass conversion. 2008 , 19, 218-27	79
1495	Parallel algorithms for molecular dynamics with induction forces. 2008 , 178, 384-392	5
1494	Accurate and efficient methods for modeling colloidal mixtures in an explicit solvent using molecular dynamics. 2008 , 179, 320-329	53
1493	Accelerating molecular dynamics simulations using Graphics Processing Units with CUDA. 2008 , 179, 634-641	104
1492	An all-atom simulation study of the ordering of liquid squalane near a solid surface. 2008 , 457, 357-361	17
1491	Molecular dynamics simulations of dislocations and nanocrystals. 2008 , 8, 494-497	12
1490	Molecular dynamics study of liquid metal infiltration during brazing. 2008 , 56, 1802-1812	13
1489	Void growth in metals: Atomistic calculations. 2008, 56, 3874-3886	196
1488	Sample shape and temperature strongly influence the yield strength of metallic nanopillars. 2008 , 56, 4816-4828	70
1487	Molecular dynamics simulations of shock compression of nickel: From monocrystals to nanocrystals. 2008 , 56, 5584-5604	89
1486	Continuum interpretation of virial stress in molecular simulations. 2008 , 45, 4340-4346	281
1485	Dislocation nucleation in B asymmetric tilt grain boundaries. 2008 , 24, 191-217	100
1484	Molecular simulation of permeation through alkyl-functionalized mesoporous ceramic membranes. 2008 , 314, 173-182	9
1483	Strain-driven grain boundary motion in nanocrystalline materials. 2008 , 493, 33-40	61

1482	Computer simulation study of the structural stability and materials properties of DNA-intercalated layered double hydroxides. 2008 , 130, 4742-56	109
1481	Grain boundary effects on plastic deformation and fracture mechanisms in Cu nanowires: Molecular dynamics simulations. 2008 , 77,	77
1480	Edge-stress-induced warping of graphene sheets and nanoribbons. 2008, 101, 245501	298
1479	Molecular dynamics simulations of nanoscratching of 3C SiC. 2008 , 265, 956-962	39
1478	Premelting of iron at high pressures under conditions of contact with amorphous argon. 2008 , 46, 795-799	4
1477	Alternating starvation of dislocations during plastic yielding in metallic nanowires. 2008, 59, 219-222	25
1476	Dislocation-assisted grain growth in nanocrystalline copper under large deformation. 2008, 59, 792-795	5
1475	Shock-induced shear bands in an energetic molecular crystal: Application of shock-front absorbing boundary conditions to molecular dynamics simulations. 2008 , 78,	95
1474	Non-equilibrium molecular dynamics study of nanoscale thermal contact resistance. 2008 , 34, 679-687	8
1473	Large-Scale Atomic/Molecular Massively Parallel Simulator (LAMMPS) Simulations of the Effects of Chirality and Diameter on the Pullout Force in a Carbon Nanotube Bundle. 2008 ,	7
1472	MD-tracks: a productive solution for the advanced analysis of molecular dynamics and Monte Carlo simulations. 2008 , 48, 2414-24	20
1471	Simulation of the Adsorption of Nucleotide Monophosphates on Carbon Nanotubes in Aqueous Solution. 2008 , 112, 6271-6278	27
1470	Self-assembled ordered polymer nanocomposites directed by attractive particles. 2008 , 128, 164903	18
1469	Water in nanoconfinement between hydrophilic self-assembled monolayers. 2008 , 24, 5209-12	44
1468	Coarse-grained molecular modeling of non-ionic surfactant self-assembly. 2008 , 4, 2454	196
1467	Quantitative description of plastic deformation in nanocrystalline Cu: Dislocation glide versus grain boundary sliding. 2008 , 77,	97
1466	Simulation of the mechanical strength of a single collagen molecule. 2008 , 95, 33-9	72
1465	Double bilayers and transmembrane gradients: a molecular dynamics study of a highly charged peptide. 2008 , 95, 3161-73	9

1404	High resolution approach to the native state ensemble kinetics and thermodynamics. 2008 , 95, 5524-32	16
1463	A Molecular Dynamics Study of Epoxy-Based Networks: Cross-Linking Procedure and Prediction of Molecular and Material Properties. 2008 , 41, 6837-6842	288
1462	Nanoscale fluid transport: size and rate effects. 2008 , 8, 2988-92	206
1461	Computer simulations of biaxial nematics. 2008 , 20, 463101	98
1460	Role of counterion condensation in the self-assembly of SDS surfactants at the water-graphite interface. 2008 , 112, 1987-2000	90
1459	Formation of two conjoint fivefold deformation twins in copper nanowires with molecular dynamics simulation. 2008 , 92, 041913	24
1458	Force Field Validation for Molecular Dynamics Simulations of IRMOF-1 and Other Isoreticular Zinc Carboxylate Coordination Polymers. 2008 , 112, 5795-5802	128
1457	A molecular dynamics study of alkaline earth metal-chloride complexation in aqueous solution. 2008 , 112, 14243-50	91
1456	Molecular Dynamics Study on Nanoparticle Diffusion in Polymer Melts: A Test of the StokesEinstein Law. 2008 , 112, 6653-6661	177
1455	Simulations of nanotribology with realistic probe tip models. 2008 , 24, 1240-6	107
	Elasticity size effects in ZnO nanowiresa combined experimental-computational approach. 2008,	
1454	8, 3668-74	344
		294
	8, 3668-74	
1453	8, 3668-74 Collagen. 2008, An examination of surface stress effects and deformation mechanisms in Allu nanowires. 2008, 16, 045005	294
1453 1452	8, 3668-74 Collagen. 2008, An examination of surface stress effects and deformation mechanisms in AlŒu nanowires. 2008, 16, 045005	294
1453 1452 1451	8, 3668-74 Collagen. 2008, An examination of surface stress effects and deformation mechanisms in Alūu nanowires. 2008, 16, 045005 Simulated anchoring of a nematic liquid crystal at a polymer surface. 2008, 77, 021707	29456
1453 1452 1451 1450	8, 3668-74 Collagen. 2008, An examination of surface stress effects and deformation mechanisms in AlCu nanowires. 2008, 16, 045005 Simulated anchoring of a nematic liquid crystal at a polymer surface. 2008, 77, 021707 Thermal Transport for Applications in Micro/Nanomachining. 2008, On Brownian Dynamics Simulation of Nanoparticle Aggregation. 2008, 47, 3338-3345	2945613

1446	Molecular Dynamics Study of Thermal Transport Phenomena in Cross-linked Polymer: Epon 862 with Curing Agent W (DETDA). 2008 ,	1
1445	Thermo-Mechanical Behavior of Nano Aluminum Particles with Oxide Layers. 2008,	1
1444	Hydrogen-bond dynamics for water confined in carbon tetrachloride-acetone mixtures. 2008 , 112, 10675-83	24
1443	Amorphous Inclusions in Irradiated Silicon and Their Effects on Material and Device Properties. 2008 , 55, 2992-2999	23
1442	Nanoparticle ordering via functionalized block copolymers in solution. 2008 , 2, 1259-65	44
1441	Peridynamics for multiscale materials modeling. 2008, 125, 012078	92
1440	Formation of stable ultra-thin pentagon Cu nanowires under high strain rate loading. 2008, 20, 335206	27
1439	Molecular simulation of the carbon nanotube growth mode during catalytic synthesis. 2008 , 92, 233121	45
1438	Computer simulation of architectural and molecular weight effects on the assembly of amphiphilic linear-dendritic block copolymers in solution. 2008 , 24, 3030-6	36
1437	Review of Fluid Slip over Superhydrophobic Surfaces and Its Dependence on the Contact Angle. 2008 , 47, 2455-2477	219
1436	Melting and vaporization of Cu and Ni films during electron-beam heating. 2008, 103, 054316	11
1435	Chapter 2 Electrostatics in Biomolecular Simulations: Where Are We Now and Where Are We Heading?. 2008 , 60, 49-89	55
1434	Effects of layer-charge distribution on the thermodynamic and microscopic properties of Cs-smectite. 2008 , 72, 1837-1847	61
1433	Atomistic simulations of tensionBompression asymmetry in dislocation nucleation for copper grain boundaries. 2008 , 44, 351-362	79
1432	Effect of atomic scale plasticity on hydrogen diffusion in iron: Quantum mechanically informed and on-the-fly kinetic Monte Carlo simulations. 2008 , 23, 2757-2773	46
1431	Parallel Computing Experiences with CUDA. 2008 , 28, 13-27	269
1430	Surface Tension and Surface Orientation of Perfluorinated Alkanes. 2008, 112, 5029-5035	28
1429	Molecular Structure and Dynamics in Thin Water Films at the Silica and Graphite Surfaces. 2008 , 112, 13587-13599	203

(2008-2008)

1428	Accurate Simulation of Surfaces and Interfaces of Face-Centered Cubic Metals Using 12B and 9B Lennard-Jones Potentials. 2008 , 112, 17281-17290	566
1427	Numerical analysis of nanograin collision by classical molecular dynamics. 2008 , 112, 042017	3
1426	Recent Advances in the Field of Integral Equation Theories: Bridge Functions and Applications to Classical Fluids. 2008 , 1-84	28
1425	Reconsideration of Continuum Thermomechanical Quantities in Atomic Scale Simulations. 2008 , 13, 221-266	52
1424	Relating biophysical properties across scales. 2008 , 81, 461-83	32
1423	Aqueous electrolytes near hydrophobic surfaces: dynamic effects of ion specificity and hydrodynamic slip. 2008 , 24, 1442-50	93
1422	Enhancement in hydrogen storage in carbon nanotubes under modified conditions. 2008 , 19, 155702	13
1421	Accelerating Molecular Dynamics Simulations with Reconfigurable Computers. 2008, 19, 764-778	21
1420	Structure and Dynamics of Squalane Films on Solid Surfaces. 2008,	
1419	Impact of multicores on large-scale molecular dynamics simulations. 2008,	5
	Impact of multicores on large-scale molecular dynamics simulations. 2008, An improved molecular dynamics algorithm for the larger momentum molecular system. 2008,	5
	An improved molecular dynamics algorithm for the larger momentum molecular system. 2008 , Molecular dynamics studies of nanoconfined water in clinoptilolite and heulandite zeolites. 2008 ,	34
1418	An improved molecular dynamics algorithm for the larger momentum molecular system. 2008 , Molecular dynamics studies of nanoconfined water in clinoptilolite and heulandite zeolites. 2008 , 10, 800-7	
1418	An improved molecular dynamics algorithm for the larger momentum molecular system. 2008 , Molecular dynamics studies of nanoconfined water in clinoptilolite and heulandite zeolites. 2008 , 10, 800-7	34
1418 1417 1416	An improved molecular dynamics algorithm for the larger momentum molecular system. 2008, Molecular dynamics studies of nanoconfined water in clinoptilolite and heulandite zeolites. 2008, 10, 800-7 Application Performance Tuning for Clusters with ccNUMA Nodes. 2008, Asymmetric interactions in symmetric multi-core systems: Analysis, enhancements and evaluation.	34
1418 1417 1416 1415	An improved molecular dynamics algorithm for the larger momentum molecular system. 2008, Molecular dynamics studies of nanoconfined water in clinoptilolite and heulandite zeolites. 2008, 10, 800-7 Application Performance Tuning for Clusters with ccNUMA Nodes. 2008, Asymmetric interactions in symmetric multi-core systems: Analysis, enhancements and evaluation. 2008,	3457
1418 1417 1416 1415	An improved molecular dynamics algorithm for the larger momentum molecular system. 2008, Molecular dynamics studies of nanoconfined water in clinoptilolite and heulandite zeolites. 2008, 10, 800-7 Application Performance Tuning for Clusters with ccNUMA Nodes. 2008, Asymmetric interactions in symmetric multi-core systems: Analysis, enhancements and evaluation. 2008, Aqueous divalent metal-nitrate interactions: hydration versus ion pairing. 2008, 10, 4793-801	345770

1410	ZEOBUILDER: A GUI toolkit for the construction of complex molecular structures on the nanoscale with building blocks. 2008 , 48, 1530-41	46
1409	Molecular simulation of the influence of interface faceting on the shock sensitivity of a model plastic bonded explosive. 2008 , 112, 14898-904	18
1408	Polyelectrolyte-macroion complexation in 1:1 and 3:1 salt contents: a Brownian dynamics study. 2008 , 112, 16505-16	3
1407	Mechano-chemical stability of gold nanoparticles coated with alkanethiolate SAMs. 2008 , 24, 773-83	34
1406	Conformation of a Spherical Polyelectrolyte Brush in the Presence of Oppositely Charged Linear Polyelectrolytes. 2008 , 41, 5477-5484	38
1405	Probing peptide nanotube self-assembly at a liquid-liquid interface with coarse-grained molecular dynamics. 2008 , 8, 3626-30	30
1404	High thermal conductivity of single polyethylene chains using molecular dynamics simulations. 2008 , 101, 235502	281
1403	Heterogeneous directional mobility in the early stages of polymer crystallization. 2008 , 128, 014903	37
1402	Effects of pressure on structure and dynamics of model elastomers: a molecular dynamics study. 2008 , 129, 154905	16
1401	Molecular simulation of the effect of temperature and architecture on polyethylene barrier properties. 2008 , 112, 5646-60	25
1400	Structural and Dielectric Properties of Quartz Water Interfaces. 2008, 112, 19986-19994	62
1399	Molecular dynamics simulation of ss-DNA translocation between copper nanoelectrodes incorporating electrode charge dynamics. 2008 , 112, 1712-7	20
1398	Developing improved MD codes for understanding processive cellulases. 2008 , 125, 012049	2
1397	Role of host layer flexibility in DNA guest intercalation revealed by computer simulation of layered nanomaterials. 2008 , 130, 12485-95	53
1396	Effects of Polymer Modification on Properties and Microstructure of Model Asphalt Systems. 2008 , 22, 3363-3375	102
1395	Surface Stability of Platinum Nanoparticles Surrounded by High-Index Facets. 2008 , 112, 3247-3251	9
1394	Effect of the bridging conformation of polyelectrolytes on the static and dynamic behavior of macroions. 2008 , 24, 10138-44	5
1393	Electrophoresis of ssDNA through nanoelectrode gaps from molecular dynamics: impact of gap width and chain length. 2008 , 112, 12851-8	2

(2008-2008)

1392	Nanopatterns in Tethered Membranes of Weakly Charged Chains with Hydrophobic Backbones. 2008 , 41, 6612-6614	1
1391	Critical Carbon Nanotube Length in Fibers. 2008,	5
1390	Atomistic Simulation of the Sorption of Small Gas Molecules in Polyisobutylene. 2008, 41, 6228-6238	16
1389	Hydrogen bonding and binding of polybasic residues with negatively charged mixed lipid monolayers. 2008 , 24, 1654-8	28
1388	Coupling strategies for hybrid moleculardontinuum simulation methods. 2008 , 222, 797-806	35
1387	Water penetration of damaged self-assembled monolayers. 2008 , 24, 5734-9	35
1386	Atomistic simulation of the effect of Ga on crack tip opening in Al bicrystals. 2008, 16, 075001	7
1385	Nanocomposites. 2008,	15
1384	Thermal entanglement in a two-qubit Heisenberg XY chain with the Dzyaloshinskii Moriya interaction. 2008 , 17, 2800-2803	13
1383	Micellar crystals in solution from molecular dynamics simulations. 2008 , 128, 184906	30
1382	Surface-controlled dislocation multiplication in metal micropillars. 2008, 105, 14304-7	184
1381		
	An Evaluation of the Oak Ridge National Laboratory Cray XT3. 2008 , 22, 52-80	11
1380	An Evaluation of the Oak Ridge National Laboratory Cray XT3. 2008, 22, 52-80 Can software reliability outperform hardware reliability on high performance interconnects?. 2008,	3
1380		
	Can software reliability outperform hardware reliability on high performance interconnects?. 2008, Molecular dynamics analysis of multiple site growth and coalescence effects on homogeneous and	3
1379	Can software reliability outperform hardware reliability on high performance interconnects?. 2008, Molecular dynamics analysis of multiple site growth and coalescence effects on homogeneous and heterogeneous nucleations. 2008, 128, 154523	3
1379	Can software reliability outperform hardware reliability on high performance interconnects?. 2008, Molecular dynamics analysis of multiple site growth and coalescence effects on homogeneous and heterogeneous nucleations. 2008, 128, 154523 Rheological study of polymer flow past rough surfaces with slip boundary conditions. 2008, 129, 144902 Packing of poly(tetrafluoroethylene) in the liquid state: Molecular dynamics simulation and theory.	3 14 27

1374	On gravitational defects, particles and strings. 2008, 2008, 126-126	5
1373	Simulations of an Interface Crack Nucleation During Nanoindentaion : Molecular Dynamics and Finite Element Coupling Approach. 2008 , 1086, 1	1
1372	Modelling of strain fields in quantum wires with continuum methods and molecular statics. 2008 , 20, 485215	5
1371	Computational exploration of polymer nanocomposite mechanical property modification via cross-linking topology. 2008 , 129, 124903	18
1370	Factors influencing deformation stability of binary glasses. 2008 , 128, 104508	5
1369	Rheological complexity in simple chain models. 2008 , 128, 184905	5
1368	Interfacial properties of semifluorinated alkane diblock copolymers. 2008, 128, 214903	31
1367	The importance of polarizability in the modeling of solubility: quantifying the effect of solute polarizability on the solubility of small nonpolar solutes in popular models of water. 2008 , 129, 024508	32
1366	Unsteady nanoscale thermal transport across a solid-fluid interface. 2008 , 104, 064306	33
1365	Improvement of Channel Mobility in Inversion-Type n-Channel GaN Metal®xideBemiconductor Field-Effect Transistor by High-Temperature Annealing. 2008 , 47, 7784-7787	21
1364	Molecular dynamics simulations of homogeneous solids using multi-layered structures. 2008 , 83, 10003	
1363	The angle of repose of spherical grains in granular HeleBhaw cells: a molecular dynamics study. 2008 , 2008, P04026	6
1362	Engineering molecular mechanics: an efficient static high temperature molecular simulation technique. 2008 , 19, 285706	9
1361	MUPHY: A parallel high performance MUlti PHYsics/Scale code. 2008,	2
1360	Grain boundary motion assisted via radiation cascades in bcc Fe. 2008 , 78,	17
1359	Nanoparticle formation by crosslinking a macromolecule. 2008 , 84, 46001	14
1358	Granular flow in a rapidly rotated system with fixed walls. 2008, 77, 031308	19
1357	Evolution of displacements and strains in sheared amorphous solids. 2008 , 20, 244128	35

1356	Atomic-scale time and space resolution of terahertz frequency acoustic waves. 2008, 101, 014302	14
1355	Molecular dynamics study on low-energy sputtering properties of MgO surfaces. 2008, 103, 073518	10
1354	High-throughput pairwise point interactions in Anton, a specialized machine for molecular dynamics simulation. 2008 ,	10
1353	Metastability of multitwinned Ag nanorods: Molecular dynamics study. 2008 , 78,	17
1352	Limits of hardness at the nanoscale: Molecular dynamics simulations. 2008, 78,	42
1351	Solid-liquid phase equilibria from free-energy perturbation calculations. 2008 , 78,	5
1350	Atomistic simulation study of the structure and dynamics of a faceted crystal-melt interface. 2008 , 78, 031605	47
1349	Molecular dynamics simulations of the Debye-Waller effect in shocked copper. 2008, 78,	9
1348	Nonaffine deformation of inherent structure as a static signature of cooperativity in supercooled liquids. 2008 , 101, 095501	22
1347	Atomistic calculations of interface elastic properties in noncoherent metallic bilayers. 2008, 77,	89
1346	Chapter 6 Blue Matter: Scaling of N-Body Simulations to One Atom per Node. 2008 , 60, 159-180	2
1345	Molecular Dynamics Simulation of Nanometric Machining Under Realistic Cutting Conditions. 2008,	9
1344	Asperity contacts at the nanoscale: Comparison of Ru and Au. 2008, 104, 074320	37
1343	A NEMD Study of the Thermal Conductivity and Surface Roughness of Silicon Thin Films. 2008,	
1342	Interfacial Thermal Resistance in Nanoscale Heat Transfer. 2008,	
1341	Message-passing implementation of the data diffusion communication model in fast multipole methods: large scale biomolecular simulations. 2008 , 2, 557-579	1
1340	Review of Mathematical Models for Pebble Dynamics. 2008,	
1339	Advances in Molecular Dynamics Simulations of Nanotribology. 2008,	

Simulation of liquid Rb by the methods of classical and first-principle molecular dynamics and statistical geometrical analysis of the atomic structure models using the Voronoi-Delaunay method. **2008**, 98, 042023

	2008, 98, 042023	
1337	. 2009,	18
1336	Molecular Dynamics Computations for Proteins: A Case Study in Membrane Ion Permeation. 2009,	
1335	Strong asymmetric effect of lattice mismatch on epilayer structure in thin-film deposition. 2009 , 79,	12
1334	First-principles prediction of a metastable crystalline phase of Ga with Cmcm symmetry. 2009, 80,	9
1333	Perimeter length and form factor in two-dimensional polymer melts. 2009 , 79, 050802	23
1332	Conformational change path between closed and open forms of C2 domain of coagulation factor V on a two-dimensional free-energy surface. 2009 , 79, 041909	1
1331	Cole-Davidson dynamics of simple chain models. 2009 , 130, 024903	15
1330	Slip velocity and velocity inversion in a cylindrical Couette flow. 2009 , 79, 036312	12
1329	Nanoscale brushes: how to build a smart surface coating. 2009 , 102, 115702	66
1328	Anisotropic power law strain correlations in sheared amorphous 2D solids. 2009 , 102, 225502	49
1327	Stress-induced phase transformation and pseudo-elastic/pseudo-plastic recovery in intermetallic Ni-Al nanowires. 2009 , 20, 295705	13
1326	Shear response of the 🗓1, <1 1 0>{1 3 1} symmetric tilt grain boundary studied by molecular dynamics. 2009 , 17, 045008	23
1325	Contact configuration modification at carbon nanotube-metal interface during nanowelding. 2009 , 106, 124308	10
1324	Assessing how metal@arbon interactions affect the structure of supported platinum nanoparticles. 2009 , 35, 795-803	17
1323	Martensitic transformation of Cu on Ag(001) and Cu on Au(001) studied with classical molecular dynamics. 2009 , 79,	5
1322	Nonequilibrium molecular dynamics simulation of the in-plane thermal conductivity of superlattices with rough interfaces. 2009 , 79,	62
1321	Influence of nanoscale Cu precipitates in Fe on dislocation core structure and strengthening. 2009 , 80,	33

1320	Atomistic simulations of crystal-melt interfaces in a model binary alloy: Interfacial free energies, adsorption coefficients, and excess entropy. 2009 , 79,	38
1319	Strain hardening in bidisperse polymer glasses: separating the roles of chain orientation and interchain entanglement. 2009 , 131, 244901	32
1318	Parallelization of discrete element simulation. 2009 , 32, 825-841	4
1317	Computer simulation study of the materials properties of intercalated and exfoliated poly(ethylene)glycol clay nanocomposites. 2009 , 5, 2239	50
1316	Enhancement of charge inversion by multivalent interfacial groups. 2009 , 80, 042601	15
1315	Implementation of a Morse potential to model hydroxyl behavior in phyllosilicates. 2009 , 130, 134713	38
1314	Chapter 89 Dislocations in Shock Compression and Release. 2009 , 15, 91-197	34
1313	Atomistic simulation of CdTe solid-liquid coexistence equilibria. 2009 , 80,	13
1312	Size-dependent nucleation kinetics at nonplanar nanowire growth interfaces. 2009, 80, 050601	17
1311	Thermal rectification at water/functionalized silica interfaces. 2009 , 95, 151903	57
1310	Coarse-grained ions without charges: reproducing the solvation structure of NaCl in water using short-ranged potentials. 2009 , 131, 034107	61
1309	Size-dependent yield stress in twinned gold nanowires mediated by site-specific surface dislocation emission. 2009 , 95, 091914	64
1308	Molecular simulation of crystal nucleation in n-octane melts. 2009 , 131, 134902	69
1307	Molecular dynamics simulation of the thin film deposition of Co/Cu(111) with Pb surfactant. 2009 , 106, 044304	9
1306	Surface transformation and inversion domain boundaries in gallium nitride nanorods. 2009 , 95, 211907	15
1305	Performance analysis and projections for Petascale applications on Cray XT series systems. 2009,	1
1304	Size and surface orientation effects on thermal expansion coefficient of one-dimensional silicon nanostructures. 2009 , 105, 104309	12
1303	Heat transfer from nanoparticles: a corresponding state analysis. 2009 , 106, 15113-8	153

1302	Driven simulations of the dynamic heat capacity. 2009 , 131, 104507	5
1301	Coupled effect of size, strain rate, and temperature on the shape memory of a pentagonal Cu nanowire. 2009 , 20, 045701	32
1300	Formation of micelles in aqueous solutions of a room temperature ionic liquid: a study using coarse grained molecular dynamics. 2009 , 107, 393-401	44
1299	. 2009,	4
1298	Codimension-one tangency bifurcations of global Poincarlmaps of four-dimensional vector fields. 2009 , 22, 1091-1121	2
1297	Molecular dynamics insight into the cointercalation of hexadecyltrimethyl-ammonium and acetate ions into smectites. 2009 , 94, 143-150	46
1296	STRUCTURE OF IONS AND WATER AROUND A POLYELECTROLYTE IN A POLARIZABLE NANOPORE. 2009 , 20, 1485-1492	2
1295	A molecular dynamics study of twin width, grain size and temperature effects on the toughness of 2D-columnar nanotwinned copper. 2009 , 17, 055009	33
1294	Shear viscosity and diffusion in liquid MgSiO3: Transport properties and implications for terrestrial planet magma oceans. 2009 , 94, 975-980	25
1293	On the fluctuations that drive small ions toward, and away from, interfaces between polar liquids and their vapors. 2009 , 106, 15125-30	60
1292	Asymmetrical reorientation of bimetallic core-shell nanowires. 2009 , 20, 045601	3
1291	Micro/meso-scale computational study of dislocation-stacking-fault tetrahedron interactions in copper. 2009 , 24, 3628-3635	33
1290	Review of Hierarchical Multiscale Modeling to Describe the Mechanical Behavior of Amorphous Polymers. 2009 , 131,	62
1289	Instruction-level simulation of a cluster at scale. 2009,	14
1288	Molecular Dynamics Simulations of Normal Shocks in Dilute Gases. 2009,	
1287	An idealized polyhedral model and geometric structure for silicon nanotubes. 2009 , 21, 075301	8
1286	Intermolecular correlations in an ionic1iquid under shear. 2009 , 21, 035105	3
1285	Structural properties of Ge/Si(001) nano-islands and AlGaN nanowires by Diffraction Anomalous Fine Structure and Multiwavelength Anomalous Diffraction. 2009 , 190, 012129	6

1284	Early structural development in melt-quenched polymer PTT from atomistic molecular dynamic simulations. 2009 , 21, 505101	2
1283	The Bain versus NishiyamaWassermann path in the martensitic transformation of Fe. 2009 , 11, 103027	68
1282	Spreading of liquid droplets on permeable polymeric surfaces. 2009 , 86, 64004	6
1281	The atomistic mechanism of high temperature contact line advancement: results from molecular dynamics simulations. 2009 , 21, 464135	8
1280	Lattice strain due to an atomic vacancy. 2009 , 10, 2798-808	35
1279	Molecular Dynamics Simulation on Crack Propagation for Magnesium. 2009 , 417-418, 21-24	
1278	From the gating charge response to pore domain movement: initial motions of Kv1.2 dynamics under physiological voltage changes. 2009 , 26, 397-421	12
1277	From campus resources to federated international grids. 2009,	O
1276	Combined molecular algorithms for the generation, equilibration and topological analysis of entangled polymers: methodology and performance. 2009 , 10, 5054-89	124
1275	Letter. The influence of atomic size and charge of dissolved species on the diffusivity and viscosity of silicate melts. 2009 , 94, 1735-1738	5
1274	Mesoscale flow and heat transfer modelling and its application to liquid and gas flows. 2009 , 3, 031960	3
1273	Molecular Dynamics Simulation of Interfacial Thermal Resistance Between a (10,10) Carbon Nanotube and SiO2. 2009 , 1172, 44	
1272	Alternative ways of coupling particle behaviour with fluid dynamics in mineral processing. 2009 , 23, 109-118	20
1271	Atomistic simulation of sliding of [101[0] tilt grain boundaries in Mg. 2009 , 24, 3446-3453	9
1270	Yield strength in nanocrystalline Cu during high strain rate deformation. 2009 , 61, 76-79	36
1269	Molecular dynamics study of stable and undercooled liquid zirconium based on MEAM interatomic potential. 2009 , 116, 489-496	19
1268	Stress-induced martensitic phase transformation in Cullr nanowires. 2009 , 63, 1289-1292	36
1267	Simulation of Liquid Argon Flow along a Nanochannel: Effect of Applied Force. 2009 , 17, 734-738	7

1266	369 Tflop/s molecular dynamics simulations on the petaflop hybrid supercomputer R oadrunner□ 2009 , 21, 2143-2159	12
1265	SPEC MPI2007 application benchmark suite for parallel systems using MPI. 2009, 22, n/a-n/a	
1264	Modeling the separation of macromolecules: a review of current computer simulation methods. 2009 , 30, 792-818	116
1263	Computational screening of biomolecular adsorption and self-assembly on nanoscale surfaces. 2010 , 31, 1564-8	50
1262	Coupled NavierBtokesMolecular dynamics simulations using a multi-physics flow simulation framework. 2009 , 62, n/a-n/a	3
1261	Polymer brushes for surface tuning. 2009 , 30, 732-40	98
1260	A performance model with a fixed point for a molecular dynamics kernel. 2009 , 23, 195-201	6
1259	Roles of grain boundary and dislocations at different deformation stages of nanocrystalline copper under tension. 2009 , 373, 570-574	32
1258	Molecular dynamics simulation comparison of atomic scale intermixing at the amorphous Al2O3/semiconductor interface for a-Al2O3/Ge, a-Al2O3/InGaAs, and a-Al2O3/InAlAs/InGaAs. 2009 , 603, 3191-3200	32
1257	Molecular statics simulations of buckling and yielding of gold nanowires deformed in axial compression. 2009 , 57, 4921-4932	22
1256	Molecular dynamics simulation study of P (VP-co-HEMA) hydrogels: effect of water content on equilibrium structures and mechanical properties. 2009 , 30, 6130-41	61
1255	Shape dependent properties of CdSe nanostructures. 2009 , 362, 114-119	9
1254	BioVEC: a program for biomolecule visualization with ellipsoidal coarse-graining. 2009, 28, 140-5	10
1253	Molecular dynamics study of size, temperature and rate dependent thermomechanical properties of copper nanofilms. 2009 , 36, 838-844	12
1252	MUPHY: A parallel MUlti PHYsics/scale code for high performance bio-fluidic simulations. 2009 , 180, 1495-1502	101
1251	Virtualizing access to scientific applications with the Application Hosting Environment. 2009 , 180, 2513-2525	28
1250	The Nano-Jackhammer effect in probing near-surface mechanical properties. 2009 , 25, 2045-2058	30
1249	Effect of voids and pressure on melting of nano-particulate and bulk aluminum. 2009 , 11, 1117-1127	18

1248	The role of dislocations in the growth of nanosized voids in ductile failure of metals. 2009, 61, 35-41	47
1247	Mechanism for the Pseudoelastic Behavior of FCC Shape Memory Nanowires. 2009 , 49, 183-190	8
1246	Radiation damage in nano-crystalline tungsten: A molecular dynamics simulation. 2009 , 15, 447-452	22
1245	Molecular dynamics study of size, temperature and strain rate effects on mechanical properties of gold nanofilms. 2009 , 95, 357-362	20
1244	Multiaxial behavior of nanoporous single crystal copper: a molecular dynamics study. 2009, 22, 650-656	22
1243	Switchable helical structures formed by the hierarchical self-assembly of laterally tethered nanorods. 2009 , 5, 2092-8	35
1242	CHAMBER: Comprehensive support for CHARMM force fields within the AMBER software. 2009 , 109, 3767-3772	64
1241	Effect of chain stiffness on the morphology of diblock copolymer melts. 2009 , 47, 2556-2565	4
1240	Growth of silicon nitride films by bombarding amorphous silicon with N+ ions: MD simulation. 2009 , 267, 3245-3248	1
1239	Parallelization of pseudo-particle modeling and its application in simulating gasBolid fluidization. 2009 , 7, 317-323	4
1238	Predicting EXAFS signals from shock compressed iron by use of molecular dynamics simulations. 2009 , 5, 44-50	6
1237	Computational study of the surface properties of aluminum nanoparticles. 2009 , 603, 2042-2046	52
1236	Structure of CF4 multilayers on (0 0 0 1) surfaces of graphite and hydroxylated Equartz: A molecular dynamics study. 2009 , 603, 3374-3381	5
1235	Molecular dynamics study of scratching velocity dependency in AFM-based nanometric scratching process. 2009 , 505, 65-69	45
1234	Molecular dynamics simulation of sphere indentation in a thin copper film. 2009 , 12, 117-123	16
1233	Molecular dynamics simulation of mixed matrix nanocomposites containing polyimide and polyhedral oligomeric silsesquioxane (POSS). 2009 , 50, 1324-1332	56
1232	Molecular modeling for calculation of mechanical properties of epoxies with moisture ingress. 2009 , 50, 2736-2742	63
1231	Heat transport in epoxy networks: A molecular dynamics study. 2009 , 50, 3378-3385	56

1230	A mesoscopic network model for permanent set in crosslinked elastomers. 2009 , 50, 5613-5617	10
1229	Effects of quenching rate on amorphous structures of Cu46Zr54 metallic glass. 2009 , 209, 4601-4606	26
1228	Sample boundary effect in nanoindentation of nano and microscale surface structures. 2009 , 57, 812-827	17
1227	Molecular dynamics simulation of intragranular Xe bubble re-solution in UO2. 2009 , 392, 35-39	49
1226	A fast adaptive load balancing method for parallel particle-based simulations. 2009, 17, 1032-1042	22
1225	Wetting of hydrophobic substrates by nanodroplets of aqueous trisiloxane and alkyl polyethoxylate surfactant solutions. 2009 , 64, 4657-4667	37
1224	Implementation of Green's function molecular dynamics: An extension to LAMMPS. 2009 , 180, 1004-1010	38
1223	TiReX: Replica-exchange molecular dynamics using Tinker. 2009 , 180, 2013-2019	12
1222	Statistical mechanics of sum frequency generation spectroscopy for the liquidNapor interface of dilute aqueous salt solutions. 2009 , 470, 21-27	8
1221	Influence of pore shape on the structure of a nanoconfined GayBerne liquid crystal. 2009, 478, 161-165	25
1220	Molecular dynamics algorithms for quantum Monte Carlo methods. 2009 , 482, 165-170	13
1219	Effect of material properties on liquid metal embrittlement in the Alta system. 2009, 57, 1546-1553	50
1218	Forced chemical mixing in immiscible alloys during severe plastic deformation at elevated temperatures. 2009 , 57, 3012-3019	48
1217	Survey of computed grain boundary properties in face-centered cubic metals I I: Grain boundary mobility. 2009 , 57, 3704-3713	249
1216	Deformation characteristics and stressEtrain response of nanotwinned copper via molecular dynamics simulation. 2009 , 57, 4364-4373	78
1215	Dislocation B win interaction mechanisms for ultrahigh strength and ductility in nanotwinned metals. 2009 , 57, 4508-4518	160
1214	Are some nanotwinned fcc metals optimal for strength, ductility and grain stability?. 2009, 57, 4835-4844	78
1213	Molecular dynamics investigation on the atomic-scale friction behaviors between copper(001) and diamond(111) surfaces. 2009 , 255, 7663-7668	7

1212	Water modeled as an intermediate element between carbon and silicon. 2009 , 113, 4008-16	648
1211	Nanoscale wetting on groove-patterned surfaces. 2009 , 25, 5045-53	96
1210	Atomistic calculations on interfaces: Bridging the length and time scales. 2009, 177, 41-57	8
1209	Anomalous properties of the acoustic excitations in glasses on the mesoscopic length scale. 2009 , 106, 16907-12	99
1208	Modeling of graphenepolymer interfacial mechanical behavior using molecular dynamics. 2009 , 17, 015002	177
1207	A homogeneous nonequilibrium molecular dynamics method for calculating thermal conductivity with a three-body potential. 2009 , 130, 204106	30
1206	Comparison of different displacive processes in bcc crystals. 2009 , 73, 1188-1192	
1205	Molecular-dynamics simulation of iron premelting at high pressures. 2009 , 54, 1-5	1
1204	A Transferable Coarse Grain Non-bonded Interaction Model For Amino Acids. 2009 , 5, 2115-2124	106
1203	Configurational dependence of elastic modulus of metallic glass. 2009 , 80,	58
1202	Mechanical Properties of Glassy Polyethylene Nanofibers via Molecular Dynamics Simulations. 2009 , 42, 4887-4895	32
1201	Interfacial Structure and Dynamics of Siloxane Systems: PDMSNapor and PDMSNater. 2009 , 42, 3186-3194	57
1200	Anomalous dissipation in single-walled carbon nanotube resonators. 2009 , 9, 3699-703	22
1199	Effect of tail architecture on self-assembly of amphiphiles for polymeric micelles. 2009 , 25, 2749-56	41
1198	Toward a simple molecular understanding of sum frequency generation at air-water interfaces. 2009 , 113, 4065-74	24
1197	Molecular dynamics simulations of nanoimprinting lithography. 2009 , 25, 13244-9	15
1196	Free energy barrier for molecular motions in bistable [2]rotaxane molecular electronic devices. 2009 , 113, 2136-43	38
1195	Hydroelectric voltage generation based on water-filled single-walled carbon nanotubes. 2009 , 131, 6374-6	134

1194	Interdiffusion of Short Chain Oligomers into an Entangled Polymer Film. 2009 , 42, 7969-7973	12
1193	Effect of monomeric sequence on mechanical properties of P(VP-co-HEMA) hydrogels at low hydration. 2009 , 113, 6604-12	27
1192	Enabling ultrahigh plastic flow and work hardening in twinned gold nanowires. 2009 , 9, 1517-22	104
1191	Nanoconfined water in magnesium-rich 2:1 phyllosilicates. 2009 , 131, 8155-62	50
1190	Structural characterization of unsaturated phosphatidylcholines using traveling wave ion mobility spectrometry. 2009 , 81, 8289-97	83
1189	Nanofluidic transport in branching nanochannels: a molecular sieve based on Y-junction nanotubes. 2009 , 113, 6468-72	15
1188	Microphase Separation of Mixed Binary Polymer Brushes at Different Temperatures. 2009, 42, 7194-7202	23
1187	Are pressure fluctuation-based equilibrium methods really worse than nonequilibrium methods for calculating viscosities?. 2009 , 131, 246101	81
1186	Spherical NanoparticleBubstrate Adhesion Interaction Simulations Utilizing Molecular Dynamics. 2009 , 23, 1723-1738	4
1185	Molecular Dynamics Simulations of Solvation and Kink Site Formation at the {001} Barite™ater Interface□ 2009 , 113, 2104-2110	39
1184	Raman spectroscopic study on the solvation of p-aminobenzonitrile in supercritical water and methanol. 2009 , 113, 3143-54	18
1183	Dynamic Resizing of Parallel Scientific Simulations: A Case Study Using LAMMPS. 2009 , 175-184	4
1182	Sodium Diffusion through Aluminum-Doped Zeolite BEA System: Effect of Water Solvation. 2009 , 113, 819-826	7
1181	Structure, dimensions, and entanglement statistics of long linear polyethylene chains. 2009 , 113, 442-55	56
1180	Dynamics of a Glassy Polymer Nanocomposite during Active Deformation. 2009 , 42, 3632-3640	57
1179	Arginine, a key residue for the enhancing ability of an antifreeze protein of the beetle Dendroides canadensis. 2009 , 48, 9696-703	29
1178	Shear thinning of nanoparticle suspensions. 2009 , 79, 021401	23
1177	Initial stages of aggregation in aqueous solutions of ionic liquids: molecular dynamics studies. 2009 , 113, 9499-505	50

1176	Tensile deformation of fcc Ni as described by an EAM potential. 2009 , 89, 3435-3450	24
1175	Effects of Microalloying on the Mobility and Mechanical Response of Interfaces in Nanocrystalline Cu. 2009 , 633-634, 21-30	4
1174	Interatomic potential for copperIntimony in dilute solidIolution alloys and application to single crystal dislocation nucleation. 2009 , 44, 1258-1264	8
1173	Graphitization as a precursor to wear of diamond in machining pure iron: A molecular dynamics investigation. 2009 , 45, 358-366	75
1172	Strengthening effects of coherent interfaces in nanoscale metallic bilayers. 2009 , 45, 1129-1133	41
1171	Atomistic simulation on size-dependent yield strength and defects evolution of metal nanowires. 2009 , 46, 142-150	66
1170	A molecular dynamics simulation on surface tension of liquid Ni and Cu. 2009 , 46, 516-519	13
1169	A comparative study of Young modulus of single-walled carbon nanotube by CPMD, MD and first principle simulations. 2009 , 46, 621-625	73
1168	Molecular dynamics study on the nano-void growth in face-centered cubic single crystal copper. 2009 , 46, 749-754	99
1167	Cu/Ag EAM potential optimized for heteroepitaxial diffusion from ab initio data. 2009 , 47, 577-583	37
1166	Structure, thermodynamic and transport properties of CaAl2Si2O8 liquid. Part I: Molecular dynamics simulations. 2009 , 73, 6918-6936	36
1165	Materials properties of clay nanocomposites: onset of negative Poisson ratio in large-scale molecular dynamics simulation. 2009 , 5, 3896	15
1164	Molecular renormalization group coarse-graining of polymer chains: application to double-stranded DNA. 2009 , 96, 4044-52	70
1163	Counterion valence-induced tunnel formation in a system of polyelectrolyte brushes grafted on two apposing walls. 2009 , 113, 11625-31	12
1162	Nanoindentation of thin films: Simulations and experiments. 2009 , 24, 1135-1141	16
1161	Ab initio molecular dynamics simulations of properties of a-Al2O3/vacuum and a-ZrO2/vacuum vs a-Al2O3Ge(100)(2 x 1) and a-ZrO2Ge(100)(2 x 1) interfaces. 2009 , 130, 124717	23
1160	Atomically abrupt and unpinned Al2O3/In0.53Ga0.47As interfaces: Experiment and simulation. 2009 , 106, 124508	78
1159	Determining materials properties of natural composites using molecular simulation. 2009 , 19, 7251	17

1158	Nanoengineering heat transfer performance at carbon nanotube interfaces. 2009 , 3, 2767-75	181
1157	Recent advances in large-scale atomistic and coarse-grained molecular dynamics simulation of clay minerals. 2009 , 19, 2482	68
1156	Dislocation motion in magnesium: a study by molecular statics and molecular dynamics. 2009 , 17, 075009	86
1155	Numerical Simulation of Granular Materials. 149-315	2
1154	Strain controlled thermomutability of single-walled carbon nanotubes. 2009 , 20, 185701	115
1153	Phase boundary effects on the mechanical deformation of core/shell Cu/Ag nanoparticles. 2009 , 24, 2210-2214	10
1152	Forces between functionalized silica nanoparticles in solution. 2009 , 79, 050501	49
1151	Mechanisms of water infiltration into conical hydrophobic nanopores. 2009 , 11, 6520-4	35
1150	Thermal effect on the dynamic infiltration of water into single-walled carbon nanotubes. 2009 , 80, 061206	24
1149	Efficient implementation of the concentration-dependent embedded atom method for molecular-dynamics and Monte-Carlo simulations. 2009 , 17, 075005	63
1148	Large-scale molecular dynamics simulations of normal shock waves in dilute argon. 2009 , 21, 066101	36
1147	Size and chirality dependent elastic properties of graphene nanoribbons under uniaxial tension. 2009 , 9, 3012-5	653
1146	Theoretical evidence for a first-order liquid-liquid phase transition in gallium. 2009, 130, 221101	25
1145	Interatomic potentials for hydrogen in fron based on density functional theory. 2009, 79,	126
1144	Atomistic simulation of the premelting of iron and aluminum: Implications for high-pressure melting-curve measurements. 2009 , 80,	42
1143	Electronic structure of disordered conjugated polymers: polythiophenes. 2009 , 113, 409-15	79
1142	Numerical study of segregation using multiscale models. 2009 , 23, 81-92	14
1141	Pseudoelasticity of Cullr nanowires via stress-induced martensitic phase transformations. 2009 , 95, 021911	30

1140	Shape effects on the yield stress and deformation of silicon nanowires: A molecular dynamics simulation. 2009 , 106, 023537	40
1139	Molecular dynamics study of crystal plasticity during nanoindentation in Ni nanowires. 2009 , 24, 948-956	27
1138	Static and dynamic properties of model elastomer with various cross-linking densities: a molecular dynamics study. 2009 , 131, 034903	24
1137	Packaging of a Polyelectrolyte into a Neutral Spherical Cavity. 2009 , 42, 4874-4877	4
1136	Anomalous heat conduction in polyethylene chains: Theory and molecular dynamics simulations. 2009 , 79,	112
1135	Coarse-Grained Intermolecular Potentials Derived From The Effective Fragment Potential: Application To Water, Benzene, And Carbon Tetrachloride. 2009 , 197-218	3
1134	Microscopic dynamics of the orientation of a hydrated nanoparticle in an electric field. 2009, 103, 207801	30
1133	Structure and dynamics of a Gay-Berne liquid crystal confined in cylindrical nanopores. 2009 , 130, 234501	36
1132	Multi-Scale Modeling of Nano-Particle Reinforced Composites Using Statistical Coupling of MD and MPM. 2009 ,	
1131	Prediction of Material Properties of Nanostructured Polymer Composites Using Atomistic Simulations. 2009 ,	
1130	Atomistic Numerical Approach to Ion Evaporation from a Tungsten Surface for Electrospray Thrusters. 2009 ,	3
1129	A molecular dynamics simulation study of hydrated sulfonated poly(ether ether ketone) for application to polymer electrolyte membrane fuel cells: Effect of water content. 2009 , 1, 033101	45
1128	Parallel algorithm for spin and spin-lattice dynamics simulations. 2009 , 79, 046703	23
1127	Explicit Treatment of Hydrogen Atoms in Thermal Simulations of Polyethylene. 2009 , 13, 99-108	9
1126	Computational study of thermocompression bonding of carbon nanotubes to metallic substrates. 2009 , 106, 104308	17
1125	Solid-solid phase transitions in Fe nanowires induced by axial strain. 2009 , 20, 325704	35
1124	Finite-size effects in Fe-nanowire solid-solid phase transitions: a molecular dynamics approach. 2009 , 9, 2290-4	70
1123	Transformation pathways in the solid-solid phase transitions of iron nanowires. 2009 , 95, 191909	37

1122	Molecular dynamics simulation of the kinetic sintering of Ni and Al nanoparticles. 2009, 35, 804-811	42
1121	Atomic structure and diffusion in Cu60Zr40 metallic liquid and glass: molecular dynamics simulations. 2009 , 106, 073520	30
1120	Multiscale modeling of emergent materials: biological and soft matter. 2009 , 11, 1869-92	217
1119	Molecular models and simulations of layered materials. 2009 , 19, 2470	210
1118	Liquid crystal nanodroplets in solution. 2009 , 130, 044901	52
1117	Molecular renormalization group coarse-graining of electrolyte solutions: application to aqueous NaCl and KCl. 2009 , 113, 7785-93	68
1116	Ordering of poly(3-hexylthiophene) nanocrystallites on the basis of substrate surface energy. 2009 , 3, 2881-6	54
1115	Thermodynamic stability and growth of guest-free clathrate hydrates: a low-density crystal phase of water. 2009 , 113, 10298-307	220
1114	Computational Nanomechanics of Graphene Membranes. 2009 , 1185, 55	
1113	Nature of molecular interactions of peptides with gold, palladium, and Pd-Au bimetal surfaces in aqueous solution. 2009 , 131, 9704-14	311
1112	Atomistic study of the mechanical response of copper nanowires under torsion. 2009 , 42, 135408	45
1111	Molecular dynamics simulation of the energetic reaction between Ni and Al nanoparticles. 2009 , 105, 124310	48
1110	Thermoreversible associating polymer networks. I. Interplay of thermodynamics, chemical kinetics, and polymer physics. 2009 , 131, 224902	59
1109	Nanoclusters of room temperature ionic liquids: a molecular dynamics simulation study. 2009 , 11, 8745-51	13
1108	Aqueous solutions of imidazolium ionic liquids: molecular dynamics studies. 2009 , 5, 3475	51
1107	Near-ideal strength in gold nanowires achieved through microstructural design. 2009 , 3, 3001-8	105
1106	Adsorption of nonuniformly charged fullerene-like nanoparticles on planar polyelectrolyte brushes in aqueous solutions. 2009 , 25, 4965-72	13
1105	. 2009,	

1104	Non-bonded force field for the interaction between metals and organic molecules: a case study of olefins on aluminum. 2009 , 11, 10195-203	12
1103	Emergence of nanoscale order in room temperature ionic liquids: simulation of symmetric 1,3-didecylimidazolium hexafluorophosphate. 2009 , 19, 4343	18
1102	Performance of LAMMPS Code on Intel Quad-Core Xeon. 2009,	1
1101	Million-Atom Count Simulations of the Effects of Carbon Nanotube Length Distributions on Fiber Mechanical Properties. 2009 ,	1
1100	GPGPU supported cooperative acceleration in molecular dynamics. 2009,	1
1099	Atomistic simulations of cross-slip nucleation at screw dislocation intersections in face-centered cubic nickel. 2009 , 89, 3351-3369	27
1098	Performance Characterization of a Hierarchical MPI Implementation on Large-scale Distributed-memory Platforms. 2009 ,	
1097	GPU Acceleration of High-Speed Collision Molecular Dynamics Simulation. 2009,	1
1096	Strain distributions and electronic property modifications in Si/Ge axial nanowire heterostructures. 2009 , 105, 044310	25
1095	Growing correlation length in supercooled water. 2009 , 130, 244505	148
1095	Nonreactive spreading at high-temperature revisited for metal systems via molecular dynamics.	148 17
	Nonreactive spreading at high-temperature revisited for metal systems via molecular dynamics.	
1094	Nonreactive spreading at high-temperature revisited for metal systems via molecular dynamics. 2009, 25, 11450-8 Heterogeneous dislocation nucleation in single crystal copperEntimony solid-solution alloys. 2009, 17, 055001	17
1094	Nonreactive spreading at high-temperature revisited for metal systems via molecular dynamics. 2009, 25, 11450-8 Heterogeneous dislocation nucleation in single crystal copperEntimony solid-solution alloys. 2009, 17, 055001	17
1094 1093 1092	Nonreactive spreading at high-temperature revisited for metal systems via molecular dynamics. 2009, 25, 11450-8 Heterogeneous dislocation nucleation in single crystal copperEntimony solid-solution alloys. 2009, 17, 055001 Multiscale Modeling: A Review. 2009, 87-135 An energy-conserving two-temperature model of radiation damage in single-component and binary	17 18
1094 1093 1092	Nonreactive spreading at high-temperature revisited for metal systems via molecular dynamics. 2009, 25, 11450-8 Heterogeneous dislocation nucleation in single crystal copper8ntimony solid-solution alloys. 2009, 17, 055001 Multiscale Modeling: A Review. 2009, 87-135 An energy-conserving two-temperature model of radiation damage in single-component and binary Lennard-Jones crystals. 2009, 131, 074701 Transport properties and induced voltage in the structure of water-filled single-walled	17 18 67 31
1094 1093 1092 1091	Nonreactive spreading at high-temperature revisited for metal systems via molecular dynamics. 2009, 25, 11450-8 Heterogeneous dislocation nucleation in single crystal copperBntimony solid-solution alloys. 2009, 17, 055001 Multiscale Modeling: A Review. 2009, 87-135 An energy-conserving two-temperature model of radiation damage in single-component and binary Lennard-Jones crystals. 2009, 131, 074701 Transport properties and induced voltage in the structure of water-filled single-walled boron-nitrogen nanotubes. 2009, 3, 22411 Composition-dependent interatomic potentials: A systematic approach to modelling	17 18 67 31 20

TimeII emperature and TimeII oncentration Superposition of Nanofilled Elastomers: A Molecu Dynamics Study. 2009 , 42, 2831-2842	ılar 55
$_{ m 1085}$ Experimental-computational investigation of ZnO nanowires strength and fracture. 2009 , 9,	4177-83 167
A unified framework and performance benchmark of fourteen multiscale atomistic/continuucoupling methods. 2009 , 17, 053001	JM 266
A Molecular Dynamics Study of Thermal Conductivity in Nanocomposites via the Phonon War Packet Method. 2009 ,	ve 3
1082 HieraAnalyses – a tool for hierarchical analysis of parallel programs. 2009 , 2, 58	
$_{1081}$ Performance comparison of two virtual machine scenarios using an HPC application. 2009 ,	3
1080 A Mechanism-Based Finite-Rate Surface Catalysis Model for Simulating Reacting Flows. 2009	9 , 6
1079 LASER COMPRESSION OF NANOCRYSTALLINE METALS. 2009 ,	2
Molecular Dynamics Simulation of the Thermal Resistance of Carbon Nanotube (Substrate Interfaces. 2009,	1
1077 Notice of Retraction: Molecular dynamics study of silicate glass under shock. 2010 ,	
Numerical Simulations of Screen Performance in Standalone Screen Applications for Sand Co 2010 ,	ontrol.
1075 Computer modeling of granular rheology. 121-146	
1074 Molecular Dynamics of Crack Propagation in Nickel and Nickel-Aluminum Bimetal Interface. 2	2010,
1073 Molecular Dynamics Modeling of Heat Transport in Metals and Semiconductors. 2010 ,	
Energetics of Pb heterostructures formation on the Cu (111) in the early stage of the deposi process. 2010 , 107, 114315	tion 3
AFM-Based Nanomachining for Nano-Fabrication Processes: MD Simulation and AFM Experim Verification. 2010 ,	mental 1
Effects of the attractive interactions in the thermodynamic, dynamic, and structural anomali two length scale potential. 2010 , 133, 244506	es of a 27
1069 Plastic deformation under high-rate loading: The multiscale approach. 2010 , 52, 1386-1396	52

(2010-2010)

1068	Influence of plastic deformation on fracture of an aluminum single crystal under shock-wave loading. 2010 , 52, 1619-1624	19
1067	Molecular dynamics simulation of copper bicrystal response to shear loading. 2010 , 36, 786-788	3
1066	Surface structures of oligoglycines: A molecular dynamics simulation. 2010 , 36, 574-580	7
1065	Gramm-software package for molecular dynamics on graphical processing units. 2010 , 2, 46-54	
1064	Plasticity and dynamical heterogeneity in driven glassy materials. 2010 , 32, 165-81	36
1063	Heterogeneous nucleation of solid Al from the melt by Al3Ti: Molecular dynamics simulations. 2010 , 82,	35
1062	Self-assembly and its impact on interfacial charge transfer in carbon nanotube/P3HT solar cells. 2010 , 4, 6599-606	84
1061	Freezing, melting and structure of ice in a hydrophilic nanopore. 2010 , 12, 4124-34	223
1060	Effects of vacancies on interwall spacings of multi-walled carbon nanotubes. 2010 , 11, 714-721	1
1059	A comparative MD study of the local structure of polymer semiconductors P3HT and PBTTT. 2010 , 12, 14735-9	61
1058	Design of polymer nanocomposites in solution by polymer functionalization. 2010 , 82, 021803	22
1057	Parametrization and application of a coarse grained force field for benzene/fullerene interactions with lipids. 2010 , 114, 16364-72	29
1056	Theoretical Study of the Organic Photovoltaic Electron Acceptor PCBM: Morphology, Electronic Structure, and Charge Localization. 2010 , 114, 20479-20488	163
1055	Spontaneous asymmetry of coated spherical nanoparticles in solution and at liquid-vapor interfaces. 2010 , 104, 235501	99
1054	Chains are more flexible under tension. 2010 , 43, 9181-9190	56
1053	Theory and molecular dynamics modeling of spall fracture in liquids. 2010 , 82,	71
1052	Molecular dynamics simulation of thermal boundary conductance between carbon nanotubes and SiO2. 2010 , 81,	234
1051	Temperature and ion concentration effects on the viscosity of Price B rooks' TIP3P-PME water model. 2010 , 36, 801-804	3

Atomistic comparison of volume-dependent melt properties from four models of aluminum. 20 18, 074001	23
1049 Temperature control in molecular dynamic simulations of non-equilibrium processes. 2010 , 22,	074205 19
1048 High-efficiency mechanical energy storage and retrieval using interfaces in nanowires. 2010 , 10), 1774-9 48
Examining the origins of the hydration force between lipid bilayers using all-atom simulations. , 235, 1-15	2010
Atomistic and mesoscale simulation of polymer electrolyte membranes based on sulfonated poly(ether ether ketone). 2010 , 487, 291-296	52
1045 Dynamics of impinging nanoscale jets. 2010 , 491, 177-182	6
Prediction of hydrogen solubility in heavy hydrocarbons over a range of temperatures and pressures using molecular dynamics simulations. 2010 , 299, 94-101	7
Size and temperature effects on the fracture mechanisms of silicon nanowires: Molecular dyna simulations. 2010 , 26, 1387-1401	mics 108
1042 Multiscale modeling of thermal conductivity of polymer/carbon nanocomposites. 2010 , 49, 155	55-1560 36
A closer look at the local responses of twin and grain boundaries in Cu to stress at the nanoscal with possible transition from the PH to the inverse PH relation. 2010 , 58, 2677-2684	le ₁₂
1040 Atomistic study of edge and screw <c +="" a=""> dislocations in magnesium. 2010, 58, 4332-4343</c>	106
Activated states for cross-slip at screw dislocation intersections in face-centered cubic nickel at copper via atomistic simulation. 2010 , 58, 5547-5557	nd 41
1038 A numerical test of stress correlations in fluctuating hydrodynamics. 2010 , 375, 327-336	17
Molecular dynamic investigation of mechanical properties of armchair and zigzag double-walle carbon nanotubes under various loading conditions. 2010 , 374, 969-974	d 23
Thermal conductivity and thermal rectification in carbon nanotubes with geometric variations of doped nitrogen: Non-equilibrium molecular dynamics simulations. 2010 , 374, 4885-4889	of ₂₆
1035 GPU-accelerated molecular modeling coming of age. 2010 , 29, 116-25	281
1034 Ab initio interionic potentials for UN by multiple lattice inversion. 2010 , 404, 6-8	6
1033 DislocationInterface interaction in nanoscale fcc metallic bilayers. 2010 , 37, 315-319	38

1032	Grain boundary characterization and energetics of superalloys. 2010 , 527, 7115-7125	73
1031	A slip model for micro/nano gas flows induced by body forces. 2010 , 8, 417-422	13
1030	Molecular dynamics simulation of nanoscale liquid flows. 2010 , 9, 1011-1031	112
1029	A general inelastic internal state variable model for amorphous glassy polymers. 2010 , 213, 71-96	39
1028	Quantifying power consumption variations of HPC systems using SPEC MPI benchmarks. 2010 , 25, 155-163	14
1027	Carbon nanotube-textured sand for controlling bioavailability of contaminated sediments. 2010 , 3, 412-422	11
1026	Effects of temperature and tilt angle on the grain boundary structure in silicon oxide: Molecular dynamics study. 2010 , 16, 163-169	2
1025	Simulation of molecular dynamics of silver subcritical nuclei and crystal clusters during solidification. 2010 , 53, 3203-3208	9
1024	Molecular Dynamics Simulation of Mechanical Properties of Single-Crystal Bismuth Telluride Nanowire. 2010 , 39, 1730-1734	14
1023	A Nonequilibrium Molecular Dynamics Study of In-Plane Thermal Conductivity of Silicon Thin Films. 2010 , 39, 1616-1620	5
1022	Effect of Topological Defects on Buckling Behavior of Single-walled Carbon Nanotube. 2011, 6, 28	8
1021	Silicon nanotubes with distinct bond lengths. 2010 , 47, 569-589	8
1020	Consideration of mechanical properties of single-walled carbon nanotubes under various loading conditions. 2010 , 12, 537-543	9
1019	Thermo-mechanical behavior of nano aluminum particles with oxide layers during melting. 2010 , 12, 2989-3002	39
1018	Compressibility of Thin Film Lubricants Characterized Using Atomistic Simulation. 2010, 38, 33-38	14
1017	Dynamic fracture kinetics, influence of temperature and microstructure in the atomistic model of aluminum. 2010 , 162, 127-136	25
1016	Long-term dynamic stability of discrete dislocations in graphene at finite temperature. 2010 , 166, 215-223	16
1015	Superplasticity in intermetallic NiAl nanowires via atomistic simulations. 2010 , 64, 879-881	11

1014	A molecular dynamics simulation of (110) surface premelting in Ni. 2010 , 63, 128-131	15
1013	Defect generation in nano-twinned, nano-grained and single crystal Cu systems caused by wear: A molecular dynamics study. 2010 , 63, 1116-1119	19
1012	Nanoindentation and plasticity in nanocrystalline Ni nanowires: A case study in size effect mitigation. 2010 , 63, 1136-1139	26
1011	Rule-based spatial modeling with diffusing, geometrically constrained molecules. 2010 , 11, 307	74
1010	Clay swelling [A challenge in the oilfield. 2010 , 98, 201-216	379
1009	Comparison of the Ewald and Wolf methods for modeling electrostatic interactions in nanowires. 2010 , 84, 1541-1551	20
1008	A flexible high-performance Lattice Boltzmann GPU code for the simulations of fluid flows in complex geometries. 2010 , 22, 1-14	89
1007	Correlation between dynamic heterogeneity and local structure in a room-temperature ionic liquid: a molecular dynamics study of [bmim][PF(6)]. 2010 , 11, 2001-10	64
1006	Chemistries for patterning robust DNA microbarcodes enable multiplex assays of cytoplasm proteins from single cancer cells. 2010 , 11, 3063-9	42
1005	ForceFit: a code to fit classical force fields to quantum mechanical potential energy surfaces. 2010 , 31, 2307-16	42
1004	Molecular Origins of the Mechanical Behavior of Hybrid Glasses. 2010 , 20, 2884-2892	62
1003	Simulation Schemes, Softwares, Lab Practice and Applications. 2010 , 343-473	
1002	Atomistic study of deposition process of Al thin film on Cu substrate. 2010 , 256, 5993-5997	19
1001	Molecular dynamic simulations of nanoindentation in aluminum thin film on silicon substrate. 2010 , 256, 6284-6290	74
1000	Study of AFM-based nanometric cutting process using molecular dynamics. 2010 , 256, 7160-7165	75
999	Formation of parallel (111) twin boundaries in silicon growth from the melt explained by molecular dynamics simulations. 2010 , 312, 1411-1415	38
998	The anisotropy of shock-induced melting of Pt observed in molecular dynamics simulations. 2010 , 374, 1579-1584	21
997	Heat capacities of both PMMA stereomers: Comparison between atomistic simulation and experimental data. 2010 , 51, 2106-2111	35

Molecular dynamics simulations of deformation mechanisms of amorphous polyethylene. 2010, 51, 6071-6083 263 996 Transmission of stresses in static and sheared granular beds: The influence of particle size, shearing 995 9 rate, layer thickness and sensor size. 2010, 203, 23-32 A single degree of freedom [bllipop[model for carbon nanotube bundle formation. 2010, 58, 409-427 61 994 Molecular dynamic simulation of fission fragment induced thermal spikes in UO2: Sputtering and 993 34 bubble re-solution. 2010, 399, 175-180 Molecular dynamics study of mechanical properties of bismuth telluride nanofilm. 2010, 405, 3190-3194 992 25 Coarse-graining atomistic dynamics of brittle fracture by finite element method. 2010, 26, 1402-1414 38 991 Plastic deformation in bi-metal multilayer nanowires. 2010, 87, 426-429 990 4 989 Cascade-driven mixing at metal oxide interfaces. 2010, 268, 3114-3116 3 Lattice dynamical finite-element method. 2010, 58, 510-523 988 19 987 Structural properties of materials created through freeze casting. 2010, 58, 709-715 55 Void initiation in fcc metals: Effect of loading orientation and nanocrystalline effects. 2010, 58, 4458-4477 986 131 Mechanisms of Guinier Preston zone hardening in the athermal limit. 2010, 58, 5797-5805 985 61 Optimizing load transfer in multiwall nanotubes through interwall coupling: Theory and simulation. 984 22 2010, 58, 6324-6333 Evolution of structure and free volume in symmetric tilt grain boundaries during dislocation 983 63 nucleation. 2010, 58, 6464-6473 Dislocation drag at the nanoscale. 2010, 58, 6535-6541 982 31 981 Parallel discrete element simulation of poly-dispersed granular material. 2010, 41, 52-63 49 Adsorption and diffusion of argon confined in ordered and disordered microporous carbons. 2010, 980 43 256, 5131-5136 Atomistic modeling of ®5n surface energies and adatom diffusivity. 2010, 256, 4402-4407 979 36

978	Mechanical and tribological properties of Ni/Al multilayers molecular dynamics study. 2010 , 257, 847-851	33
977	Molecular dynamics study on the effects of stamp shape, adhesive energy, and temperature on the nanoimprint lithography process. 2010 , 257, 1562-1572	42
976	Collaborative software infrastructure for adaptive multiple model simulation. 2010 , 199, 1352-1370	11
975	Molecular dynamics simulation of self-assembly structure for AOK based reverse micelle in supercritical CO2. 2010 , 367, 148-154	17
974	A molecular dynamics study of the mechanical properties of hydrogen functionalized graphene. 2010 , 48, 898-904	390
973	Modeling the structural evolution of carbide-derived carbons using quenched molecular dynamics. 2010 , 48, 1116-1123	150
972	Molecular simulation of nanoparticle diffusion at fluid interfaces. 2010 , 495, 55-59	25
971	An investigation of the phonon properties of silicon nanowires. 2010 , 49, 1095-1102	16
970	AtomSim: web-deployed atomistic dynamics simulator. 2010 , 43, 1553-1559	1
969	Anisotropic plasticity and chain orientation in polymer glasses. 2010 , 48, 1473-1482	27
968	Molecular dynamics simulations of semicrystalline polymers: Crystallization, melting, and reorganization. 2010 , 48, 2222-2232	44
967	Mechanical fatigue of hybrid glasses. 2010 , 6, 1892-6	6
966	Buckling of Carbon Nanotubes: a Molecular Static Approach. 2010 , 10, 27-30	1
965	Mechanics of carbon nanoscrolls: a review. 2010 , 23, 484-497	38
964	A kinetic model of fracture of simple liquids. 2010 , 48, 511-517	14
963	Atomistic simulation of the interaction of an electrolyte with graphite nanostructures in perspective supercapacitors. 2010 , 48, 837-845	10
962	20. Large Scale Simulations. 2010 , 437-464	
961	. 2010,	6

960 Failure mechanisms and electromechanical coupling in semiconducting nanowires. **2010**, 6, 40010

959	Thermal Analysis of Carbon Nanotubes Suspended in PAO Mixtures. 2010 ,	1
958	Towards the design of new and improved drilling fluid additives using molecular dynamics simulations. 2010 , 82, 43-60	17
957	Direct atomistic simulation of brittle-to-ductile transition in silicon single crystals. 2010 , 1272, 1	2
956	Swelling of K $+$, Na $+$ and Ca $2+$ -montmorillonites and hydration of interlayer cations: a molecular dynamics simulation. 2010 , 19, 109101	49
955	Surface effect on the self-equilibrium state and size-dependent elasticity of FCC thin films. 2010 , 18, 085006	15
954	Examining different NEMD methods in simulating nanoscale fluid at high shear rates. 2010 , 224, 19-29	2
953	Thermomechanical properties dependence on chain length in bulk polyethylene: Coarse-grained molecular dynamics simulations. 2010 , 25, 537-544	27
952	Investigations into the applicability of rubber elastic analogy to hardening in glassy polymers. 2010 , 18, 025001	10
951	Molecular Dynamics Simulations of Uniaxial Compression of Ceria and Gadolinia Doped Ceria. 2010 , 152-153, 1180-1183	
950	Large Scale Simulations. 2010 , 71, 437-463	2
949	The Research of Data Mining Based Sales Forecast. 2010 ,	3
948	Dynamics and diffusivellonformational coupling in polymer bulk samples and surfaces: a molecular dynamics study. 2010 , 12, 023001	5
947	Characterization of Complex Engineering Silicones by 1H Multiple Quantum NMR and Large Scale Molecular Dynamics Simulations. 2010 , 75-84	1
946	Ice crystallization in water's "no-man's land". 2010 , 132, 244504	146
945	A Framework for End-to-End Simulation of High-performance Computing Systems. 2010 , 86, 331-350	13
944	Structure, mechanical and thermodynamic stability of vacancy clusters in Cu. 2010 , 18, 055009	7
943	Multiscale Modeling of Contact-Induced Plasticity in Nanocrystalline Metals. 2010 , 151-172	1

942	Simulations of tensile failure in glassy polymers: effect of cross-link density. 2010 , 18, 055005	23
941	Molecular dynamics simulation of collective behaviour of Xe in UO 2. 2010 , 19, 057102	16
940	Molecular Dynamics Simulations of Thermal Properties of Solid Uranium Dioxide. 2010 , 27, 036501	3
939	Interaction of dislocations with incoherent interfaces in nanoscale FCCBCC metallic bi-layers. 2010 , $18,055010$	33
938	Nanotribology of water confined between hydrophilic alkylsilane self-assembled monolayers. 2010 , 18, 034005	22
937	A method for computing the solubility limit of solids: application to sodium chloride in water and alcohols. 2010 , 133, 124504	59
936	Investigation of Interfacial Thermal Resistance on Nano-Structures Using Molecular Dynamics Simulations. 2010 ,	
935	Dislocation mechanism of interface point defect migration. 2010 , 82,	31
934	Charge ordering induces a smectic phase in oblate ionic liquid crystals. 2010 , 105, 137801	19
933	Fluctuation electron microscopy of medium-range order in ion-irradiated zircon. 2010 , 90, 4661-4677	8
932	Effective elasticity of a flexible filament bound to a deformable cylindrical surface. 2010 , 104, 226101	14
931	Rotational relaxation times of individual compounds within simulations of molecular asphalt models. 2010 , 132, 184502	37
930	Tuning the thermal conductivity of graphene nanoribbons by edge passivation and isotope engineering: A molecular dynamics study. 2010 , 97, 133107	134
929	Anisotropic atomic motion at undercooled crystal/melt interfaces. 2010 , 82,	10
928	Atomic transformation pathways from terahertz radiation generated by shock-induced phase transformations. 2010 , 81,	4
927	Tuning the thermal conductivity of polymers with mechanical strains. 2010 , 81,	126
926	Capillary force induced structural deformation in liquid infiltrated elastic circular tubes. 2010 , 81,	14
925	Approaches to Mesoscale Modeling of Nanoparticle Tell Membrane Interactions. 2010,	1

924	⊞n grain-boundary structure and self-diffusivity via molecular dynamics simulations. 2010 , 81,	26
923	Molecular dynamics study of the ordering of carbon in highly supersaturated & Ee. 2010 , 81,	43
922	Deformation mechanisms and pseudoelastic behaviors in trilayer composite metal nanowires. 2010 , 81,	22
921	Partial-epitaxial morphology of graphene nanoribbon on the Si-terminated SiC(0001) surfaces. 2010 , 81,	12
920	Modeling the combined effect of surface roughness and shear rate on slip flow of simple fluids. 2010 , 81, 011606	53
919	Study of defects in Pd thin films on Au(100) using molecular dynamics. 2010 , 81,	8
918	Minimal energy packings and collapse of sticky tangent hard-sphere polymers. 2010 , 105, 068001	24
917	The interaction between electrolyte and surfaces decorated with charged groups: A molecular dynamics simulation study. 2010 , 132, 024704	18
916	Nanoscale metal-metal contact physics from molecular dynamics: the strongest contact size. 2010 , 104, 215504	13
915	Shear response of the \square <110> {221} symmetric tilt grain boundary in fcc metals studied by atomistic simulation methods. 2010 , 82,	64
914	Precursor film in dynamic wetting, electrowetting, and electro-elasto-capillarity. 2010, 104, 246101	157
913	A molecular dynamics study of deformation induced phase transformations at fault bands. 2010 , 240, 012105	2
912	Size-dependent elastic properties of Au nanowires under bending and tensionBurfaces versus core nonlinearity. 2010 , 108, 083506	29
911	Superelasticity in bcc nanowires by a reversible twinning mechanism. 2010 , 82,	82
910	Frequency and polarization dependence of thermal coupling between carbon nanotubes and SiO2. 2010 , 108, 103502	34
909	Mesoscale hydrodynamics via stochastic rotation dynamics: comparison with Lennard-Jones fluid. 2010 , 132, 174106	34
908	Nanotwinned fcc metals: Strengthening versus softening mechanisms. 2010 , 82,	108
907	Towards microsecond biological molecular dynamics simulations on hybrid processors. 2010 ,	6

906	Analytical model and molecular dynamics simulations of the size dependence of flow stress in amorphous intermetallic nanowires at temperatures near the glass transition. 2010 , 81,	12
905	Compressive pseudoelastic behavior in copper nanowires. 2010 , 81,	10
904	Exploiting 162-Nanosecond End-to-End Communication Latency on Anton. 2010 ,	15
903	Contact and friction of nanoasperities: effects of adsorbed monolayers. 2010 , 81, 016102	56
902	MOLECULAR DYNAMICS SIMULATION OF NANOMETRIC CUTTING. 2010 , 14, 423-439	13
901	Inverse martensitic transformation in Zr nanowires. 2010 , 81,	23
900	The multiscale coarse-graining method. VI. Implementation of three-body coarse-grained potentials. 2010 , 132, 164107	92
899	Thermal boundary resistance from mode energy relaxation times: Case study of argon-like crystals by molecular dynamics. 2010 , 108, 094324	47
898	Efficient non-reflecting boundary condition constructed via optimization of damped layers. 2010 , 81,	11
897	Carrier heating in disordered conjugated polymers in electric field. 2010 , 81,	12
896	Compression-induced transformation of aldehydes into polyethers: a first-principles molecular dynamics study. 2010 , 132, 134513	7
895	Rotation-dependent epitaxial relations between graphene and the Si-terminated SiC substrate. 2010 , 82,	8
894	Strain-induced Wurtzite to h-BN Phase Transformation in Zinc Oxide nanorods. 2010,	
893	Carbon nanotube initiated formation of carbon nanoscrolls. 2010 , 97, 081909	64
892	Quantum chemistry and molecular dynamics studies of the entropic elasticity of localized molecular kinks in polyisoprene chains. 2010 , 133, 084903	9
891	In silico assembly and nanomechanical characterization of carbon nanotube buckypaper. 2010 , 21, 265706	77
890	Dependencies of the thermal conductivity of individual single-walled carbon nanotubes. 2010 , 224, 41-54	2
889	Deformation micromechanisms of collagen fibrils under uniaxial tension. 2010 , 7, 839-50	96

888	protein A to human brain microvascular endothelial cells: identification of critical mutations that prevent E. coli meningitis. 2010 , 285, 37753-61	27
887	Investigations on the deformation behavior of polycrystalline Cu nanowires and some factors affecting the modulus and yield strength. 2010 , 18, 055011	4
886	Energetics and structure of <0 0 1> tilt grain boundaries in SiC. 2010 , 18, 075009	35
885	Shear deformation kinematics of bicrystalline grain boundaries in atomistic simulations. 2010 , 18, 015002	34
884	Asymptotic solution for first and second order linear Volterra integro-differential equations with convolution kernels. 2010 , 43, 375203	17
883	Loading path effect on the mechanical behaviour and fivefold twinning of copper nanowires. 2010 , 43, 335402	14
882	Molecular Dynamics Study on Interaction between Voids for Pure Aluminum. 2010 , 452-453, 845-848	
881	A molecular dynamics study of void interaction in copper. 2010 , 10, 012175	6
880	A topology preserving method for generating equilibrated polymer melts in computer simulations. 2010 , 133, 164902	14
879	Main phase transition in lipid bilayers: Phase coexistence and line tension in a soft, solvent-free, coarse-grained model. 2010 , 132, 155104	57
878	Large Scale Molecular Dynamics Simulations of Vapor Phase Lubrication for MEMS. 2010 , 24, 2453-2469	13
877	Anomalous heat conduction behavior in thin finite-size silicon nanowires. 2010 , 21, 155704	31
876	Thermal conductivity of GaAs/AlAs superlattices and the puzzle of interfaces. 2010, 22, 475001	29
875	Coupled effects of size and uniaxial force on phase transitions in copper nanowires. 2010 , 21, 185703	11
874	A plasticity model with microstructure evolution for quasi-static granular flows. 2010,	2
873	Quantum mechanics based force field for carbon (QMFF-Cx) validated to reproduce the mechanical and thermodynamics properties of graphite. 2010 , 133, 134114	16
872	On the hydration of the phosphocholine headgroup in aqueous solution. 2010 , 133, 145103	70
871	Toward Distinct Element Method Simulations of Carbon Nanotube Systems. 2010 , 1,	10

870	NANOSCALE VOID GROWTH IN MAGNESIUM: A MOLECULAR DYNAMICS STUDY. 2010 , 02, 191-205	15
869	Identifying software usage at HPC centers with the automatic library tracking database. 2010,	4
868	Coarse-grained models to study dynamics of nanoscale biomolecules and their applications to the ribosome. 2010 , 22, 453101	30
867	Micromechanics of Soft Particle Glasses. 2010 , 117-161	58
866	Grain boundary sliding in irradiated stressed Fe-Ni bicrystals: a molecular dynamics study. 2010 , 22, 345006	2
865	The thermomutability of single-walled carbon nanotubes by constrained mechanical folding. 2010 , 21, 365708	9
864	Simplified particulate model for coarse-grained hemodynamics simulations. 2010 , 82, 056710	37
863	1D-to-3D transition of phonon heat conduction in polyethylene using molecular dynamics simulations. 2010 , 82,	88
862	An atomistic study of dislocation-solute interaction in Mg-Al alloys. 2010 , 10, 012177	5
861	Molecular Dynamics Modeling of Nanodroplets and Nanoparticles. 2010 , 151-183	1
860	Cleavage Energy of Alkylammonium-Modified Montmorillonite and Relation to Exfoliation in Nanocomposites: Influence of Cation Density, Head Group Structure, and Chain Length. 2010 , 22, 1595-1605	85
859	Two-phase thermodynamic model for efficient and accurate absolute entropy of water from molecular dynamics simulations. 2010 , 114, 8191-8	218
858	Reply to Comment on E ntangled Polymer Melts: Relation between Plateau Modulus and Stress Autocorrelation Function 2010 , 43, 3984-3985	3
857	Design of Very High-Strength Aligned and Interconnected Carbon Nanotube Fibers Based on Molecular Dynamics Simulations. 2010 ,	
856	A direct method to calculate thermal conductivity and its application in solid HMX. 2010 , 22, 185404	21
855	Molecular Modeling of Matter: Impact and Prospects in Engineering. 2010 , 49, 3026-3046	86
854	Recrystallization of picosecond laser-melted ZnO nanoparticles in a liquid: a molecular dynamics study. 2010 , 132, 164504	20
853	Phase behavior of repulsive polymer-tethered colloids. 2010 , 132, 014901	8

852	Stress-temperature scaling for steady-state flow in metallic glasses. 2010 , 104, 205701	162
851	Molecular Dynamics Simulation of Shock Wave Propagation through RDX Crystal Lattice. 2010 , 28, 78-91	
850	Liquid crystal phase and waterlike anomalies in a core-softened shoulder-dumbbells system. 2010 , 132, 164505	18
849	A Magnetically Controlled Molecular Nanocontainer as a Drug Delivery System: The Effects of Carbon Nanotube and Magnetic Nanoparticle Parameters from Monte Carlo Simulations. 2010 , 114, 21299-2	1308
848	Improved united-atom force field for 1-alkyl-3-methylimidazolium chloride. 2010 , 114, 4572-82	68
847	Hydrogen bond networks in graphene oxide composite paper: structure and mechanical properties. 2010 , 4, 2300-6	568
846	Many-body interactions and coarse-grained simulations of structure of nanoparticle-polymer melt mixtures. 2010 , 133, 144904	28
845	Boundary conditions at the liquid-liquid interface in the presence of surfactants. 2010 , 26, 10693-702	18
844	The geometric structure of single-walled nanotubes. 2010 , 2, 859-72	28
843	A systematically coarse-grained model for DNA and its predictions for persistence length, stacking, twist, and chirality. 2010 , 132, 035105	100
842	Molecular dynamics investigation on the atomic-scale indentation and friction behaviors between diamond tips and copper substrate. 2010 , 19, 723-728	12
841	Structural, Electronic, and Thermoelectric Properties of BiSb Nanotubes. 2010 , 114, 21234-21239	12
840	Visualization and analysis of atomistic simulation data with OVITOE Open Visualization Tool. 2010 , 18, 015012	5508
839	Micellization behavior of coarse grained surfactant models. 2010 , 132, 114902	64
838	Modeling of Thermal Conductance at Transverse CNTIINT Interfaces. 2010 , 114, 16223-16228	70
837	Island shape controls magic-size effect for heteroepitaxial diffusion. 2010 , 108, 023521	10
836	Coarse-Grained Computer Simulations of Polymer/Fullerene Bulk Heterojunctions for Organic Photovoltaic Applications. 2010 , 6, 526-37	148
835	Surface segregation of bimetallic alloys in nanoscale confinement. 2010 , 97, 153107	7

834	Amorphous precursors in the nucleation of clathrate hydrates. 2010 , 132, 11806-11	306
833	Molecular dynamics simulation of O2 sticking on Pt(111) using the ab initio based ReaxFF reactive force field. 2010 , 133, 084703	42
832	Water is the key to nonclassical nucleation of amorphous calcium carbonate. 2010 , 132, 17623-34	283
831	Molecular dynamics simulations as a way to investigate the local physics of contact mechanics: a comparison between experimental data and numerical results. 2010 , 43, 455406	13
830	Clay minerals mediate folding and regioselective interactions of RNA: a large-scale atomistic simulation study. 2010 , 132, 13750-64	56
829	Limitations and recommendations for the calculation of shear viscosity using reverse nonequilibrium molecular dynamics. 2010 , 132, 014103	53
828	Historical Perspective and Current Outlook for Molecular Dynamics As a Chemical Engineering Tool. 2010 , 49, 3059-3078	86
827	Temperature and strain-rate dependent fracture strength of graphene. 2010 , 108, 064321	258
826	Zwitterionic lipid assemblies: molecular dynamics studies of monolayers, bilayers, and vesicles using a new coarse grain force field. 2010 , 114, 6836-49	208
825	Kinetics of Diblock Copolymer Micellization by Dissipative Particle Dynamics. 2010 , 43, 3521-3531	82
824	Nucleation pathways of clathrate hydrates: effect of guest size and solubility. 2010 , 114, 13796-807	149
823	Coupling between chemical and dynamic heterogeneities in a multicomponent bulk metallic glass. 2010 , 81,	66
822	Static properties of polymer melts in two dimensions. 2010 , 132, 184904	45
821	Nanoscale modelling of mechanical properties of asphaltEggregate interface under tensile loading. 2010 , 11, 393-401	34
820	Model for random packing of polydisperse frictionless spheres. 2010 , 6, 2949	42
819	A molecular simulation probing of structure and interaction for supramolecular sodium dodecyl sulfate/single-wall carbon nanotube assemblies. 2010 , 10, 985-91	133
818	Structural disjoining potential for grain-boundary premelting and grain coalescence from molecular-dynamics simulations. 2010 , 81, 031601	40
817	First-principles and classical molecular dynamics simulation of shocked polymers. 2010 , 81,	205

816	Fluctuations of water near extended hydrophobic and hydrophilic surfaces. 2010 , 114, 1632-7	223
815	Eigenstress model for surface stress of solids. 2010 , 81,	58
814	Multi-scale simulation of partially unzipped CNT hetero-junction Tunneling Field Effect Transistor. 2010 ,	4
813	Large-scale density functional theory investigation of failure modes in ZnO nanowires. 2010 , 10, 3432-8	32
812	Supported bimetallic Pt-Au nanoparticles: Structural features predicted by molecular dynamics simulations. 2010 , 81,	32
811	Molecular dynamics simulations of CO2 at an ionic liquid interface: adsorption, ordering, and interfacial crossing. 2010 , 114, 11827-37	90
810	Interfacial reactions of ozone with surfactant protein B in a model lung surfactant system. 2010 , 132, 2254-63	44
809	Effect of the stress field of an edge dislocation on carbon diffusion in ∃ron: Coupling molecular statics and atomistic kinetic Monte Carlo. 2010 , 82,	37
808	Molecular dynamics study of the structures and dynamics of the iodine molecules confined in AlPO(4)-11 crystals. 2010 , 114, 16481-6	25
807	Reactive forcefield for simulating gold surfaces and nanoparticles. 2010 , 81,	52
806	Self-Assembly of Star-Polymer-Attached Nanospheres for Polymer Nanocomposites. 2010 , 114, 5732-5740	13
805	Dislocation detection algorithm for atomistic simulations. 2010 , 18, 025016	105
804	Unsteady Shear of Dense Assemblies of Cohesive Granular Materials under Constant Volume Conditions. 2010 , 49, 5153-5165	6
803	Splaying of aliphatic tails plays a central role in barrier crossing during liposome fusion. 2010 , 114, 11061-8	53
802	Spontaneous curling of graphene sheets with reconstructed edges. 2010 , 4, 4840-4	77
801	Time resolved studies of interfacial reactions of ozone with pulmonary phospholipid surfactants using field induced droplet ionization mass spectrometry. 2010 , 114, 9496-503	30
800	A many-body dissipative particle dynamics study of spontaneous capillary imbibition and drainage. 2010 , 26, 9533-8	57
799	Molecular dynamics of ion hydration in the presence of small carboxylated molecules and implications for calcification. 2010 , 114, 10488-95	43

Numerical study of stress tensors in Poiseuille flow of suspensions. **2010**, 82, 021401

797	Molecular dynamics simulations of grafted layers of bottle-brush polyelectrolytes. 2010 , 26, 18374-81	18
796	Defining Condensed Phase Reactive Force Fields from ab Initio Molecular Dynamics Simulations: The Case of the Hydrated Excess Proton. 2010 , 6, 3223-32	36
795	Molecular origin of fast water transport in carbon nanotube membranes: superlubricity versus curvature dependent friction. 2010 , 10, 4067-73	537
794	Implementation of molecular dynamics and its extensions with the coarse-grained UNRES force field on massively parallel systems; towards millisecond-scale simulations of protein structure, dynamics, and thermodynamics. 2010 , 6, 890-909	37
793	Molecular Dynamics Simulations of Folding of Supported Graphene. 2010 , 114, 22472-22477	46
79²	Adhesion of nanoparticles. 2010 , 26, 12973-9	75
791	Molecular dynamics study of the behavior of selected nanoscale building blocks in a gel-phase lipid bilayer. 2010 , 114, 9165-72	13
790	Structure and dynamics of tetrahalomethane adsorption on (001) surfaces of graphite and Equartz. 2010 , 114, 13970-81	6
789	Melt Structure and Dynamics of Unentangled Polyethylene Rings: Rouse Theory, Atomistic Molecular Dynamics Simulation, and Comparison with the Linear Analogues. 2010 , 43, 10692-10713	94
788	Molecular Simulation of Polyelectrolye Conformational Dynamics under an AC Electric Field. 2010 , 43, 4805-4813	18
787	Role of local order in the small-scale plasticity of model amorphous materials. 2010 , 82, 066116	42
786	Designed AB Copolymers as Efficient Stabilizers of Colloidal Particles. 2010 , 43, 5442-5449	16
785	Formation of Interconnected Aggregates in Aqueous Dicationic Ionic Liquid Solutions. 2010 , 6, 873-9	41
784	A two-temperature model of radiation damage in Equartz. 2010 , 133, 144711	23
783	Janssen effect and the stability of quasi-two-dimensional sandpiles. 2010 , 82, 031302	3
782	Molecular Simulation of the Thermal and Transport Properties of Three Alkali Nitrate Salts. 2010 , 49, 559-571	53
781	Molecular dynamics simulation of fractal aggregate diffusion. 2010 , 82, 051402	11

7 ⁸ 0	Polyelectrolyte Brushes: MD Simulation and SCF Theory. 2010 , 43, 7845-7851	31
779	Effect of the Electrostatic Interactions on Stretching of Semiflexible and Biological Polyelectrolytes. 2010 , 43, 2589-2604	15
778	Viscosities of the mixtures of 1-ethyl-3-methylimidazolium chloride with water, acetonitrile and glucose: a molecular dynamics simulation and experimental study. 2010 , 114, 5790-4	51
777	Water nanoconfinement induced thermal enhancement at hydrophilic quartz interfaces. 2010 , 10, 279-85	60
776	Atomistic simulations of structure of solvated sulfonated poly(ether ether ketone) membranes and their comparisons to nafion: II. Structure and transport properties of water, hydronium ions, and methanol. 2010 , 114, 8367-73	34
775	Brownian Dynamics Simulations on Self-Assembly Behavior of H-Shaped Copolymers and Terpolymers 2010 , 43, 6903-6911	16
774	Coarse-grained molecular dynamics simulations of DNA condensation by block copolymer and formation of core-corona structures. 2010 , 114, 6225-32	42
773	Predicting polymer nanofiber interactions via molecular simulations. 2010 , 2, 1164-72	25
772	Understanding Dynamics in Binary Mixtures of Entangledcis-1,4-Polybutadiene Melts at the Level of Primitive Path Segments by Mapping Atomistic Simulation Data onto the Tube Model. 2010 , 43, 8239-8250	28
771	Optimal Utilization of Heterogeneous Resources for Biomolecular Simulations. 2010 ,	10
77°	A MD-based method to calculate free energy for crystalline structures: from basic theory to application. 2010 , 43, 455002	1
769	Lattice Green⊠ function for crystals containing a planar interface. 2010 , 82,	5
768	A Graphics Processing Unit Implementation of Coulomb Interaction in Molecular Dynamics. 2010 , 6, 3058-65	32
767	Force-matched embedded-atom method potential for niobium. 2010 , 81,	97
766	Viscoplasticity and large-scale chain relaxation in glassy-polymeric strain hardening. 2010 , 82, 041803	22
765	Single and multi-step phase transformation in CuZr nanowire under compressive/tensile loading. 2010 , 18, 679-687	39
764	Asymmetry in structural and thermo-mechanical behavior of intermetallic NiAl nanowire under tensile/compressive loading: A molecular dynamics study. 2010 , 18, 1565-1571	16
763	Atomistic simulations of stress corrosion cracking. 2010 , 52, 1247-1257	12

762	Molecular dynamics investigation of MgOtaOBiO2 liquids: Influence of pressure and composition on density and transport properties. 2010 , 275, 50-57	32
761	MD simulations of molybdenum disulphide (MoS2): Force-field parameterization and thermal transport behavior. 2010 , 48, 101-108	131
760	Bioinspired nanoporous silicon provides great toughness at great deformability. 2010 , 48, 303-309	46
759	Molecular dynamics study on thermo-mechanical properties of bismuth telluride bulk. 2010 , 48, 343-348	18
758	Cluster dynamics method for simulation of dynamic processes of continuum mechanics. 2010 , 49, S32-S36	2
757	Dynamical properties of deeply undercooled and amorphous systems: Combined classical and ab initio molecular dynamics simulations approaches. 2010 , 49, S272-S275	O
756	On the atomistic mechanisms of grain boundary migration in [001] twist boundaries: Molecular dynamics simulations. 2010 , 48, 773-782	12
755	Atomistic model of type-II twin boundary. 2010 , 49, 882-887	5
754	Effects of pores on shear bands in metallic glasses: A molecular dynamics study. 2010 , 50, 211-217	35
753	Buckling behavior of carbon nanotube-based intramolecular junctions under compression: Molecular dynamics simulation and finite element analysis. 2010 , 50, 253-259	41
752	Self-assembly of carbon nanotubes and boron nitride nanotubes into coaxial structures. 2010 , 50, 645-650	9
751	Computing free energies of protein conformations from explicit solvent simulations. 2010 , 52, 115-21	12
75°	The strength of single crystal copper under uniaxial shock compression at 100 GPa. 2010 , 22, 065404	60
749	Phonon instabilities in uniaxially compressed fcc metals as seen in molecular dynamics simulations. 2010 , 81,	20
748	Plastic deformation of nanocrystalline copper-antimony alloys. 2010 , 25, 411-421	27
747	Shear rheology of extended nanoparticles. 2010 , 82, 010201	10
746	Atomistic modeling of interfaces and their impact on microstructure and properties. 2010, 58, 1117-1151	379
745	Second-generation charge-optimized many-body potential for Si/SiO2 and amorphous silica. 2010 , 82,	79

744	Supercritical fluid behavior at nanoscale interfaces: Implications for CO2 sequestration in geologic formations. 2010 , 90, 2339-2363	96
743	Atom-by-atom simulations of chemical vapor deposition of nanoporous hydrogenated silicon nitride. 2010 , 107, 083501	20
742	Distribution and Diffusion of Water in Model Epoxy Molding Compound: Molecular Dynamics Simulation Approach. 2010 , 33, 333-339	20
741	Mechanical properties of methyl functionalized graphene: a molecular dynamics study. 2010 , 21, 115709	92
740	Coarse-grained potential models for phenyl-based molecules: II. Application to fullerenes. 2010 , 114, 6394-400	35
739	Water filling of hydrophilic nanopores. 2010 , 133, 034513	37
738	Liquid-vapor oscillations of water nanoconfined between hydrophobic disks: thermodynamics and kinetics. 2010 , 114, 7320-8	41
737	The anomalously high melting temperature of bilayer ice. 2010 , 132, 124511	74
736	Comment on "pumping of confined water in carbon nanotubes by rotation-translation coupling". 2010 , 105, 209401; author reply 209402	30
735	Molecular dynamics simulation on plasticity deformation mechanism and failure near void for magnesium alloy. 2010 , 20, s519-s522	9
734	Energetics and Vibronics Analyses of the Enzymatic Coupled Electron Proton Transfer From NfsA Nitroreductase to Trinitrotoluene. 2010 , 9, 543-553	5
733	Sponge Behaviors of Functionalized Few-Walled Carbon Nanotubes. 2010 , 114, 14868-14875	6
732	Effect of particle shape and charge on bulk rheology of nanoparticle suspensions. 2010 , 132, 184509	47
731	Stress relaxation in entangled polymer melts. 2010 , 105, 068301	80
730	Molecular dynamics simulations of supramolecular polymer rheology. 2010 , 133, 184904	16
729	Electron-ion coupling effects on simulations of radiation damage in pyrochlore waste forms. 2010 , 22, 225405	17
728	Numerical investigations into mechanical properties of hexagonal silicon carbon nanowires and nanotubes. 2010 , 2, 1733-9	9
727	Detailed molecular dynamics simulations of a model NaPSS in water. 2010 , 114, 9391-9	46

Molecular dynamics simulations of oblique phonon scattering at semiconductor interfaces. **2010**,

7 2 5	A Component-Based Framework for Smoothed Particle Hydrodynamics Simulations of Reactive Fluid Flow in Porous Media. 2010 , 24, 228-239	13
724	Atomistic simulations of structure of solvated sulfonated poly(ether ether ketone) membranes and their comparisons to nafion: I. Nanophase segregation and hydrophilic domains. 2010 , 114, 8357-66	57
723	Mechanomutable properties of a PAA/PAH polyelectrolyte complex: rate dependence and ionization effects on tunable adhesion strength. 2010 , 6, 4175	78
722	Nanomechanics of biologically inspired helical silica nanostructures. 2010 , 224, 93-100	2
721	Large-scale atomistic simulation of a nanosized fibril formed by thiophenepeptide holecular chimeras 2010 , 6, 1453	7
720	Tuning Thermal Conductivity With Mechanical Strain. 2010,	
719	Effects of twin and surface facet on strain-rate sensitivity of gold nanowires at different temperatures. 2010 , 81,	33
718	The crucial role of chemical detail for slip-boundary conditions: molecular dynamics simulations of linear oligomers between sliding aluminum surfaces. 2010 , 18, 034004	19
717	Molecular Dynamics Study of Size Effect on Uniaxial Tension of Single Crystal Cu Nanowires. 2010 , 160-162, 682-686	
716	Fluorescence resonance energy transfer between phenanthrene and PAMAM dendrimers. 2010 , 12, 9285-91	33
715	Geometric methods for microstructure rendition and atomic characterization of poly- and nano-crystalline materials. 2010 , 90, 2191-2222	23
714	Reconfigurable assemblies of shape-changing nanorods. 2010 , 4, 2585-94	43
713	Cluster Formation by Charged Nanoparticles on a Surface in Aqueous Solution. 2010 , 114, 3754-3762	20
712	Modeling of Mechanical Behavior of Pillard Graphene Structures. 2010,	1
711	Multiscale Modeling of Nanoparticle Reinforced Polymers Using Statistical Coupling of MD and MPM. 2010 ,	
710	Atomistic Modeling of Cross-linked Epoxy Polymer. 2010,	5
709	Simulation of Gas-Surface Interactions Using ReaxFF Molecular Dynamics: Oxygen Adsorption on Platinum. 2010 ,	2

(2023-2010)

708	Modeling Air-SiO2 Surface Catalysis Under Hypersonic Conditions with ReaxFF Molecular Dynamics. 2010 ,	3
707	Atomistic Modeling of the Decomposition of Charring Ablators. 2010,	2
706	Improvements in Nanoparticle Dispersion Methods for Solid Propellants. 2010,	
705	Electron-beam-assisted superplastic shaping of nanoscale amorphous silica. 2010 , 1, 24	244
704	THOR: A Transparent Heterogeneous Open Resource framework. 2010 ,	2
703	Predicting water sorption and volume swelling in dense polymer systems via computer simulation. 2010 , 114, 17013-24	31
702	Discrete plasticity in sub-10-nm-sized gold crystals. 2010 , 1, 144	240
701	Study on nanometer cutting mechanism of single crystal silicon at different temperatures. 2023 , 93, 275-286	Ο
700	The interplay between solute atoms and vacancy clusters in magnesium alloys. 2023 , 249, 118805	О
699	Diffusion bonding of high entropy alloy and stainless steel at a relative lower temperature via surface nano-crystallization treatment. 2023 , 24, 475-487	Ο
698	Influence of matrix recrystallization and nanofiller porosity on the interfacial properties of holey graphene-aluminium nanocomposites. 2023 , 312, 116856	0
697	Effect of graphene substrate on melting of Cu nanoparticles. 2023, 657, 414817	O
696	A comprehensive atomistic investigation on the cascade induced helium bubble motion in bcc iron for neutron irradiated RAFM steels. 2023 , 578, 154373	0
695	The effect of glass structure and local rare earth site symmetry on the optical properties of rare earth doped alkaline earth aluminosilicate glasses. 2023 , 249, 118811	O
694	A multiscale and multiphysics framework to simulate radiation damage in nano-crystalline materials. 2023 , 578, 154347	О
693	Molecular dynamics study of grain boundary and radiation effects on tritium population and diffusion in zirconium. 2023 , 578, 154376	O
692	Irradiation-accelerated corrosion/oxidation of the Cr coating prepared by arc-ion plating. 2023, 406, 112252	О
691	Effects of cooling rate on the glass formation process and the microstructural evolution of Silver mono-component metallic glass. 2023 , 569, 111873	O

690	Atomistic modeling to the investigation of irradiation effect on optical properties of LiI/ZnS scintillator in a research reactor-based neutron radiography facility. 2023 , 538, 1-7	O
689	Performance enhancement of nanoscale heat pipe with hydrophilic/hydrophobic pattern. 2023 , 144, 106767	O
688	A chemo-mechanical coupling model of oxidation and interlayer cracking of copper nanowires. 2023 , 174, 105259	O
687	Atomic-scale deformation mechanisms of nano-polycrystalline Cu/Al layered composites: a´molecular dynamics simulation. 2023 , 24, 1177-1189	O
686	Atomic and electronic structure of grain boundaries in a-Al2O3: A combination of machine learning, first-principles calculation and electron microscopy. 2023 , 229, 115368	O
685	Prediction of photogalvanic effect enhancement in Janus transition metal dichalcogenide monolayers induced by spontaneous curling. 2023 , 619, 156730	O
684	Atomistic simulations of defect clustering evolution in heavily irradiated Ti35 alloy. 2023, 211, 111952	O
683	Inhibition of voltage-gated sodium ion channel by corannulene and computational inversion blockage underlying mechanisms. 2023 , 656, 70-77	O
682	Tailored rigid-flexible interphase of M40X composites via block copolymers: A combined method of experimental analysis and molecular dynamic simulation. 2023 , 257, 110674	O
681	Free standing nanoindentation of penta-graphene via molecular dynamics: Mechanics and deformation mechanisms. 2023 , 180, 104628	O
680	Multiscale analysis of nano-powder compaction process using the FEMMD technique. 2023 , 423, 118507	Ο
679	Mesoscale modeling to study isolated asphaltene agglomerates. 2023 , 379, 131249	O
678	Exploring the basal/prismatic slip transfer at grain boundaries in magnesium: A molecular dynamic simulation. 2023 , 212, 111995	O
677	Origin of enhanced zone lines in field evaporation maps. 2023 , 230, 115406	O
676	Dilute viscoelastic polymer solutions for dielectric heat transfer applications: A molecular dynamics study. 2023 , 18, 100333	O
675	A nanoscroll robustly formed by self-folding a Egraphyne ribbon on a CNT. 2023 , 225, 112163	O
674	Revealing multiple strengthening transitions in crystalline-amorphous nanolaminates through molecular dynamics. 2023 , 35, 105675	O
673	First-principles calculations of the viscosity in multicomponent metallic melts: Al-Cu-Ni as a test case. 2023 , 380, 121751	O

672	Effect of functionalization and defects on thermal conductivity of graphene sheets modified asphalt nanocomposites. 2023 , 621, 156804	О
671	Dislocation reactions dominated pop-in events in nanoindentation of Ni-based single crystal superalloys. 2023 , 200, 112883	О
670	MgO/Molten salt interfacial thermal transport and its consequences on thermophysical property enhancement: A molecular dynamics study. 2023 , 207, 124022	О
669	Diffraction and transmission antiresonances of lattice waves in sparse two-dimensional arrays of defect atoms. 2023 , 553, 117663	O
668	Molecular dynamics study on the kinematic viscosity, density and structure of fuel blends containing n-decane and biofuel compound of ethyl decanoate or ethyl dodecanoate. 2023 , 379, 121680	О
667	Molecular dynamics simulations of CaCl2NaCl molten salt based on the machine learning potentials. 2023 , 254, 112275	Ο
666	Size-dependent shape characteristics of 2D crystal blisters. 2023 , 175, 105286	0
665	Influence of HCP/BCC interface orientation on the tribological behavior of Zr/Nb multilayer during nanoscratch: A combined experimental and atomistic study. 2023 , 249, 118832	1
664	Atomistic characterization of impact bonding in cold spray deposition of copper. 2023, 28, 101736	О
663	Small-data-based machine learning interatomic potentials for graphene grain boundaries enabled by structural unit model. 2023 , 11, 100260	O
662	The study on the dielectric properties of structural changes of surfactant aqueous solution by molecular dynamics simulation. 2023 , 379, 121622	О
661	Water desalination through FAU zeolite studied by using molecular dynamics simulations. 2023 , 380, 121683	O
660	Effects of pressure on microstructure evolution of liquid Fe BB i alloy during rapid solidification: A molecular dynamics study. 2023 , 121, 108456	0
659	A physically-based constitutive model for a novel heat resistant martensitic steel under different cyclic loading modes: Microstructural strengthening mechanisms. 2023 , 165, 103611	O
658	Effects of temperature on the deformation of 6HBiC during nanoscratching. 2023, 523, 204843	О
657	The molecular dynamics description of electric field effect on nano-pumping performance of boron-nitride nanotube (BNNT) in the presence of vacancy defect. 2023 , 666, 131322	O
656	Properties of Pluronic F68 and F127 micelles interacting furosemide from coarse-grained molecular simulations as validated by experiments. 2023 , 666, 131352	0
655	Stress overshoot behavior in polymer nanocomposites filled with spherical nanoparticles under steady shear flow via molecular dynamics simulation. 2023 , 35, 105573	O

654	Dynamic microstructure evolution of charged kaolinites with counterions during hydration large-scale molecular dynamics study. 2023 , 158, 105334	O
653	Bauschinger effect on wear of cold-worked Cu and Mg 🖪 study combining molecular dynamics modeling and experimental investigation. 2023 , 522, 204726	O
652	Rejuvenation behavior and microstructural evolution of Cu-Zr metallic glass during multiple recovery annealing treatment via molecular dynamic simulation. 2023 , 945, 169294	0
651	The MD simulation of friction heat dissipation and generation in high-speed dry sliding system. 2023 , 9, 101-112	O
650	Sustainable steady-state serrated flow induced by modulating deformation sequence in bulk metallic glass. 2023 , 946, 169308	O
649	Probing plastic mechanisms in gradient dual-phase high-entropy alloys under nanoindentation. 2023 , 946, 169424	O
648	Fundamental abrasive contact at high speeds: Scratch testing in experiment and simulation. 2023 , 522, 204696	0
647	Controlling self-assembling co-polymer coatings of hydrophilic polysaccharide substrates via co-polymer block length ratio. 2023 , 640, 809-819	O
646	How droplets pin on solid surfaces. 2023, 640, 940-948	O
645	Full-scale simulation and experimental verification of the phase-transition temperature of a VO2 nanofilm as smart window materials. 2023 , 35, 105758	O
644	Research on CO2 capture by imidazolium and alkali metal salt hybrid ionic liquids. 2023, 379, 121646	O
643	Surface modification strategy for controlling wettability and ionic diffusion behaviors of calcium silicate hydrate. 2023 , 622, 156993	O
642	Combining tensile test results with atomistic predictions of elastic modulus of graphene/polyamide-6,6 nanocomposites. 2023 , 35, 105636	0
641	Effect of interfacial stability on microstructure and properties of carbon fiber reinforced aluminum matrix composites. 2023 , 38, 102816	O
640	Molecular dynamics simulations of warm laser shock peening for monocrystalline nickel. 2023, 35, 105626	0
639	A comprehensive experimental study and numerical analysis of coefficient of friction of nanocomposite coatings. 2023 , 301, 127550	O
638	On ionic transport through pores in a borophenegraphene membrane. 2023 , 30, 101512	О
637	Effects of $\chi'(\chi'=2.5, SO2)$ and N2O) mole fractions on adsorption behavior and phase equilibrium properties of CO2 $'+\chi'$ mixed gas hydrate. 2023 , 380, 121661	O

636	Effect of molecular aspect ratio on structure, dynamics and phase stability of thermotropic liquid crystals studied by molecular dynamics simulation. 2023 , 366-367, 115147	0
635	Exploring the potential of MXene nanoslit for water desalination through molecular dynamics simulations. 2023 , 556, 116560	O
634	Investigation of the mechanical stability of polyethylene glycol hydrogel reinforced with cellulose nanofibrils for wound healing: Molecular dynamics simulation. 2023 , 151, 1-7	O
633	Stability and structure of multiply occupied sII CO2 clathrate hydrates: A possibility for carbon capturing. 2023 , 380, 121746	1
632	Controlled stretching and splitting behaviors of nanodroplets by designing surface wettability patterns. 2023 , 273, 118635	O
631	Molecular dynamics simulation of phase transformation and wear behavior of Ni35Al30Co35 high temperature shape memory alloy. 2023 , 522, 204849	O
630	Role of temperature and preexisting dislocation network on the shock compression of copper crystals. 2023 , 165, 103599	0
629	Investigation of physio-mechanical properties of cross-linked Bis-GMA/TEGDMA dental resins: A molecular dynamics study. 2023 , 35, 105926	O
628	An exploration of efficiency of proposed drug delivery system including BNNT, C48N12, and TMZ in treating of glioblastoma through classical molecular dynamics. 2023 , 379, 121625	0
627	Phononic origin of strain-controlled friction force. 2023 , 184, 108474	O
626	A localized stress field approach for calculating the critical stress intensity factor for an isotropic solid at atomistic scale. 2023 , 181, 104632	0
625	TEM-MD characterization of KDP deformation mechanisms under nanoindentation. 2023 , 43, 3844-3848	O
624	Shock compression and spall damage of dendritic high-entropy alloy CoCrFeNiCu. 2023, 947, 169650	O
623	Anisotropic cutting mechanisms on the surface quality in ultra-precision machining of R-plane sapphire. 2023 , 622, 156868	O
622	Coarse-grained methods for heterogeneous vesicles with phase-separated domains: Elastic mechanics of shape fluctuations, plate compression, and channel insertion. 2023 , 209, 342-361	0
621	Enhancing thermal transport across diamond/graphene heterostructure interface. 2023, 209, 124123	O
620	Orientation-dependent ductility and deformation mechanisms in body-centered cubic molybdenum nanocrystals. 2023 , 154, 107-113	O
619	Chemical inhomogeneity inhibits grain boundary fracture: A comparative study in CrCoNi medium entropy alloy. 2023 , 153, 228-241	O

618	Complex strengthening mechanisms in nanocrystalline Ni-Mo alloys revealed by a machine-learning interatomic potential. 2023 , 952, 169964	O
617	New approaches to study of mismatched interfaces structure on low-index surfaces by molecular dynamics simulation. 2023 , 623, 157072	O
616	Sputtering of coinage metals with bismuth cluster ions: Experiment and computer simulation. 2023 , 213, 112070	O
615	Molecular dynamics simulation of CO2-oil miscible fluid distribution and flow within nanopores. 2023 , 380, 121769	O
614	Spall damage of solution-treated hot-rolled Inconel 718 superalloy under plate impact. 2023 , 952, 170090	O
613	Phase transition in yttrium under shock compression by atomistic simulations. 2023 , 250, 108330	O
612	Investigation of the heat transport in intersected graphene. 2023 , 209, 124162	O
611	Phonon thermal transport in polycrystalline graphene:Effects of grain, vacancy and strain. 2023 , 209, 124057	O
610	Molecular simulations of adsorption of surfactant micelles on partially and fully covered iron surfaces. 2023 , 379, 121685	O
609	A molecular dynamics study on the influence of vacancies and interstitial helium on mechanical properties of tungsten. 2023 , 580, 154378	O
608	A molecular investigation on the effects of OMEX addition on soot inception of diesel pyrolysis. 2023 , 346, 128357	O
607	Transfer or blockage: Unraveling the interaction between deformation twinning and grain boundary in tantalum under shock loading with molecular dynamics. 2023 , 156, 118-128	O
606	Multiscale modeling of irradiation-induced defect evolution in BCC multi principal element alloys. 2023 , 953, 170084	O
605	Molecular dynamics data-driven study of leidenfrost phenomena in context to liquid thin film phase transformation. 2023 , 209, 124107	O
604	Atomistic simulations of martensitic transformation processes for metastable FeMnCoCr high-entropy alloy.	Ο
603	Twisting Dynamics of Large Lattice-Mismatch van der Waals Heterostructures.	O
602	Ordered and amorphous phases of polyacrylonitrile: Effect of tensile deformation of structure on relaxation and glass transition. 2023 , 125969	O
601	Nano-tribological behavior of CuCoCrFeNi high-entropy alloys at cryogenic temperature: A molecular dynamics study. 2023 , 133, 155901	O

600	Prominently improved CO2/N2 separation efficiency by ultrathin-ionic-liquid-covered MXene membrane. 2023 , 311, 123296	О
599	Entrance loss of capillary flow in narrow slit nanochannels. 2023 , 35, 042005	O
598	Machine learning-based prediction for single-cell mechanics. 2023 , 180, 104631	0
597	Atomistic origin of shear induced quasi-plastic deformation in boron carbide. 2023, 249, 118828	O
596	Unveiling load carriers between nanoparticles capable of passing through a glassy disordered phase: A theoretical multiscale analysis. 2023 , 252, 118950	0
595	Atomistic investigation of the mechanical and tribological responses of the ferrite-cementite interface with a Bagaryatskii orientation. 2023 , 184, 108480	O
594	Analysis of grain-boundary segregation of hydrogen in bcc-Fe polycrystals via a nano-polycrystalline grain-boundary model. 2023 , 225, 112196	0
593	Crack tip enhanced phase-field model for crack evolution in crystalline Ti6Al from concurrent crystal plasticity FE-molecular dynamics simulations. 2023 , 100, 104983	O
592	Concentration dependence of yield stress of bentonite suspension and corresponding particle interactions. 2023 , 157, 105358	O
591	Dislocation-assisted diffusion-mediated atomic reshuffling in the Kolbe mechanism for micro-twinning in Ni-based superalloys from molecular dynamics simulation. 2023 , 232, 115475	O
590	Improved liquid mixture viscosity predictions with the TLVMie force field. 2023, 570, 113782	O
589	Influence of V and Al in enhancing the strength and ductility of Co-rich high-entropy alloys. 2023 , 948, 169745	O
588	Atomistic simulations of enhanced irradiation resistance and defect properties in body-centered cubic W-V-Cr and W-Ta-V alloys. 2023 , 948, 169744	0
587	The influence of gadolinium concentration on the twin propagation rate in magnesium alloys. 2023 , 948, 169635	O
586	Modeling microstructural mechanical behavior of expansive soil at various water contents and dry densities by molecular dynamics simulation. 2023 , 158, 105371	0
585	Multi-scale simulation of the fracture behavior of non-stoichiometric gadolinia-doped ceria solid electrolytes under the coupled mechanical and electrochemical field. 2023 , 100, 104989	O
584	Stress-induced phase transformation and phase boundary sliding in Ti: An atomically resolved in-situ analysis. 2023 , 152, 30-36	O
583	Multiscale modelling of irradiation damage behavior in high entropy alloys. 2023 , 2, 100114	O

582	Evaluation of the BET and GAB models for interpretation of soil water isotherms: A molecular simulation study. 2023 , 159, 105454	0
581	Morphology engineering of biomass-derived porous carbon from 3D to 2D towards boosting capacitive charge storage capability. 2023 , 642, 736-746	Ο
580	Combining MD-LAMMPS and MC-McChasy2 codes for dislocation simulations of Ni single crystal structure. 2023 , 540, 38-44	0
579	Composition effects on thermodynamic properties and interfacial structure in styrene-butadiene rubber: A combined experimental and simulation study. 2023 , 275, 118750	O
578	Dielectric permittivity of C-S-H. 2023 , 169, 107178	0
577	Predictive modelling for enhanced scratching of brittle ceramics with magneto-plasticity. 2023 , 249, 108272	O
576	Influence of High Concentration Vacancy-Type Defects on the Mobility of Edge Dislocation in ∃ron: An Atomistic Investigation. 2022 ,	Ο
575	Diffusion in undoped and Cr-doped amorphous UO2. 2023 , 576, 154270	O
574	Molecular dynamics simulation of the mechanical characteristics of brick structure reinforced with graphene nanosheet. 2023 , 361, 115078	Ο
573	Liquid Dynamics Determine Transition Metal- N -Heterocyclic Carbene Complex Formation. 2023 , 29,	O
57 ²	Strengthening Fe50+xMn25Cr15Ni10-x medium-entropy alloys by Ni/Fe replacement: Experiments and molecular dynamics study. 2023 , 155, 107833	Ο
571	The interactions between dislocations and displacement cascades in FeCoCrNi concentrated solid-solution alloy and pure Ni. 2023 , 576, 154286	O
57°	Quantitative analysis of grinding performance of cubic silicon carbide surface texture lubricated with water film. 2023 , 180, 108267	O
569	Fracture universality in amorphous nanowires. 2023 , 173, 105210	Ο
568	Polishing process of 4H-SiC under different pressures in a water environment. 2023 , 133, 109710	Ο
567	Reactive-dynamic characteristics of a nanobubble collapse near a solid boundary using molecular dynamic simulation. 2023 , 35, 022003	Ο
566	Limitations of meta-atom potential for analyzing dislocation core structure in TWIP steel. 2023 , 178, 104563	0
565	An atomistic study of fundamental bulk and defect properties in Euranium. 2023, 576, 154289	O

564	Tunable local piezopotential properties of zinc oxide nanowires grown by remote epitaxy. 2023 , 157, 107345	О
563	Evolution of the microstructure and lubrication mechanism of AgTaO3 films at high temperatures: A MD simulation study. 2023 , 180, 108282	О
562	Segregation of solute elements and strengthening effects of CoCrNiCux medium-entropy alloys: A combined experimental and simulation study. 2023 , 941, 169015	1
561	Structural features, thermal stability and catalytic implication of FeIII nanoparticles. 2023, 320, 123863	О
560	Molecular dynamics study of shock-induced deformation phenomena and spallation failure in Ni-based single crystal superalloys. 2023 , 162, 103539	0
559	Towards accurate and efficient process simulations based on atomistic and neural network approaches. 2022 ,	O
558	Nanocutting mechanisms of Cu50Zr50 amorphous alloy: A molecular dynamics simulation. 2023 , 605, 122161	0
557	Discontinuous segregation patterning across disconnections. 2023 , 246, 118724	О
556	Practical compatibility between self-consistent field theory and dissipative particle dynamics. 2023 , 269, 125733	0
555	Evolution of dislocations and grain boundaries during multi-axial forging of tantalum. 2023, 112, 106120	О
554	Achieving exceptional high-temperature resistant Al matrix composites via two-dimensional BN pinning grain rotation. 2023 , 253, 110570	0
553	Mechanism of polishing lutetium oxide single crystals with polyhedral diamond abrasive grains based on molecular dynamics simulation. 2023 , 616, 156549	O
552	Directional transport and coalescence behavior on Titanium-Tantalum alloy surface: Insights from experiment and molecular dynamics simulation. 2023 , 180, 108303	0
551	Efficient Task-Mapping of Parallel Applications Using a Space-Filling Curve. 2022 ,	О
550	Mechanochemical reclaiming and thermoplastic re-processing of waste Acrylonitrile-butadiene rubber (NBR)/poly (Vinyl Chloride) (PVC) insulation materials. 2023 , 158, 153-163	0
549	A concurrent multiscale method based on smoothed molecular dynamics for large-scale parallel computation at finite temperature. 2023 , 406, 115898	O
548	Unveiling the mutual ion-storage mechanism of dual-carbon NaTFSI-WiSE Cells: A molecular dynamics study. 2023 , 205, 383-393	0
547	The role of resonant coupling in vibrational sum-frequency-generation spectroscopy: Liquid acetonitrile at the silica interface. 2023 , 375, 121315	О

546	AppEKG: A Simple Unifying View of HPC Applications in Production. 2022,	0
545	Strain rate sensitivity in Zr-based metallic glass: Experiments and molecular dynamics study. 2023 , 605, 122168	O
544	Microstructure of a heavily irradiated metal exposed to a spectrum of atomic recoils. 2023, 13,	0
543	Formation and growth kinetics of the initial amorphous oxide film on the aluminum melt: A ReaxFF molecular dynamics simulation. 2023 , 220, 112035	O
542	A discrete-to-continuum model of weakly interacting incommensurate two-dimensional lattices: The hexagonal case. 2023 , 173, 105229	0
541	Tilt grain boundary stability in uranium dioxide and effect on xenon segregation. 2023 , 577, 154302	O
540	Uncovering wear mechanism of a Fe2Ni2CrAl multi-principal elements alloy. 2023, 58, 2660-2675	0
539	Strain-Rate Dependence of Plasticity and Phase Transition in [001]-Oriented Single-Crystal Iron. 2023 , 13, 250	O
538	Probing the atomic-scale deformation mechanism of single-crystal nanowires coated with a multi-component alloyed shell. 2023 , 220, 112056	0
537	One-dimensional harmonic chain model of vibration-mode matching in solid-liquid interfacial thermal transport. 2023 , 107,	O
536	Distinct relaxation mechanism at room temperature in metallic glass. 2023, 14,	O
535	CHARMM-GUI PDB Manipulator: Various PDB Structural Modifications for Biomolecular Modeling and Simulation. 2023 , 167995	O
534	Nanoscale investigation of surface wettability distribution on bubble nucleation with variable temperature boundary condition. 1-12	0
533	Molecular Modeling to Predict the Optimal Mineralogy of Smectites as Binders of Aflatoxin.	O
532	Bifunctional electrolyte regulation towards low-temperature and high-stability Zn-ion hybrid capacitor. 2023 , 79, 495-504	0
531	Atomistic analysis of plastic deformation and shear band formation in FCC/FCC metallic nanolayered composites. 2023 , 38, 1386-1395	O
530	Interface-independent sound speed and thermal conductivity of atomic-layer-deposition-grown amorphous AlN/Al2O3 multilayers with varying oxygen composition. 2023 , 7,	0
529	Designed Y3+ Surface Segregation Increases Stability of Nanocrystalline Zinc Aluminate. 2023 , 127, 4239-42	50 0

528	IPMPI: Improved MPI Communication Logger. 2022,	0
527	Dispersion Free Energy of Carbon Nanotubes in Water Systems. 2023 , 52, 156-159	O
526	Statistical Mechanical Design Principles for Coarse-Grained Interactions across Different Conformational Free Energy Surfaces. 2023 , 14, 1354-1362	0
525	A neural network parametrized coagulation rate model for <3´nm titanium dioxide nanoclusters. 2023 , 158, 084301	O
524	The brittle-to-ductile transition in aluminosilicate glasses is driven by topological and dynamical heterogeneity. 2023 , 247, 118740	0
523	Towards a multi-abrasive grinding model for the material point method. 3,	O
522	Influence of nano-indentation depth on the elasticplastic transformation of 6H-SiC simulated. 2023 , 13, 025118	0
521	Temperature-dependent elasticity of single crystalline graphite. 2023 , 220, 112045	O
520	Machine-learning inspired density-fluctuation model of local structural instability in metallic glasses. 2023 , 247, 118741	1
519	Degradation and lifetime prediction of thermoplastic polyurethane encapsulants in seawater for underwater acoustic sensor applications. 2023 , 209, 110281	O
518	On the replacement behavior of CO2 in nanopores of shale oil reservoirs: Insights from wettability tests and molecular dynamics simulations. 2023 , 223, 211528	0
517	Material point simulations as a basis for determining JohnsonLook hardening parameters via instrumented scratch tests. 2023 , 267, 112146	O
516	Enhancing the toughness of nano-composite coating for light alloys by the plastic phase transformation of zirconia. 2023 , 163, 103555	О
515	Investigation of the Impact of High Concentration LiTFSI Electrolytes on Silicon Anodes with Reactive Force Field Simulations. 2023 , 3, 132-158	O
514	Evidence That Less Can Be More for Transferable Force Fields. 2023 , 63, 1188-1195	0
513	Molecular Dynamics Simulations of the Thermal Evolution of Voids in Cu Bulk and Grain Boundaries. 2023 , 1001-1010	O
512	Competing Nuclear Quantum Effects and Hydrogen-Bond Jumps in Hydrated Kaolinite. 2023 , 14, 1542-1547	0
511	Nanostructure, Plastic Deformation, and Influence of Strain Rate Concerning Ni/Al2O3 Interface System Using a Molecular Dynamic Study (LAMMPS). 2023 , 13, 641	O

510	Development and Validation of a ReaxFF Reactive Force Field for Modeling SiliconCarbon Composite Anode Materials in Lithium-Ion Batteries. 2023 , 127, 2818-2834	0
509	Dislocation mechanisms in strengthening and softening of nanotwinned materials. 2023 , 133, 055106	O
508	Scaling Law for Impact Resistance of Amorphous Alloys Connecting Atomistic Molecular Dynamics with Macroscale Experiments. 2023 , 15, 13449-13459	0
507	Molecular Study of Nonequilibrium Transport Mechanism for Proton and Water in Porous Proton Exchange Membranes. 2023 , 2023, 1-13	O
506	Mechanism Study on Mechanical Properties of Physical Themical Hybrid Hydrogels by Coarse-Grained Molecular Dynamics Simulations. 2023 , 5, 1707-1714	0
505	Device-to-Materials Pathway for Electron Traps Detection in Amorphous GeSe-Based Selectors. 2023 , 9,	O
504	StressEtress correlations reveal force chains in gels. 2023 , 158, 114104	0
503	Multiple polarity kinases inhibit phase separation of F-BAR protein Cdc15 and antagonize cytokinetic ring assembly in fission yeast. 12,	O
502	Modes of strain accommodation in Cu-Nb multilayered thin film on indentation and cyclic shear. 2023 , 37, 102712	0
501	Size- and temperature-dependent thermal transport across a Culliamond interface: Non-equilibrium molecular dynamics simulations. 2023 , 37, 102736	O
500	Simulation of thermal decomposition of &Fe4N using molecular dynamics method. 2023, 13, 025234	0
499	The profile of extreme tension wave front in aluminum. 2023 , 58, 3360-3374	O
498	Mechanism of Aluminum Element Segregation in As-Cast Medium-Entropy Alloy CrCoNiAl0.014: A Hybrid MD/MC Simulation and Experimental Study. 2023 , 13, 331	0
497	The evolution of deformation twinning microstructures in random face-centered cubic solid solutions. 2023 , 133, 055107	O
496	Solution-Processed Synthesis of Nano-Sized Argyrodite Solid Electrolytes with Cavitation Effect for High Performance All-Solid-State Lithium-Ion Batteries. 2023 , 6,	0
495	Impeded thermal transport in aperiodic BN/C nanotube superlattices due to phonon Anderson localization.	O
494	Atomistic Study for the Tantalum and Tantalum II ungsten Alloy Threshold Displacement Energy under Local Strain. 2023 , 24, 3289	0
493	Determination of optimal potential parameters for the self-assembly of various lattice structures. 2023 , 9, 18-29	O

492	The low-cyclic fatigue response and its dependence of specific surface area for open-cell nanoporous Cu. 2023 , 133, 065103	0
491	Melting conditions and entropies of superionic water ice: Free-energy calculations based on hybrid solid/liquid reference systems. 2023 , 158, 064502	O
490	Breakdown of Reye⊠ theory in nanoscale wear. 2023 , 173, 105236	О
489	Surface-Dependent Adhesion Properties of Graphene on Diamonds for the Fabrication of Nanodevices: A Molecular Dynamics Investigation. 2023 , 6, 2942-2951	O
488	Bioinformatics and Cheminformatics Tools in Early Drug Discovery. 2023, 147-181	O
487	Cooperative diffusion in body-centered cubic iron in Earth and super-Earths[Inner core conditions. 2023 , 35, 154002	1
486	Automated determination of grain boundary energy and potential-dependence using the OpenKIM framework. 2023 , 220, 112057	O
485	Bringing Quantum Mechanics to Coarse-Grained Soft Materials Modeling. 2023 , 35, 1470-1486	O
484	Unidirectional Droplet Propulsion onto Gradient Brushes without External Energy Supply. 2023 , 39, 2818-28	328 0
483	Local Reactivity on Carbon Quantum Dots: The Influence of the Geometries and Chemical Doping for Chemical Sensor Applications. 2023 , 127, 3819-3829	O
482	Atomistic insight of torsional behavior of CNT-nanocrystalline Al nanocomposites. 2023, 134, 109768	0
481	Detecting Microstructural Criticality/Degeneracy through Hybrid Learning Strategies Trained by Molecular Dynamics Simulations.	O
480	Atomistic simulations for investigation of substrate effects on lipid in-source fragmentation in secondary ion mass spectrometry. 2023 , 18, 011003	O
479	Hydrophobic Nanoconfinement Enhances CO2 Conversion to H2CO3. 2023 , 14, 1693-1701	1
478	Molecular-Level Understanding of the Effect of Water on Oil Transport in Graphene Nanochannels. 2023 , 127, 3671-3681	O
477	Statics, Dynamics and Linear Viscoelasticity from Dissipative Particle Dynamics Simulation of Entangled Linear Polymer Melts.	O
476	4.2V polymer all-solid-state lithium batteries enabled by high-concentration PEO solid electrolytes. 2023 , 57, 171-179	O
475	Universality of grain boundary phases in fcc metals: Case study on high-angle [111] symmetric tilt grain boundaries. 2023 , 107,	O

474	Molecular Dynamics Studies of Primary Irradiation Damage in ⊞ype Ti35 Alloy. 2023 , 260,	0
473	Separation of ion component from solid hydrocarbon materials by laser ablation. 2023 , 72, 075201	O
472	The mechanism in surface morphology of YSZ ceramics influencing its corrosion resistance to CMAS melt: Molecular dynamics research. 2023 , 606, 122194	0
471	Molecular dynamics simulation of thermal characteristics of globulin protein dissolved in dilute salt solutions using equilibrium and non-equilibrium methods. 2023 , 113, 103505	1
470	Effect of TiO2 nanoparticles on the mass transfer process of absorption of toluene: Experimental investigation and molecular dynamics simulation. 2023 , 11, 109474	0
469	MDSuite: comprehensive post-processing tool for particle simulations. 2023 , 15,	O
468	Exploring durability and environmental impact of cementitious composites modified by fluoroalkyl-silane based additive. 2023 , 370, 130665	0
467	Enhanced resistance to helium irradiations through unusual interaction between high-entropy-alloy and helium. 2023 , 248, 118765	O
466	Thermal Transport Study in a Strained Carbon Nanotube and Graphene Junction Using Phonon Wavepacket Analysis. 2023 , 9, 21	0
465	Anharmonic thermo-elasticity of tungsten from accelerated Bayesian adaptive biasing force calculations with data-driven force fields. 2023 , 7,	O
464	Monocrystalline Nickel Nanogrinding Subsurface Deformation-Layer Depth Study Based on Orthogonal Tests. 2023 , 13, 410	0
463	Water-driven expansion of boron nitride nanosheets for self-healing tobermorite composite. 2023 , 235, 109954	O
462	Unveiling the Machinery behind Chromosome Folding by Polymer Physics Modeling. 2023 , 24, 3660	0
461	Interface enhancing strategy for low-temperature bonding of Ag-based nanoalloy. 2023, 339, 134050	O
460	C60 filling-enabled tribological improvement of graphene in conformal contact with a rough substrate. 2023 , 206, 157-165	0
459	Theoretical Evaluation of the Persistence of Transverse Phonons across a Liquid-like Transition in Superionic Conductor KAg3Se2. 2023 , 35, 1780-1787	O
458	Melting of MgSiO3 determined by machine learning potentials. 2023 , 107,	0
457	Flexural behavior and microstructural material properties of sandwich foam core under arctic temperature conditions. 109963622311570	0

456	Aminosilane modified graphene oxide for reinforcing nitrile butadiene rubber: Experiments and molecular dynamic simulations. 2023 , 235, 109956	О
455	Release Behavior Research of <i>In-situ</i> Helium-3 Resources Extraction in Moon under Heating. 2021 , 41, 787	O
454	Confined ionic liquids films under shear: The importance of the chemical nature of the solid surface. 2023 , 158, 094712	0
453	Probing single-chain conformation and its impact on the optoelectronic properties of donorEccepter conjugated polymers.	O
452	The synergistic effect between imidazole reagents and kinetic hydrate inhibitors. 2023, 376, 121466	О
45 ¹	Modulation of thermal conductivity of single-walled carbon nanotubes by fullerene encapsulation: the effect of vacancy defects. 2023 , 25, 7734-7740	Ο
450	Modelling the dynamic physical properties of vulcanised polymer models by molecular dynamics simulations and machine learning. 2023 , 221, 112081	0
449	Study of controlling phase separation in Yb3+-doped fluorophosphate glasses via molecular dynamics simulations. 2023 , 606, 122202	Ο
448	Effect of the thermodynamic factor on the intrinsic and tracer diffusivities in binary mixtures. 2023 , 107,	0
447	Modelling of nanocrystalline insulators response to swift heavy ion irradiation. 2023 , 221, 112078	O
446	Computational Mesoscale Framework for Biological Clustering and Fractal Aggregation.	О
445	MoSDeF-GOMC: Python Software for the Creation of Scientific Workflows for the Monte Carlo Simulation Engine GOMC. 2023 , 63, 1218-1228	1
444	Mechanical properties and deformation behaviors of the hydroxyl-terminated polybutadiene and ammonium perchlorate interface by molecular dynamics simulation. 2023 , 221, 112077	0
443	Non-reactive facet specific adsorption as a route to remediation of chlorinated organic contaminants. 3,	O
442	Triple junction solute segregation in Al-based polycrystals. 2023, 7,	0
441	Nanogel Degradation at Soft Interfaces and in Bulk: Tracking Shape Changes and Interfacial Spreading. 2023 , 56, 1289-1302	O
440	Molecular dynamics simulation of effects of Al on the evolution of displacement cascades in Al CoCrFeNi high entropy alloys. 2023 , 577, 154342	О
439	Tamping effect during additive manufacturing of copper coating by cold spray: A comprehensive molecular dynamics study. 2023 , 66, 103448	Ο

438	Direct Observation of Transient Structural Dynamics of Atomically Thin Halide Perovskite Nanowires. 2023 , 145, 4800-4807	Ο
437	The highest melting point material: Searched by Bayesian global optimization with deep potential molecular dynamics. 2023 , 12, 803-814	О
436	Diffusion mobility increases linearly on liquid binodals above triple point. 2023, 13,	О
435	Electron and ion transport in semi-dilute conjugated polyelectrolytes: view from a coarse-grained tight binding model.	О
434	Calculation of Thermodynamic Characteristics and Sound Velocity for Two-Dimensional Yukawa Fluids Based on a Two-Step Approximation for the Radial Distribution Function. 2023 , 8, 72	O
433	Thermal batteries based on inverse barocaloric effects. 2023 , 9,	O
432	Phase selection in aluminum rare-earth metallic alloys by molecular dynamics simulations using machine learning interatomic potentials. 2023 , 7,	O
431	Surface and Constriction Engineering of Nanoparticle Based Structures Towards Ultra-Low Thermal Conductivity as Prospective Thermoelectric Materials. 2023 , 27, 25-41	О
430	Controlling interfacial composition and improvement in bonding strength of compound casted Al/steel bimetal via Cr interlayer. 2023 , 23, 4385-4395	O
429	Formation and evolution of topologically closepacked crystals during the rapid solidification of liquid metal tungsten. 2023 , 25, 1792-1802	О
428	Thermo-mechanical analysis of hydrogen permeation in lubricated rubbing contacts. 2023, 182, 108355	O
427	Enhanced graphene oxide adhesion on steel surface through boronizing functionalization treatment: Toward the robust ultralow friction. 2023 , 206, 201-210	O
426	End-to-End Fluctuation of cis-Poly(isoprene) under Constraints from Slow Poly(tert-butyl styrene). 2023 , 56, 1379-1389	O
425	The effect of configurational complexity in hetero-polymers on the coil-globule phase transition. 2023 , 138,	O
424	Unraveling the ultrahigh modulus of resilience of Core-Shell SU-8 nanocomposite nanopillars fabricated by vapor-phase infiltration. 2023 , 227, 111770	O
423	Microwave-assisted design of nanoporous graphene membrane for ultrafast and switchable organic solvent nanofiltration. 2023 , 14,	O
422	An In-depth Benchmarking of Evolutionary and Swarm Intelligence Algorithms for Autoscaling Parameter Sweep Applications on Public Clouds. 2023 , 2023, 1-26	0
421	Atomistic insight into three-dimensional twin embryo growth in Mg alloys. 2023 , 58, 3972-3995	О

420	Electrolyte design principles for developing quasi-solid-state rechargeable halide-ion batteries. 2023 , 14,	О
419	Influence of the Hydrogen Doping Method on the Atomic Structure, Mechanical Properties and Relaxation Behaviors of Metallic Glasses. 2023 , 16, 1731	O
418	Thermal transport across copperWater interfaces according to deep potential molecular dynamics. 2023 , 25, 6746-6756	О
417	Utilizing Machine Learning to Greatly Expand the Range and Accuracy of Bottom-Up Coarse-Grained Models through Virtual Particles.	1
416	Early-Stage Liquid Infiltration in Nanoconfinements. 2023 , 39, 3301-3311	О
415	A Machine Learning-Combined Flexible Sensor for Tactile Detection and Voice Recognition. 2023 , 15, 12551-12559	O
414	Molecular Dynamics of Nanodroplet Coalescence in Quasi-Saturated Vapor. 2023, 8, 77	О
413	The surface effect on the mechanical behavior of MG nanowires: A molecular dynamic simulation. 2023 , 606, 122224	O
412	Molecular dynamics simulations of displacement cascades in vanadium: Generation and types of dislocation loops. 2023 , 34, 101394	O
411	Active Brownian particles in random and porous environments. 2023, 158, 104907	O
410	Modelling shear thinning of Imidazolium-based ionic liquids. 2023 , 816, 140387	O
409	Ligand-Triggered Self-Assembly of Flexible Carbon Dot Nanoribbons for Optoelectronic Memristor Devices and Neuromorphic Computing. 2207688	O
408	Effect of electronic stopping in molecular dynamics simulations of collision cascades in gallium arsenide. 2023 , 7,	О
407	Quantification of the impact of water on the wetting behavior of hydrophilic ionic liquid: a molecular dynamics study. 2023 , 49, 525-535	O
406	A deep learning approach to predict thermophysical properties of metastable liquid Ti-Ni-Cr-Al alloy. 2023 , 133, 085102	O
405	Multiscale Modeling of Metal-Oxide-Metal Conductive Bridging Random-Access Memory Cells: From Ab Initio to Finite-Element Calculations. 2023 , 19,	O
	Janiah talia tala tala a CNI anno anti anno anni a havorda a atau atu an Itana aiti anno di anna a anni an I	
404	Insights into the role of Nb segregation on grain boundary structural transition and mechanical response in a NiNb system. 2023 , 299, 127531	Ο

402	High-surface-area functionalized nanolaminated membranes for energy-efficient nanofiltration and desalination in forward osmosis. 2023 , 1, 187-197	О
401	Unraveling the influence of surface roughness on oil displacement by Janus nanoparticles. 2023,	O
400	Energy harvesting from mechanical vibrations: Self-rectification effect.	О
399	Electrostatic Fields Stimulate Absorption of Small Neutral Molecules in Gradient Polyelectrolyte Brushes.	Ο
398	Interaction between Grain Dislocation and Symmetrical Tilt Grain Boundary in TiC Single Crystal. 2022 ,	0
397	A general expression for the statistical error in a diffusion coefficient obtained from a solid-state molecular-dynamics simulation.	O
396	Boron Nitride Nanotubes: Force Field Parameterization, Epoxy Interactions, and Comparison with Carbon Nanotubes for High-Performance Composite Materials. 2023 , 6, 3513-3524	0
395	Towards the realisation of high permi-selective MoS2 membrane for water desalination. 2023, 6,	Ο
394	Theoretical study of void collapse and hot spot formation mechanism for energetic material. 1-18	0
393	Decoding the phonon transport of structural lubrication at silicon/silicon interface. 2023 , 34, 215704	Ο
392	Insights on oxide ion transport in yttria-doped ceria from molecular dynamics simulations. 2023 , 58, 4499-4	1 512 0
391	Shock-induced energy localization and reaction growth considering chemical-inclusions effects for crystalline explosives. 2023 ,	Ο
390	The dynamics of shear band propagation in metallic glasses. 2023 , 248, 118787	0
389	Machine learning quantitatively characterizes the deformation and destruction of explosive molecules. 2023 , 25, 8692-8704	Ο
388	Atomistic study on high temperature creep of nanocrystalline 316L austenitic stainless steels. 2023 , 39,	0
387	Phonon-Induced Localization of Excitons in Molecular Crystals from First Principles. 2023 , 130,	Ο
386	Revealing the Correlation between the Solvation Structures and the Transport Properties of Water-in-Salt Electrolytes. 2023 , 35, 2088-2094	O
385	The conformational phase diagram of neutral polymers in the presence of attractive crowders. 2023 , 158, 114903	O

384	Investigating the dynamic behavior of the nano-bubble in two-phase systems of argon and water: A molecular dynamics simulation approach. 2023 , 17, 100977	0
383	Scheme for the excitation of thorium-229 nuclei based on electronic bridge excitation. 2023, 34,	О
382	Nanoscale crack propagation in clay with water adsorption through reactive MD modeling. 2023 , 47, 1103-1133	О
381	Thermal transport in grapheneHMX composites with grafted interface. 2023 , 58, 4668-4678	O
380	From Green-Kubo to the full Boltzmann kinetic approach to heat transport in crystals and glasses. 2023 , 107,	0
379	Theoretical study on uniaxial compressive mechanical properties of three-dimensional graphene. 2023 , 249, 108250	0
378	Mechanical Properties and Microstructure Evolution of Cryorolled AlCoCrFeNi-Reinforced Aluminum Matrix Composites Tensile Tested at Room and Cryogenic Temperatures.	0
377	Ultrathin Mo2S3 Nanowire Network for High-Sensitivity Breathable Piezoresistive Electronic Skins. 2023 , 17, 4862-4870	O
376	A Theoretical and Experimental Study on High-Efficiency and Ultra-Low Damage Machining of Diamond. 2023 , 145,	0
375	Carbon nanowires made by the insertion-and-fusion method toward carbonflydrogen nanoelectronics. 2023 , 15, 6143-6155	Ο
374	A study of grain boundary effects on the stress-induced martensitic transformation and superelasticity in NiTi alloy via atomistic simulation. 2023 , 133, 085106	0
373	Pseudo-Elasticity and Variable Electro-Conductivity Mediated by Size-Dependent Deformation Twinning in Molybdenum Nanocrystals. 2206380	Ο
372	Tribochemistry of 1-Octene on Three Transition Metal Surfaces: Fe(100), Pt(111) and Ni(111). 2023 , 71,	0
371	Investigation of bubble nucleation on inhomogeneous wettability surfaces. 2023, 49, 608-616	O
370	A monofluoride ether-based electrolyte solution for fast-charging and low-temperature non-aqueous lithium metal batteries. 2023 , 14,	0
369	GAFF-AIC: reoptimisation of the GAFF force field for realistic densities and viscosities in aromatic isocyanates. 2023 , 49, 576-588	O
368	Atomistic study of internal stress effect on scratching behavior in titanium single crystal. 2023 , 23, 5230-5238	8 0
367	A Monte Carlo code for the collisional evolution of porous aggregates (CPA). 2023 , 672, A50	О

366	Insights into the solubility of H2 in various polyethylene matrices at high pressure: A coarse-grained MC/MD study. 2023 ,	0
365	Structural Spectrum of 2D Materials in Solution: Toward Establishing 2D AssembliesDigital Factory. 2023 , 10,	O
364	Resonant increase of ionic conductance of yttria-stabilized zirconia in an alternating external electric field. 2023 , 27, 1177-1184	Ο
363	Giant Gateable Osmotic Power Generation from a Goldilocks Two-Dimensional Polymer. 2023 , 145, 5261-5269	9 o
362	Thermodynamics of diamond formation from hydrocarbon mixtures in planets. 2023, 14,	1
361	Polyamide membranes with nanoscale ordered structures for fast permeation and highly selective ion-ion separation. 2023 , 14,	O
360	Microphase behaviors and shear moduli of double-network gels: The effect of crosslinking constraints and chain uncrossability. 2023 , 158, 114906	О
359	A Study of Compression Deformation Behavior of 🔁 Interface in (TiAl) Alloy Using Molecular Dynamics Simulation.	O
358	Surface enrichment dictates block copolymer orientation. 2023 , 15, 6901-6912	0
357	Machine Learning Molecular Dynamics Simulations for Evaluation of High-Temperature Properties of Nuclear Fuel Materials. 2023 , 62, 175-181	O
356	Machine learning coarse-grained models of dissolutive wetting: a droplet on soluble surfaces. 2023 , 25, 7487-7495	О
355	Mechanical Behavior and Physical Properties of Mg Binary Alloys via Y-doping: Molecular Dynamic Study.	O
354	Physics of molecular deformation mechanism in 6H-SiC. 2023 , 31, 035006	О
353	Atomistic simulations of defect accumulation and evolution in heavily irradiated titanium for nuclear-powered spacecraft. 2023 ,	O
352	Superelasticity Induced by a Strain Gradient.	О
351	A heterogeneous processing-in-memory approach to accelerate quantum chemistry simulation. 2023 , 116, 103017	O
350	Impact of interfacial compositional diffusion on interfacial phonon scattering and transmission in GaN/AlN heterostructure. 2023 , 133, 095101	0
349	Experimental and theoretical study of synthesis and properties of Cu2O/TiO2 heterojunction for photoelectrochemical purposes. 2023 , 37, 102751	Ο

348	Impact of Ionic Correlations on Selective Salt Transport in Ligand-Functionalized Polymer Membranes. 2023 , 56, 2194-2208	0
347	Interfacial Adsorption Kinetics of Methane in Microporous Kerogen. 2023, 39, 3742-3751	O
346	Appropriate clusterset selection for the prediction of thermodynamic properties of liquid water with QCE theory. 2023 , 25, 9846-9858	О
345	Effects of surface defects on mechanical properties and fracture mechanism of gallium selenide/graphene heterostructure. 2023 , 180, 104610	O
344	Phage Display Screening as a Rational Approach to Design Additives for Selective Crystallization Control in Construction Systems.	O
343	Microscopic Mechanism of Tunable Thermal Conductivity in Carbon Nanotube-Geopolymer Nanocomposites. 2023 , 127, 2267-2276	o
342	Atomistic simulations of temperature-induced switchable morphology in graphene nanodrum. 2023 , 222, 112102	0
341	Physics-separating artificial neural networks for predicting sputtering and thin film deposition of AlN in Ar/N2 discharges on experimental timescales. 2023 , 56, 194001	О
340	Recrystallization in string-fluid complex plasmas. 2023 , 5,	0
339	Fracture resistance of graphene origami under nanoindentation. 2023, 207, 67-76	О
338	Interfacial nanobubbles@rowth at the initial stage of electrocatalytic hydrogen evolution.	0
337	Suppressing the Surface Amorphization of Ba0.5Sr0.5Co0.8Fe0.2O3 Perovskite toward Oxygen Catalytic Reactions by Introducing the Compressive Stress. 2023 , 62, 4373-4384	o
336	Crystal orientation-dependent tensile mechanical behavior and deformation mechanisms of	
	zinc-blende ZnSe nanowires. 2023 , 13,	0
335	zinc-blende ZnSe nanowires. 2023 , 13, Self-assembly of amphiphilic polyelectrolytes in trivalent salt solution. 2023 , 25, 10042-10053	0
335	Self-assembly of amphiphilic polyelectrolytes in trivalent salt solution. 2023 , 25, 10042-10053	O
335	Self-assembly of amphiphilic polyelectrolytes in trivalent salt solution. 2023 , 25, 10042-10053 Achieving superb strength in single-phase FCC alloys via maximizing volume misfit. 2023 , 63, 108-119	0

330	Interactions of Oil Shale and Hydrogen-Rich Wastes during Co-pyrolysis: Co-pyrolysis of Oil Shale and Waste Tire. 2023 , 37, 4222-4232	O
329	Quantifying the Molecular Polarization Response of Liquid Water Interfaces at Heterogeneously Charged Surfaces. 2023 , 19, 1843-1852	O
328	Mechanism on Material Strengthening of Metastable Precipitate and Edge Dislocation in AlMgBi Alloy. 2200478	0
327	The anomalous annealing hardening behaviors in commercial pure Tantalum foil. 2023, 870, 144878	O
326	Reactive force-field MD simulation on the pyrolysis process of phenolic with various cross-linked and branched structures. 2023 , 272, 118606	O
325	Ultrasonic study and molecular dynamics simulation of propylene glycol at pressures up to 1.4 GPa. 2023 , 98, 045016	O
324	Untra-fine-grained equiatomic CoCrNi medium entropy alloys with high density stacking faults and strengthening mechanisms. 2023 , 870, 144880	O
323	Density anomaly in water-alcohol mixtures: Minimum model for structure makers and breakers. 2023 , 107,	O
322	ReaxFF molecular dynamics simulation of the thermal decomposition reaction of bio-based polyester materials. 2023 , 25, 9445-9453	0
321	Effect of oxidation on mechanical properties of copper nanowire: A ReaxFF (reactive force field) molecular dynamics study. 2023 , 133, 095302	O
320	An atomistic study on tensile behaviors of nanocrystalline copper. 2023 , 98, 045902	0
319	Molecular dynamics simulation of energy transfer in reaction process near supported nanoparticle catalyst. 2023 , 18, 22-00384-22-00384	O
318	Uncertainty-aware molecular dynamics from Bayesian active learning for phase transformations and thermal transport in SiC. 2023 , 9,	O
317	Two-Dimensional Carbon Networks with a Negative Poisson Ratio. 2023, 13, 442	O
316	Effect of surfactants on the elasticity of the liquid I quid interface. 2023, 158, 124901	0
315	Micro-mechanical insights into the stress transmission in strongly aggregating colloidal gel. 2023 , 158, 124902	O
314	Isolating Chemical Reaction Mechanism as a Variable with Reactive Coarse-Grained Molecular Dynamics: Step-Growth versus Chain-Growth Polymerization. 2023 , 56, 2225-2233	O
313	Impact of oxygen and nitrogen-containing species on performance of NO removal by coal pyrolysis gas. 2023 , 173, 229-236	O

312	Water clusters in liquid organic matrices of different polarity. 2023, 378, 121580	0
311	Dislocation density transients and saturation in irradiated zirconium. 2023 , 164, 103590	O
310	Modeling Catalyzed Reactions on Metal-Doped Amorphous Silicates: The Case of Niobium-Catalyzed Ethylene Epoxidation. 2023 , 127, 4984-4997	0
309	Formation of Wear-Protective Tribofilms on Different Steel Surfaces During Lubricated Sliding.	О
308	Development of Deep Potentials of Molten MgCl2NaCl and MgCl2RCl Salts Driven by Machine Learning.	О
307	Anharmonic phonon behavior via irreducible derivatives: Self-consistent perturbation theory and molecular dynamics. 2023 , 107,	O
306	Quantum-mechanics-based molecular dynamics simulations of the structure and performance of sulfur-enriched Li3PS4 cathodes. 2023 , 4, 101326	О
305	Hydrogen-Induced Attractive Force Between Two Partials of Edge Dislocation in Nickel. 2023, 90,	O
304	Nanotwin stability in alloyed copper under ambient and cryo-temperature dependent deformation states. 2023 , 871, 144866	0
303	Thermal cloaking phenomenon in the convex structure silicon film. 2023 , 364, 115131	O
302	Combining Machine Learning and Molecular Dynamics to Predict Mechanical Properties and Microstructural Evolution of FeNiCrCoCu High-Entropy Alloys. 2023 , 13, 968	0
301	Machine learning and molecular dynamics based models to predict the temperature dependent elastic properties of silver nanowires. 1-9	O
300	Structural mechanisms of enhanced mechanical properties in amorphousBanocrystalline ZrCu alloys under irradiation. 2023 , 58, 5061-5071	O
299	Quantum Informed Machine-Learning Potentials for Molecular Dynamics Simulations of CO2B Chemisorption and Diffusion in Mg-MOF-74. 2023 , 17, 5579-5587	O
298	Integrating Machine Learning in the Coarse-Grained Molecular Simulation of Polymers. 2023, 127, 2302-2322	0
297	AUTOCORRELATION FUNCTIONS OF TRANSLATIONAL AND ROTATIONAL VELOCITIES IN MOLECULAR DYNAMIC MODELS OF WATER AND THEIR SPECTRA. 2023 , 64, 208-215	O
296	Molecular dynamics study of the finite-size effect in 2D nanoribbon silicene. 2023, 49, 655-663	0
295	Molecular dynamics study on the thermodynamic stability and structural evolution of crown-jewel structured PdCu nanoalloys. 2023 , 13, 7963-7971	O

294	Profiling the off-center atomic displacements in CuCl at finite temperatures with a deep-learning potential. 2023 , 7,	Ο
293	Effect of Grain-Size in Nanocrystalline Tungsten on Hardness and Dislocation Density: A Molecular Dynamics Study. 2023 , 13, 469	O
292	Kelvin-Helmholtz instability in a compressible dust fluid flow. 2023 , 13,	0
291	Strain-induced dark exciton generation in rippled monolayer MoS2. 2023 , 25, 9894-9900	O
290	Impact of ethylene glycol on ions influencing corrosion in pores between iron oxide and calcium carbonate. 2023 , 49, 664-677	О
289	Atomistic simulation of $\{0001\}$ <\$\$overline $\{1\}$ \$\$2\$\$overline $\{1\}$ \$\$0> crack propagation with Nb precipitates in \boxtimes r. 2023 , 42, 1663-1669	O
288	Insights on the dissolution of water in an albite melt at high pressures and temperatures from a direct structural analysis. 2023 , 13,	О
287	Desorption of a Flexible Polymer with Activity from a Homogeneous Attractive Surface. 2023 , 56, 2542-2550	O
286	A general-purpose machine learning Pt interatomic potential for an accurate description of bulk, surfaces, and nanoparticles. 2023 , 158, 134704	О
285	Molybdenum disulfide under extreme conditions: An ab initio study on its melting. 2023 , 133, 105102	O
284	Computational Investigation on Water and Ion Transport in MoS2 Nanoporous Membranes: Implications for Water Desalination. 2023 , 6, 4465-4476	Ο
283	Bridging necking and shear-banding mediated tensile failure in glasses. 2023, 7,	О
282	A comprehensive modeling approach for polymorph selection in Lennard-Jones crystallization. 2023 , 158, 134505	О
281	On the Uniqueness of Wear Coefficient for Abrasive Wear at Nanoscale. 2023 , 145,	О
280	Implementation of probe rheology simulation technique in atomistically detailed molecular dynamics simulations.	0
279	Phospholipid-based nanodrill technology for enhanced intracellular delivery of nano-sized cargos. 2023 , 4, 493-503	O
278	Symbolic Regression in Materials Science: Discovering Interatomic Potentials from Data. 2023 , 1-30	0
277	Study on Interface Mechanical Properties of Graphene/Copper Matrix Composites. 2023, 13, 3559	O

276	Understanding the graphene-polymer interfacial mechanical behavior via coarse-grained modeling. 2023 , 222, 112109	0
275	Solvent effects determine the sign of the charges of maximum entropy and capacitance at silver electrodes. 2023 , 158, 121102	O
274	A multi-modal pre-training transformer for universal transfer learning in metalorganic frameworks. 2023 , 5, 309-318	0
273	Post-Hydration Crosslinking of Ion Exchange Membranes to Control Water Content. 2023 , 127, 5613-5621	1
272	Absorbing stress via molecular crumple zones: Strain engineering flexibility into the rigid UiO-66 material. 2023 ,	O
271	Atomistic simulation of mechanical behavior of Cu/Cu3Sn solder interface with Kirkendall void under shear and tensile deformation. 2023 , 129,	Ο
270	Performance analysis of thermal cloak with porous silicon structure. 2023 , 143, 106730	Ο
269	Structure and Growth Mechanism of the 2D Ice on the Hydrophobic Metal Surface. 2023 , 45-72	Ο
268	Experimental and Theoretical Study on Thermal Stability of Mixture R1234ze(E)/R32 in Organic Rankine Cycle.	0
267	Wide-Humidity Range Applicable, Anti-Freezing, and Healable Zwitterionic Hydrogels for Ion-Leakage-Free Iontronic Sensors.	Ο
266	Size-Polydisperse Model Ionic Liquid in Bulk. 2023 , 127, 2739-2748	0
265	Kinetics and Mechanisms of Pressure-Induced Ice Amorphization and Polyamorphic Transitions in a Machine-Learned Coarse-Grained Water Model. 2023 , 127, 2847-2862	O
264	Effect of the fractal dimension of nanoparticle aggregates on enhanced thermal transport in nanofluids had molecular dynamics study. 2023 , 49, 690-700	O
263	Dissolution of Forsterite Surface in Brine at CO2 Geo-storage Conditions: Insights from Molecular Dynamic Simulations. 2023 , 39, 4304-4316	Ο
262	Using Molecular Dynamic Simulation to Understand the Deformation Mechanism in Cu, Ni, and Equimolar Cu-Ni Polycrystalline Alloys. 2023 , 2, 77-88	О
261	Molecular dynamic simulations of the liquid structure and fast growth of Y3Al5O12.	O
260	Machine learned interatomic potential for dispersion strengthened plasma facing components. 2023 , 158, 114101	О
259	Equation of State, Compressibility, and Vibrational Properties of Brucite over Wide Pressure and Temperature Ranges: Atomistic Computer Simulations with the Modified ClayFF Classical Force Field. 2023 , 13, 408	1

258	Thermodynamic analysis of the interaction between metal vacancies and hydrogen in bulk Cu. 2023 , 25, 9168-9175	О
257	Numerical Simulation of Shear Viscosity of Magnetic Fluid Polishing Liquid Based on Molecular Dynamics. 2023 , 12, 1098-1106	O
256	Regulated Thermal Boundary Conductance between Copper and Diamond through Nanoscale Interfacial Rough Structures. 2023 , 15, 16162-16176	О
255	Reactive Bimetallic Nanostructures Based on Triply Periodic Minimal Surfaces: A Molecular Dynamics Study toward the Limits of Performance.	O
254	Mechanical behavior and microstructure evolution of Al/AlCu alloy interface. 2023, 58, 5489-5502	О
253	Effect of silver nanoparticle volume fraction on thermal conductivity, specific heat and viscosity of ethylene glycol base silver nanofluid: A molecular dynamics investigation. 2023 , 378, 121635	O
252	Ultrafast hole relaxation dynamics in quantum dots revealed by two-dimensional electronic spectroscopy. 2023 , 6,	О
251	Programmable Transport of C60 by Straining Graphene Substrate. 2023 , 39, 4483-4494	O
250	Heterostrain and temperature-tuned twist between graphene/h-BN bilayers. 2023, 13,	О
249	Interfacial Features Govern Nanoscale Jumping Droplets. 2023 , 39, 4317-4325	O
249 248	Interfacial Features Govern Nanoscale Jumping Droplets. 2023 , 39, 4317-4325 Matrix transformation of lunar regolith and its use as a feedstock for additive manufacturing. 2023 , 26, 106382	0
	Matrix transformation of lunar regolith and its use as a feedstock for additive manufacturing. 2023 ,	
248	Matrix transformation of lunar regolith and its use as a feedstock for additive manufacturing. 2023, 26, 106382 Elemental zoning enhances mass transport in zeolite catalysts for methanol to hydrocarbons. 2023,	0
248 247	Matrix transformation of lunar regolith and its use as a feedstock for additive manufacturing. 2023, 26, 106382 Elemental zoning enhances mass transport in zeolite catalysts for methanol to hydrocarbons. 2023, 6, 254-265 Laser shock peening strengthens additively manufactured high-entropy alloy through novel surface	0
248 247 246	Matrix transformation of lunar regolith and its use as a feedstock for additive manufacturing. 2023, 26, 106382 Elemental zoning enhances mass transport in zeolite catalysts for methanol to hydrocarbons. 2023, 6, 254-265 Laser shock peening strengthens additively manufactured high-entropy alloy through novel surface grain rotation. 2023, 871, 144886	0 0
248 247 246 245	Matrix transformation of lunar regolith and its use as a feedstock for additive manufacturing. 2023, 26, 106382 Elemental zoning enhances mass transport in zeolite catalysts for methanol to hydrocarbons. 2023, 6, 254-265 Laser shock peening strengthens additively manufactured high-entropy alloy through novel surface grain rotation. 2023, 871, 144886 Cation-controlled permeation of charged polymers through nanocapillaries. 2023, 107,	0 0
248 247 246 245	Matrix transformation of lunar regolith and its use as a feedstock for additive manufacturing. 2023, 26, 106382 Elemental zoning enhances mass transport in zeolite catalysts for methanol to hydrocarbons. 2023, 6, 254-265 Laser shock peening strengthens additively manufactured high-entropy alloy through novel surface grain rotation. 2023, 871, 144886 Cation-controlled permeation of charged polymers through nanocapillaries. 2023, 107, Capillary Filling of Polymer Chains in Nanopores. 2023, 56, 2258-2267	0 0 0

240	Effects of neutron irradiation on densities and elastic properties of aggregate-forming minerals in concrete. 2023 ,	0
239	Transferability of Zr-Zr interatomic potentials. 2023 , 154391	O
238	Uncovering the bridging role of slow atoms in unusual caged dynamics and 骨elaxation of binary metallic glasses. 2023 , 158, 134511	O
237	Grain size responsive uniaxial tensile behavior of polycrystalline nanocopper under different temperatures and strain rates. 2023 , 19, 507-521	O
236	The LINC Complex Inhibits Excessive Chromatin Repression. 2023 , 12, 932	0
235	Adsorption Studies at the Graphene Oxidelliquid Interface: A Molecular Dynamics Study. 2023 , 127, 5920-5930	O
234	Role of genome topology in the stability of viral capsids. 2023 , 5,	О
233	Mechanism of sluggish diffusion under rough energy landscape. 2023 , 4, 101337	O
232	Atomistic study on crystal orientation-dependent crack propagation and resultant microstructure anisotropy in NiTi alloys. 2023 , 250, 108320	О
231	Rediscovering the intrinsic mechanical properties of bulk nanocrystalline indium arsenide.	O
230	Velocity distributions of particles sputtered from supported two-dimensional MoS2 during highly charged ion irradiation. 2023 , 107,	0
229	Electronic properties of twisted bilayer graphene suspended and encapsulated with hexagonal boron nitride. 2023 , 107,	O
228	Model reduction for molecular diffusion in nanoporous media. 2023, 7,	О
227	Molecular Dynamics Simulation Study on the Influence of the Abrasive Flow Process on the Cutting of Iron-Carbon Alloys (Fe). 2023 , 14, 703	O
226	Efficient Hi-C inversion facilitates chromatin folding mechanism discovery and structure prediction.	О
225	A defect formation mechanism induced by structural reconstruction of a well-known silicon grain boundary 2023 , 250, 118827	O
224	Effect of Segregation on Deformation Behaviour of Nanoscale CoCrCuFeNi High-Entropy Alloy. 2023 , 13, 4013	1
223	Magnetization relaxation dynamics in polydisperse ferrofluids. 2023 , 107,	O

222	Mechanically Robust and Self-Healing Elastomers Based on Dynamic Oxime©arbamate Bonds: A Combined Experiment and All-Atom Simulation Study. 2023 , 5, 3161-3172	0
221	Insight into Biophysicochemical Principles of Biopolymers through Simulation and Theory.	O
220	Data-Driven Design of High-Performance Graphene-Based Seawater Desalination Membranes. 2023 , 6, 5889-5900	О
219	Percolating contacts network and force chains during interface shear in granular media. 2023 , 25,	Ο
218	Spall fracture in aluminum bicrystals: Molecular dynamics study. 2023,	O
217	Revisiting the Mechanisms of Charge Transport in Solutions of Redox-Active Molecules Using Computer Simulations: When and Why Do Analytical Theories Fail?. 2023 , 127, 2968-2978	0
216	Modeling Cracks in Clay at the Nanoscale through Molecular Dynamics. 2023,	0
215	Misorientation and Temperature Dependence of Small Angle Twist Grain Boundaries in Silicon: Atomistic Simulation of Directional Growth. 2023 , 23, 2893-2904	O
214	Theoretical and computational analysis of the electrophoretic polymer mobility inversion induced by charge correlations. 2023 , 107,	О
213	Theory of Cation Solvation and Ionic Association in Nonaqueous Solvent Mixtures. 2023 , 2,	O
212	Molecular dynamics investigation on micro-friction behavior of cylinder liner-piston ring assembly.	O
211	Initial Response of Pentaerythritol Tetranitrate (PETN) under the Coupling Effect of Preheating, Shock and Defect via the Molecular Dynamics Simulations with the Multiscale Shock Technique Method. 2023 , 28, 2911	O
2 10	Molecular Dynamics Study on the Effect of Interfacial Cellullose Polymers in Strengthening the Stress Transfer Between Alumina Nanoparticles and Epoxy. 2023 , 22,	O
209	Superionic effect and anisotropic texture in Earth inner core driven by geomagnetic field. 2023 , 14,	O
208	Machine Learning Understands Knotted Polymers. 2023 , 56, 2899-2909	О
207	The evaluation of density and diffusion properties in hydrogen/oxygen mixture modelled by Lennard-Jones fluid.	O
206	Deformation characteristics and dislocation quantification of aluminum-magnesium alloy with different <0 0 1> tilt grain boundaries using MD simulation. 2023 ,	0
205	Development of three-dimensional GPU DEM codeBenchmarking, validation, and application in mineral processing.	0

204	Modeling of surface phenomena of liquid AlNi alloys using molecular dynamics. 2023, 13,	O
203	High-throughput manufacturing of epitaxial membranes from a single wafer by 2D materials-based layer transfer process.	Ο
202	Surface Ligands Dictate the Mechanical Properties of Inorganic Nanomaterials. 2023, 17, 6698-6707	0
201	Thermal conductivity of 2D diamond superstructures in interlayer-bonded twisted bilayer graphene. 2023 , 122, 133101	O
200	Atomistic-Continuum Constitutive Modeling Connection for Gold Foams under Compression at High Strain Rates: The Dislocation Density Effect. 2023 , 13, 652	О
199	The Dynamic Nature of Graphene Active Sites in the H2O Gasification process: A ReaxFF and DFT Study. 2023 , 29,	O
198	Molecular Simulations in Macromolecular Science.	O
197	Short-range ordering alters the dislocation nucleation and propagation in refractory high-entropy alloys. 2023 ,	O
196	Molecular Dynamics Study of Clathrate-like Ordering of Water in Supersaturated Methane Solution at Low Pressure. 2023 , 28, 2960	0
195	Factors controlling heteroepitaxial phase formation at intermetallic-Al3Sc/liquid interfaces. 2023 , 133, 124902	Ο
194	Continuum Simulation of the Elastic Behavior of Nanosized Diamond Single Crystals. 2023, 45, 1-9	O
193	Molecular dynamics study of nano-indentation deformation behavior of Al/Al90Sm10 nanolaminate. 2023 , 29,	O
192	Understanding the efficient seawater desalination performance of carbon honeycomb via reverse osmosis. 2023 , 223, 112130	0
191	Linear Catenanes in Channel Confinement. 2023 , 56, 2736-2746	O
190	Impact of Atomic Void Clusters on the Tensile Behavior and its Features of Silicon Carbide Polycrystal through Molecular Dynamics Analysis.	0
189	Recognition of Synthesized Intermetallic Interlayers at the Interface in Ti@Al "Core Ishell" Nanoparticles Based on Computer Molecular-Dynamic Simulation. 2023 , 29-36	O
188	Experiment and Simulation Reveal Residue Details for How Target Binding Tunes Calmodulin Calcium-Binding Properties. 2023 , 127, 2900-2908	О
187	Mechanistic Insights on Permeation of Water over Iron Cations in Nanoporous Silicon Oxide Films for Selective H2 and O2 Evolution. 2023 , 15, 17814-17824	O

186	Optimization of interfacial thermal conductance based on nanodot embedding. 2023 , 0	O
185	Efficient Non-Destructive Detection of Interface Adhesion State by Interfacial Thermal Conductance: A Molecular Dynamics Study. 2023 , 11, 1032	O
184	Phase behavior of active and passive dumbbells. 2023, 107,	O
183	Effects of Crack Formation on the Mechanical Properties of Bilayer Graphene: A Comparative Analysis. 2023 , 13, 584	О
182	Machine learning transferable atomic forces for large systems from underconverged molecular fragments.	O
181	Morphological evolution of irregularly shaped Au nanoparticles during the sintering process and their mechanical performance.	O
180	Atomic-scale study of the nano-cutting deformation mechanism of nickel-based single crystal superalloy containing Cr, Co, and 四 2023 , 129,	0
179	Multiple Scratching: An Atomistic Study. 2023 , 71,	O
178	Fast general two- and three-body interatomic potential. 2023 , 107,	0
177	Spontaneous transport of nanodroplets in 2D nanochannels. 2023 ,	O
176	Investigation of structural and transport properties of highly oxygen-permeable ionomer in polymer electrolyte membrane fuel cells using molecular dynamics simulations. 2023 ,	0
175	Influences of C, Si and Mn on the wear resistance of coiled tubing steel. 2023 , 204854	O
174	The physicochemical properties of the CeF3 IFLiNaK molten mixture: an in silico study. 2023, 49, 845-854	О
173	The Nanoscale Density Gradient as a Structural Stabilizer for Glass Formation. 2023,	O
172	Network Structure and Water Absorption of Soil Moisture Gel by Coarse-Grained Molecular Dynamics Simulations. 63, 1-12	O
171	Influence of short-range order on diffusion in multiprincipal element alloys from long-time atomistic simulations. 2023 , 7,	O
170	The Importance of Morphology on Ion Transport in Single-Ion, Comb-Branched Copolymer Electrolytes: Experiments and Simulations. 2023 , 56, 2790-2800	0
169	Topological Data Analysis for Revealing the Structural Origin of Density Anomalies in Silica Glass. 2023 , 127, 3302-3311	O

168	Microstructure and Thermophysical Property Prediction for Chloride Composite Phase Change Materials: A Deep Potential Molecular Dynamics Study. 2023 , 127, 6852-6860	О
167	Theoretical study of entropy-induced friction in graphene. 2023 , 186, 110724	О
166	Spinlattice relaxation time in water/graphene-oxide dispersion. 2023, 158, 124709	О
165	Displacement cascades database from molecular dynamics simulations in tungsten. 2023 , 580, 154415	Ο
164	Sequential hydrogen storage in phosphorene nanotubes: A molecular dynamics study. 2023,	0
163	Mechanisms during Strain Rate-Dependent Crack Propagation of Copper Nanowires Containing Edge Cracks. 2023 , 13, 1231	Ο
162	An energy minimization strategy based on an improved nonlinear conjugate gradient method for accelerating the charged polymer dynamics simulation.	0
161	Disorder-order transition in multiprincipal element alloy: A free energy perspective. 2023 , 7,	O
160	Universal preference for low-energy core-shifted grain boundaries at the surfaces of fcc metals. 2023 , 5,	0
159	A method for extracting effective interactions from Hi-C data with applications to interphase chromosomes and inverted nuclei.	О
158	Small bimetallic clusters Agn-1M (M´=´Au, Co, Cu, Ni, Pd, Pt; n´=´3, 9, 15): Density functional theory and genetic algorithm. 2023 , 733, 122290	0
157	Understanding the Effect of Oil-Based Lubricants on the Tribological Behavior of Fettr Alloys from Reactive Molecular Dynamics. 2023 , 39, 5145-5155	О
156	Untangling the Interactions between Anionic Polystyrene Nanoparticles and Lipid Membranes Using Laurdan Fluorescence Spectroscopy and Molecular Simulations. 2023 , 145, 7962-7973	0
155	Hybrid interatomic potential for Sn. 2023 , 7,	O
154	Brittle-to-ductile transition and theoretical strength in a metalorganic framework glass.	0
153	Sintering Rate of Nickel Nanoparticles by Molecular Dynamics. 2023 , 127, 6802-6812	O
152	Solvation Environments in Porous Ionic Liquids Determine Selectivity in CO2 Conversion to Cyclic Carbonates. 2023 , 127, 3266-3277	0
151	Oxidization-Temperature-Triggered Rapid Preparation of Large-Area Single-Crystal Cu(111) Foil.	Ο

150	Entropy-driven atomic activation in supercooled liquids and its link to the fragile-to-strong transition. 2023 , 66,	O
149	Beyond steric selectivity of ions using figstrffi-scale capillaries.	О
148	Water-Structure-Specific Entropic Dominance in the Filling of Boron Nitride Nanotubes. 2023 , 127, 7009-7018	О
147	Computer Simulation of a Silicene Anode on a Silicone Carbide Substrate. 2023 , 17, 113-121	O
146	Molecular dynamics simulation of mechanical properties of carbon nanotube reinforced cellulose. 2023 , 29,	0
145	Atomistic modeling of the mechanical properties: the rise of machine learning interatomic potentials.	O
144	High changing curvature regions detect chromatin enrichment in single cell data.	О
143	Molecular Dynamics Simulation Prediction of the Partitioning Constants (KH, Kiw, Kia) of 82 Legacy and Emerging Organic Contaminants at the WaterAir Interface. 2023 , 57, 6296-6308	O
142	Charge-optimized many-body interaction potential for AlN revisited to explore plasmaBurface interactions. 2023 , 13,	O
141	Ion Separation Together with Water Purification via a New Type of Nanotube: A Molecular Dynamics Study. 2023 , 24, 6677	О
140	Energetic and Structural Characterizations of the PETWater Interface as a Key Step in Understanding Its Depolymerization. 2023 , 127, 3543-3555	O
139	Hierarchical lath colonies induced by dislocation rearrangement improve thermal cyclic stability of NiTi shape memory alloy. 2023 , 231, 115469	O
138	Effect of amorphous complexions on plastic deformation of nanolayered composites. 2023, 231, 115470	О
137	Pressure-Induced Stability of Methane Hydrate from Machine Learning Force Field Simulations. 2023 , 127, 7071-7077	О
136	Atomic-scale origin of the low grain-boundary resistance in perovskite solid electrolyte Li0.375Sr0.4375Ta0.75Zr0.25O3. 2023 , 14,	0
135	Cyclic-polymer grafted colloids in spherical confinement: insights for interphase chromosome organization.	О
134	Complex Strain Scapes in Reconstructed Transition-Metal Dichalcogenide Moir Superlattices.	O
133	Molecular insights into enhanced water evaporation from a hybrid nanostructured surface with hydrophilic and hydrophobic domains. 2023 , 465, 142838	O

132	Lithium Trapping and Irreversible Atomic-Scale Structure Evolution during Delithiation of Silicon Oxides as Lithium-Ion Battery Anodes. 2023 , 170, 040514	Ο
131	Dynamic Observation of the Coulomb Explosion and Field Evaporation of a Few-Layer Graphene Nanoribbon.	O
130	Accurate Interaction Energies of CO2 with the 20 Naturally Occurring Amino Acids.	0
129	Atomistic Simulation of Flow-Induced Microphase Separation and Crystallization of an Entangled Polyethylene Melt Undergoing Uniaxial Elongational Flow and the Role of Kuhn Segment Extension. 2023 , 15, 1831	O
128	Nanostructure-property relation of 5 grain boundary in HfNbZrTi high-entropy alloy under shear. 2023 , 58, 6757-6774	0
127	Competition between phonon-vacancy and four-phonon scattering in cubic boron arsenide by machine learning interatomic potential. 2023 , 7,	O
126	Supercritical fluids behave as complex networks. 2023, 14,	O
125	Influence of Host-Framework Flexibility on Gas Transport Properties of Nanosheets and Finite-Size Nanomaterials. 2023 , 127, 7445-7460	O
124	Initial stage of titanium oxidation in Ti/CuO thermites: a molecular dynamics study using ReaxFF forcefields.	0
123	Tailoring planar slip to achieve pure metal-like ductility in body-centred-cubic multi-principal element alloys.	O
122	Engineering Peculiar Cathode Electrolyte Interphase toward Sustainable and High-Rate Liß Batteries.	0
121	Influence of the twin boundary and Cr segregation on the spalling of Ni-base alloys by large-scale molecular dynamic simulations. 2023 , 133, 145901	Ο
120	The structure and energy of symmetric tilt grain boundaries in tungsten. 2023, 581, 154442	0
119	Piezoelectric and dielectric constants of topologically defected boron nitride nanotubes.	O
118	Karamelo: A Multi-CPU/GPU C++ Parallel MPM Code. 2023 , 205-225	Ο
117	Tool and Techniques on Computer-Aided Drug Design for Targeted Cancer Therapy. 2023 , 781-829	O
116	ពិgstrom-Depth Resolution with Chemical Specificity at the Liquid-Vapor Interface. 2023, 130,	O
115	Chemical short range order and deformation mechanism of a refractory high entropy alloy HfNbTaZr under nanoindentation: An atomistic study. 2023 , 24, 3588-3598	O

114	Understanding the wetting of transition metal dichalcogenides from an ab initio perspective. 2023 , 5,	O
113	A neural network model for high entropy alloy design. 2023 , 9,	O
112	Modular development of deep potential for complex solid solutions. 2023, 107,	O
111	Molecular Dynamics Simulation on Tensile Behavior of Cellulose at Different Strain Rates. 2023 , 2023, 1-10	O
110	Effects of void shape and location on the fracture and plastic deformation of Cu (crystalline) /Cu64Zr36 (amorphous) composites. 2023 , 24, 4177-4189	О
109	Molecular dynamics study of the tensile properties of gold nanocrystalline films irradiated by gallium Ions. 2023 , 581, 154448	O
108	Grain boundary softening from stress assisted helium cavity coalescence in ultrafine-grained tungsten. 2023 , 252, 118948	O
107	Buckling and Interfacial Deformation of Fluorescent Poly(N-isopropylacrylamide) Microgel Capsules.	O
106	Understanding How Metalligand Coordination Enables Solvent Free Ionic Conductivity in PDMS.	O
105	A Computational Study of Cluster Dynamics in Structural Lubricity: Role of Cluster Rotation.	O
104	Diffusion behavior determined by the new n-body potential in highly immiscible W/Cu system through molecular dynamics simulations. 2023 , 24, 3731-3745	O
103	Detecting LiquidIliquid Phase Separations Using Molecular Dynamics Simulations and Spectral Clustering.	O
102	High-Accuracy Neural Network Interatomic Potential for Silicon Nitride. 2023, 13, 1352	0
101	An atomistic study of plastic deformation of SmCo5 by amorphous shear bands. 2023 , 106002	O
100	Topological Data analysis of Ion Migration Mechanism. 2023 , 158, 144116	O
99	Phonon Interference Effects In Graphene Nanomesh. 2023 , 0	O
98	Water transport in reverse osmosis membranes is governed by pore flow, not a solution-diffusion mechanism. 2023 , 9,	0
97	Evaluation of Various Shear-Thinning Models for Squalane Using Traction Measurements, TEHD and NEMD Simulations. 2023 , 11, 178	O

96	Development of a Ni-Al reactive force field for Ni-based superalloy: Revealing electrostatic effects on mechanical deformation. 2023 ,	O
95	Kinetic reconstruction of free energies as a function of multiple order parameters. 2023 , 158, 144502	O
94	Computational simulation of self-cleaning carbon-based membranes with zeolite porous structure for desalination. 2023 , 136, 109925	O
93	Shear Responsive Gelation of Aqueous Polyacrylic Acid-co-polyacrylamide: Molecular Mechanism and Tribological Applications.	O
92	The nature of dynamic local order in CH3NH3PbI3 and CH3NH3PbBr3. 2023,	О
91	A review of GEMC method and its improved algorithms.	Ο
90	Review on Molecular Dynamics Simulations of Effects of Carbon Nanotubes (CNTs) on Electrical and Thermal Conductivities of CNT-Modified Polymeric Composites. 2023 , 7, 165	O
89	Study on Sintering Mechanism and Mechanical Properties of Nano-Cu based on Molecular Dynamics Simulation. 2023 ,	O
88	Atomistic Insights on Surface Quality Control via Annealing Process in AlGaN Thin Film Growth. 2023 , 13, 1382	O
87	Ultra-flexible two-dimensional Janus heterostructure superlattice: A novel intrinsic wrinkled structure.	O
86	Quantum Mechanical and Classical Calculation of the Transport and Relaxation Properties of HeCO2 Complex Using a New PES.	O
85	Insight into Oxygen Transport in Solid and High-Surface-Area Carbon Supports of Proton Exchange Membrane Fuel Cells.	O
84	Effects of location and size of Kirkendall voids on mechanical response of Cu/Sn solder joint under tension. 1-8	0
83	Liquid-Phase Friction of Two-Dimensional Molybdenum Disulfide at the Atomic Scale.	O
82	A Deep Neural Network Potential to Study the Thermal Conductivity of MnBi2Te4 and Bi2Te3/MnBi2Te4 Superlattice.	0
81	Graph theory-based structural analysis on density anomaly of silica glass. 2023 , 225, 112190	O
80	Influence of Curing Agents Molecular Structures on Interfacial Characteristics of Graphene/Epoxy Nanocomposites: A Molecular Dynamics Framework.	0
79	Rapid activation of non-oriented mechanophores via shock loading and spallation. 2023, 7,	O

78	Insights into nanoparticle shape transformation by energetic ions. 2023, 13,	O
77	Effects of structure and strain rate on deformation mechanism of twin lamellar Al0.3CoCrFeNi alloys. 2023 , 954, 170174	O
76	Interfacial thermal resistance calculations for weak solid[]quid atom interactions using equilibrium molecular dynamics. 1-12	0
75	Super Proton Conductivity Through Control of Hydrogen-Bonding Networks in Flexible Metal Drganic Frameworks.	O
74	Insights into the role of water concentrations on nanomechanical behavior of type I collagen-hyaluronan interfaces in annulus fibrosus: A molecular dynamics investigation.	O
73	Conformability of flexible sheets on spherical surfaces. 2023 , 9,	O
72	Enhanced antimony removal within lamellar nanoconfined interspaces through a self-cleaning MXene@CNF@FeOOH water purification membrane. 2023 , 465, 143018	О
71	Thermal Conductivity of a Two-Dimensional Diamondene Sheet: A Molecular Study.	О
70	Restricted CO2/CH4 diffusion in nanopores: A quantitative framework to characterize nanoconfinement effect of shale organic pore. 2023 , 210, 124178	0
69	n-Pentanol Lubrication of Silica Layers Passivated with Hydroxyl Groups Under Constant Shear Stress and Load and Isothermal Conditions. 2023 , 71,	O
68	Viscosity of Fe2O3-Water nanofluids by molecular dynamics simulations: Effects of nanoparticle content, temperature and size. 2023 , 121859	О
67	Collaborative mechanisms boost the nanoscale boiling heat transfer at functionalized gold surfaces. 2023 , 210, 124179	O
66	The effect of grain boundary on irradiation resistance of CoCrCuFeNi high entropy alloy. 2023, 225, 112185	0
65	Single-Molecule Structure and Topology of Kinetoplast DNA Networks. 2023 , 13,	O
64	Atomic-resolution observations of silver segregation in a [111] tilt grain boundary in copper. 2023 , 107,	O
63	Compositional effects on dislocation properties in NiCo and NiFe alloys using atomistic simulations. 2023 , 225, 112191	O
62	Quantitative tests revealing hydrogen-enhanced dislocation motion in ∃ron.	О
61	Generalization of the Hall-Petch and inverse Hall-Petch behaviors by tuning amorphous regions in 2D solids. 2023 , 20220058	O

60	Analysis of the effect of tool geometry on the cutting process of polycrystalline Fe-Cr-W alloy based on molecular dynamics simulation. 2023 , 95, 405-414	О
59	Amorphous Zirconia-doped Tantala modeling and simulations using explicit multi-element spectral neighbor analysis machine learning potentials (EME-SNAP). 2023 , 7,	O
58	Annealing coatings of graphene on silicon and application to tribology. 2023, 108539	0
57	Thermal Conductivities of PtX2 ($X = S$, Se , and Te) Monolayers: A Comprehensive Molecular Dynamics Study.	O
56	Graphullerite: A Thermally Conductive and Remarkably Ductile Allotrope of Polymerized Carbon.	0
55	Hydrodynamic effects in kinetics of phase separation in binary fluids: Critical versus off-critical compositions. 2023 , 107,	O
54	Effect of Pressure on the Dynamics of Iodide Defects in Methylammonium Lead Iodide: An Atomistic Simulation.	О
53	Breathable MOFs Layer on Atomically Grown 2D SnS 2 for Stable and Selective Surface Activation.	O
52	Characterizing Soft Matter Self-Assembly and Material Properties with Advanced Molecular Dynamics and Data-Driven Methods. 2023 , 1197-1220	О
51	Nanoporous Amorphous Carbon with Exceptional Ultra-High Strength. 2023 , 13, 1429	O
50	Improvement in CO2 geo-sequestration in saline aquifers by viscosification: From molecular scale to core scale. 2023 , 125, 103888	0
49	Laser assisted fabrication of mechanochemically robust Ti3Au intermetallic at Au-Ti interface. 2023 , 42, 101413	O
48	Percolation transitions of confinement-induced layering and intralayer structural orders in three-dimensional Yukawa liquids. 2023 , 107,	О
47	Crystal Polymorph Selection Mechanism of Hard Spheres Hidden in the Fluid.	O
46	Inhibition mechanisms of HAIB on Q235 rebar in the simulated concrete pore solution. 2023, 106565	0
45	Regulating the dislocation-nanocluster interactions by electrical pulses to alleviate material hardening. 2023 , 145064	O
44	Atomistic simulation of the dislocation interactions with the Al2Ca Laves phase in MgAl Ω a alloy. 2023 ,	Ο
43	Thermal transport properties and lattice vibration modes in crystalline and amorphous LaMgAl11O19. 2023 , 170245	Ο

42	Quadruple H-Bonding and Polyrotaxanes Dual Cross-linking Supramolecular Elastomer for High Toughness and Self-healing Conductors.	0
41	Quadruple H-Bonding and Polyrotaxanes Dual Cross-linking Supramolecular Elastomer for High Toughness and Self-healing Conductors.	O
40	A molecular dynamics study of thermal conductivity and viscosity in colloidal suspensions: From well-dispersed nanoparticles to nanoparticle aggregates. 2023 , 229, 120651	0
39	Registry-Dependent Potential for Interfaces of Water with Graphene. 2023 , 127, 8704-8713	O
38	Dynamic crosslinking compatibilizes immiscible mixed plastics. 2023 , 616, 731-739	О
37	Comparative analysis of frictional behavior and mechanism of molybdenum ditelluride with different structures.	O
36	Visualizing the disordered nuclear transport machinery in situ. 2023 , 617, 162-169	0
35	Surface water in C-S-H: Effect of the temperature on (de)sorption. 2023 , 169, 107179	O
34	MD-Bench: A Generic Proxy-App Toolbox for State-of-the-Art Molecular Dynamics Algorithms. 2023 , 321-332	0
33	Impact dynamics of droplets on the well-designed wrinkled surfaces: Enhancement of bounding ability. 2023 , 669, 131521	O
32	Numerical investigation of ejecta mass of twice-shocked liquid Sn. 2023 , 133,	О
31	Molecular dynamics simulation for radiation response of Nb bicrystal having 13 , 129 , and 185 grain boundary. 2023 , 133,	O
30	Unified description for the temperature dependence of mobility in liquids. 2023, 158,	О
29	DNA Detection Using a Single-Layer Phosphorene Nanopore. 2023 , 6, 7814-7820	O
28	Dissipative solitary waves in a two-dimensional complex plasma: Amorphous versus crystalline. 2023 , 107,	0
27	Unexpected Behavior in Thermal Conductivity of Confined Monolayer Water. 2023 , 127, 4090-4098	O
26	Roles of Hydrogen Bonds and Alignment in Oriented Attachment of Gibbsite Nanoparticles: Insights from Molecular Dynamics. 2023 , 127, 8695-8703	O
25	The effects of the shape of a capsid on the ejection rate of a single polymer chain through a nanopore. 2023 , 158,	O

24	Thermal Conductivities of Uniform and Random Sulfur Crosslinking in Polybutadiene by Molecular Dynamic Simulation. 2023 , 15, 2058	O
23	Origins of strengthening and toughening effects in twinned nanocrystalline alloys of low stacking fault energy with heterogeneous grain structure. 2023 , 176, 105305	O
22	The growth and coalescence of helium bubbles in bicrystal copper under tension. 2023 , 582, 154489	O
21	Effect of the kinetic energy on particle ejection process from carbon nanotubes bombarded by kilo-electron-volt C60. 2023 , 41,	O
20	Dislocation loop bias and void swelling in irradiated <code>Bron</code> from mesoscale and atomistic simulations. 2023 , 4,	O
19	The effects of hydrogen and vacancy on the tensile deformation behavior of B symmetric tilt grain boundaries in pure fe. 2023 ,	O
18	An Approach for Quantitative EHD Friction Prediction Based on Rheological Experiments and Molecular Dynamics Simulations. 2023 , 71,	0
17	Monoclinic-to-tetragonal transition in HfO2 induced by swift heavy ions: Effects of thermal spike and oxygen defects. 2023 , 254, 118992	O
16	Critical contact angle for triggering dynamic Leidenfrost phenomenon at different surface wettability: A molecular dynamics study. 2023 , 382, 121982	0
15	Molecular dynamics of solution strengthening of Si and Cu atoms in aluminum alloy.	О
14	Transition in helium bubble strengthening of copper from quasi-static to dynamic deformation. 2023 , 254, 118987	0
13	Intercalated water-induced hysteretic friction behavior of graphene, h-BN, and MoS2. 2023, 630, 157442	O
12	Molecular dynamics simulation of twin nucleation and growth in Ni-based superalloys. 2023, 166, 103645	0
11	Understanding the role of surface mechanical properties in SiC surface machining. 2023, 163, 107594	O
10	Insights into the carbonization mechanism of PAN-derived carbon precursor fibers and establishment of a kinetics-driven accelerated reaction template for atomistic simulation.	О
9	Thermal Expansion and Thermal Conductivity of Ni/Graphene Composite: Molecular Dynamics Simulation. 2023 , 16, 3747	O
8	Short- and medium-range structure synergistically control fracture toughness of densified aluminoborate glasses. 2023 , 7,	O
7	Scratching a soft layer above a hard substrate. 1-12	O

6	Ring structural transitions in strongly coupled dusty plasmas. 2023, 107,	O
5	Ridge-twin boundaries as prolific dislocation sources in low stacking-fault energy metals and alloys.	O
4	Prediction of Adsorption and Diffusion of Shale Gas in Composite Pores Consisting of Kaolinite and Kerogen using Molecular Simulation.	О
3	Developing a variable charge potential for Hf/Nb/Ta/Ti/Zr/O system via machine learning global optimization. 2023 , 230, 111999	O
2	Structuring thermal transport in pristine graphene with h-BN nanorings. 2023, 180, 111414	О
1	Thermal Conductivity Enhancement of Graphene/Epoxy Nanocomposites by Reducing Interfacial Thermal Resistance.	O